AWARD NUMBER: W81XWH-08-1-0508

TITLE: "The Isolation and Characterization of Human Prostate Cancer Stem Cells"

PRINCIPAL INVESTIGATOR: Ganesh S. Palapattu, MD

CONTRACTING ORGANIZATION: The University of Michigan
Ann Arbor, MI 48109

REPORT DATE: May 2015

TYPE OF REPORT: Final Summary

PREPARED FOR: U.S. Army Medical Research and Materiel Command
Fort Detrick, Maryland 21702-5012

REPORT DOCUMENTATION PAGE

Form Approved
OMB No. 0704-0188

1. REPORT DATE	2. REPORT TYPE	3. DATES COVERED
May 2015	Final Summary	01 Aug 2008– 28 Feb 2015

4. TITLE AND SUBTITLE

The Isolation and Characterization of Human Prostate Cancer Stem Cells

5a. CONTRACT NUMBER
W81XWH-08-1-0508

5b. GRANT NUMBER
W81XWH-08-1-0508

5c. PROGRAM ELEMENT NUMBER

6. AUTHOR(S)

Ganesh S. Palapattu, MD

E-Mail: gpalapat@med.umich.edu

5d. PROJECT NUMBER

5e. TASK NUMBER

5f. WORK UNIT NUMBER

7. PERFORMING ORGANIZATION NAME(S) AND ADDRESS(ES)

The University of Michigan Medical Schoo
3875 Taubman Center
1500 E. Medical Center Dr
Ann Arbor, MI 48109

8. PERFORMING ORGANIZATION REPORT NUMBER

9. SPONSORING / MONITORING AGENCY NAME(S) AND ADDRESS(ES)

U.S. Army Medical Research and Materiel Command
Fort Detrick, Maryland 21702-5012

10. SPONSOR/MONITOR'S ACRONYM(S)

11. SPONSOR/MONITOR'S REPORT NUMBER(S)

12. DISTRIBUTION / AVAILABILITY STATEMENT

Approved for Public Release; Distribution Unlimited

13. SUPPLEMENTARY NOTES

14. ABSTRACT

The overall objective of this proposal is to develop a durable cure for lethal prostate cancer through the elucidation of the role of cancer stem cells in the pathogenesis of the disease. During the past year, we have made the following significant findings/observations: i) 3D culture of human prostate cancer cells with magnetic nanoparticles is not optimal for tumor initiation studies, ii) in vitro co-culture of human prostate cancer cells (established cell lines and primary patient samples) with human prostate fibroblasts hold promise as models of tumor initiation/cancer stem cell activity. We continue to optimize and validate our in vitro model of prostate cancer initiation to facilitate cancer stem cell discovery as well as drug targeting.

15. SUBJECT TERMS
Prostate cancer, stem cell, in vitro assay, cancer stem cell

16. SECURITY CLASSIFICATION OF:			17. LIMITATION OF ABSTRACT	18. NUMBER OF PAGES	19a. NAME OF RESPONSIBLE PERSON
a. REPORT	b. ABSTRACT	c. THIS PAGE			USAMRMC
Unclassified	Unclassified	Unclassified	Unclassified	84	19b. TELEPHONE NUMBER *(include area code)*

Table of Contents

Introduction

The overarching goal of this proposal is to develop a durable cure for men with advanced prostate cancer through an improved understanding of the role of human prostate cancer stem cells in the pathogenesis of the disease. To this end, we have proposed the following specific aims: **1)** to identify and prospectively isolate prostate cancer stem cells from human prostate cancer tissue, **2)** to examine human prostate cancer cell lines, both primary and established, for cells that express cancer stem cell surface markers and the ability to determine therapy resistance *in vitro*, and **3)** to develop an *in vivo* model to assess human prostate cancer stem cell targeted therapy. The elucidation of the differential biology of cancer stem cells, versus the bulk population of cancer cells, has the potential to lead to the identification of novel therapeutic targets that aim to cripple the driving force behind lethal prostate cancer.

Keywords

Prostate cancer, stem cell, in vitro assay, cancer stem cell, CD44, androgen receptor, reactive oxygen species, drug resistance, castrate resistant prostate cancer

Overall Project Summary

From 01 Aug 2008- 28 Feb 2015 our lab was involved in identifying and characterizing prostate cancer stem cells using established prostate cancer cell lines. The frequently used functional definition of a cancer stem cell is a cell that is treatment resistant.

In our initial application we had planned: 1) to identify and prospectively isolate prostate cancer stem cells from human prostate cancer tissue, **2)** to examine human prostate cancer cell lines, both primary and established, for cells that express cancer stem cell surface markers and the ability to determine therapy resistance *in vitro*, and **3)** to develop an *in vivo* model to assess human prostate cancer stem cell targeted therapy. The elucidation of the differential biology of cancer stem cells, versus the bulk population of cancer cells, has the potential to lead to the identification of novel therapeutic targets that aim to cripple the driving force behind lethal prostate cancer.

The following is a summary from each annual report and concludes with our findings from the period 2014-2015.

Task 1a: Identification of prostate cancer stem cells from human prostate cancer tissue. (months 1-12)

Aim 1a: Identification of prostate cancer stem cells from human prostate cancer tissue.

Before pursuing in vivo modeling with sorted cells with markers such as CD44 we pursued establishing the technique without cell sorting (i.e., positive control). Over the past year we have performed 485 individual tissue recombination experiments from 17 different prostate cancer specimens obtained at radical prostatectomy. As discussed in our proposal, tissue recombination (TR) was performed by combining single cell suspensions made from areas of suspected prostate cancer with rodent seminal vesicle mesenchyme. Only 2 of 485 tissue recombinants displayed prostate tissue at 3 months. One showed benign human prostate and the other rodent prostate. See figure 1 below. Notably, our negative findings were corroborated by the Tang lab (collaborator) at MD Anderson. They performed a similar number of TR experiments and were unable to generate a single TR composed of human prostate cancer glands.

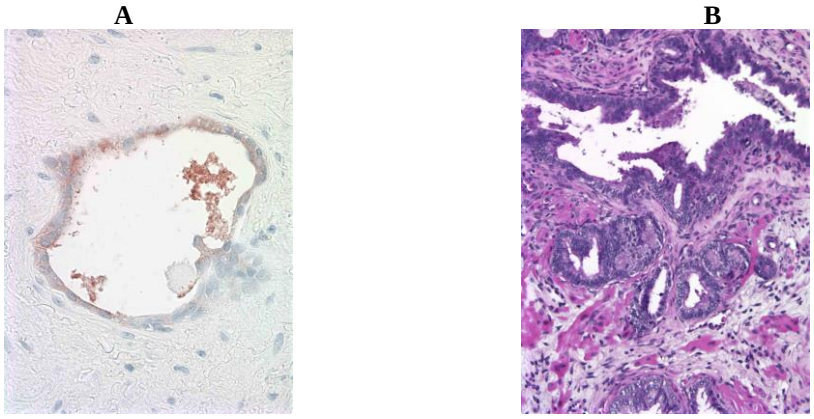

Figure 1. Tissue recombination with primary unsorted human prostate cancer cells. Of the almost 500 TRs constructed, only 2 gave evidence of prostate type tissue at harvest. **A** shows benign human prostate tissue (brown stain for PSA) and **B** displays rodent prostate tissue.

Reasons for our negative findings include: i) starting tissue was not actually prostate cancer but benign or mostly stroma, ii) collagenase/trypsin treatment was too harsh on human cells, or less likely, iii) our technique of TR was sub-optimal (we were able to generate rodent prostate when rodent UGE was combined with rSVM). At the moment, following discussions with my mentors and collaborators we have halted further TR experiments as described in this aim.

Task 1b: Prospective isolation of prostate cancer stem cells from human prostate cancer tissue. (months 13-30)

Aim 1b: Prospective isolation of prostate cancer stem cells from human prostate cancer tissue.

Given the above findings, no work on this sub-aim has been performed to date.

Task 2a: *In vitro* examination of human prostate cancer cell lines, both primary and established, for cells that express cancer stem cell surface markers. (months 6-24)

Aim 2a: *In vitro* examination of human prostate cancer cell lines, both primary and established, for cells that express cancer stem cell surface markers.

Based upon conversations with mentor Craig T. Jordan and collaborator Dean Tang, we have focused initially on CD44. We have completed a detailed analysis of CD44 expression in three common human prostate cancer cell lines and in human prostate cancer tissue. This work has been published and the DoD cited as a funding source. See reference below (reprint attached to appendix).

Palapattu GS, Wu G, Silvers C, Martin, HB, Williams K, Salamone L, Bushnell T, Huang LS, Yang Q, Huang J. Selective expression of CD44, a putative prostate cancer stem cell marker, in neuroendocrine tumor cells of human prostate cancer. *Prostate*, 15;69(7): 787-98, 2009.

We have encountered significant problems with culturing and maintaining primary human prostate cancer cells *in vitro*. Per discussions with others in the field, this is not altogether unexpected. To overcome this problem we have begun studies using rSVM as a feeder layer. This idea borrows from Cuhna's work on *in vivo* TR and work published by Witte and Isaacs on the use of feeder layers in prostate cell culture. In essence, we are creating 'TR in a dish'. Initial studies with this technique on the non-adherent cell line LAPC-9 and 2 other xenograft maintained human prostate cancer cell lines have shown promise. We have termed the 3-D structures formed by single cell suspensions upon this feeder layer 'glandoids' (see figure 2). Glandoids typically form with 21-27 days after plating on rSVM that has been irradiated to 30Gy to prevent overgrowth, and are composed of all cell types relevant in human prostate cancer (luminal cells, NE cells; no basal cells).

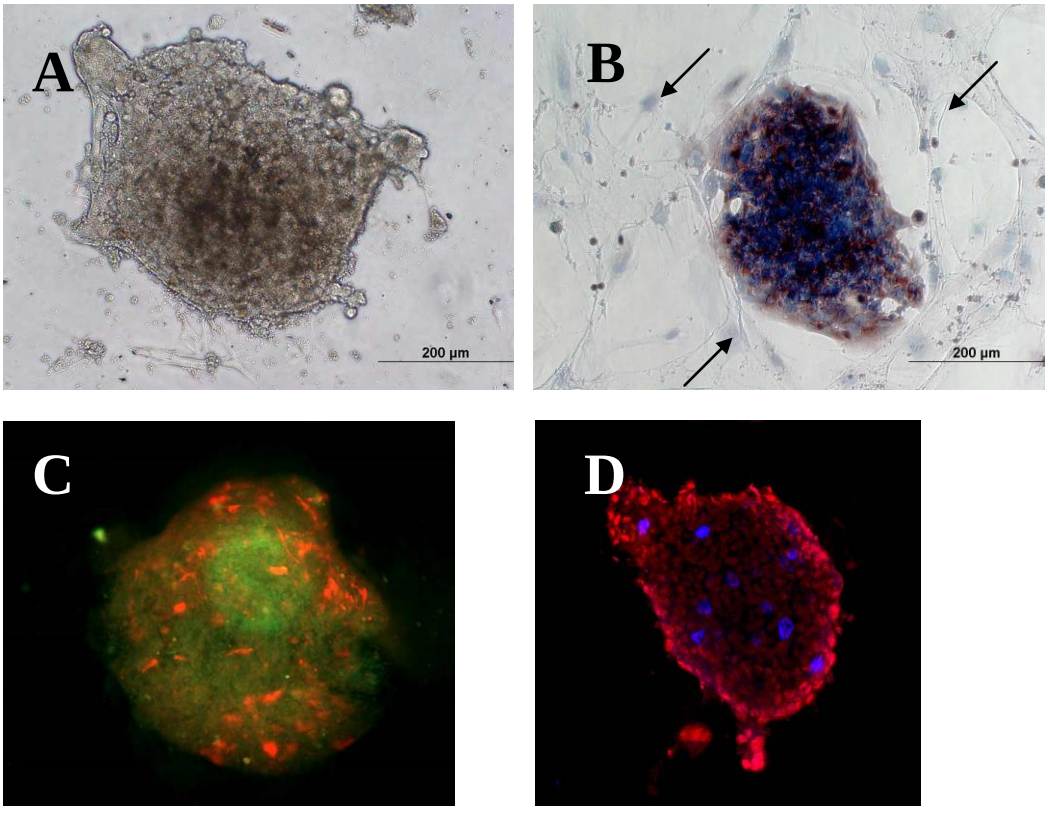

Figure 2. *In vitro* 'glandoids'. **A** represents light microscopy of a glandoid at 21 days. **B** shows a glandoid upon rSVM (arrows). Brown (DAB) stain is for PSA; blue nuclear stain. **C** shows

immunofluorescent analysis of a glandoid for PSA (green) and cytokeratin 8 (orange). Panel **D** demonstrates rare neuroendocrine cells in glandoids (blue=chromogranin A; red=cytokeratin 8).

Interestingly, we have also shown that primary glandoids can give rise to daughter (secondary) glandoids- implying this assay may also be able test self-renewal (an important attribute of stem cells). We are currently evaluating the tumorigenicity of these glandoids and testing the assay for clonogenicity and reproducibility with other human prostate cancer cell lines. We are also studying the composition and tumorigenicty of secondary glandoids. Our goal is to develop this assay as a valid model of human prostate cancer initiation with either primary human prostate cancer cells and/or non-adherent prostate cancer xenograft cell lines. The successful development of this assay will allow us to assess/screen candidate compounds *in vitro* for their impact on tumor initiation/stem cell activity.

Task 2b: Assessment of the ability of human prostate cancer cells that possess cancer stem cell surface antigen expression to determine therapy resistance *in vitro*. (months 14-28)

Aim 2b: Assessment of the ability of human prostate cancer cells that possess cancer stem cell surface antigen expression to determine therapy resistance *in vitro*.

No work on this sub-aim has been performed to date.

Task 3: Development of an *in vivo* model to assess human prostate cancer stem cell targeted therapy. (months 30-60)

Aim 3: Development of an *in vivo* model to assess human prostate cancer stem cell targeted therapy.

No work on this aim has been performed to date.

2009-2010

Revised September 4, 2009 **Revised/new Statement of Work**

Isolation and characterization of human prostate cancer stem cells

Research plan

Task 2a: *In vitro* examination of human prostate cancer cell lines, both primary and established, for cells that express cancer stem cell surface markers. (months 6-24)

We have been able to successfully create human prostate cancer in vivo from our transplanted glandoids (3D in vitro spheres) derived from xenograft human prostate cancer cell lines (i.e., LAPC9 and TRPC). Further, in appears from our data that glandoids are clonal- suggesting that such 3D structures may be a good in vitro surrogate for tumor initiation. This work has been published and the DoD cited as a funding source. See reference below (reprint attached to appendix).

Silvers CR, Williams K, Salamone L, Huang J, Jordan CT, Zhou H, **Palapattu GS**. A novel in vitro assay of tumor-initiating cells in xenograft prostate tumors. Prostate,70(13):1379-87, 2010.

The difficulty of readily obtaining rSVM as a feeder layer is a significant obstacle to the broad applicability of this assay. Further, we have tried this assay with 7-10 primary patient samples and have not been able to generate tumor initiating glandoids as described in the manuscript with xenograft only cells (cells that must be maintained in animals as they do not sit on plastic). We are currently exploring other methods of generating in vitro glandoids/spheres from xenograft and primary patient samples. These alternative strategies include: magnetic nanoparticles and using a stable (non-transformed) human prostate fibroblast cell line as a feeder layer. The former uses inert magnetic nanoparticles (3D Biosciences, Inc.) that passively diffuse into live cells that then allow 3D growth in an applied magnetic field[1]. Such a technique has been used to grow primary brain tumor cells in vitro when conventional techniques failed. The latter is a line developed by David Rowley at Baylor College of Medicine from a 19 y/o boy who died after a traumatic accident. This line has been maintained in culture for several years and is non-tumorigenic in animals.

Task 2b: Assessment of the ability of human prostate cancer cells that possess cancer stem cell surface antigen expression to determine therapy resistance *in vitro*. (months 14-28)

As noted, due to issues with developing an in vitro assay of tumor initiation no work on this sub-aim has been performed to date.

Task 3: Development of an *in vivo* model to assess human prostate cancer stem cell targeted therapy. (months 30-60)

No work on this aim has been completed to date. Given the difficulty of cultivating primary human prostate cancer cells in vitro/in vivo by us, and virtually investigators in the field, we may consider performing this aim with established cell lines (LNCaP, PC3 and DU-145). In this alternative approach, we may FACS cells by putative stem cell markers (e.g., CD44, CD144, side population) and establish xenografts from each line. Thereafter, we would treat with different therapies (hormone ablation, chemotherapy- as appropriate) once tumors became palpable (.5 cm x .5 cm).

2010-2011

This period was one of transition where I moved from the University of Rochester to The Methodist Hospital/The Methodist Research Institute.

Revised September 4, 2009 **Revised/new Statement of Work**

Isolation and characterization of human prostate cancer stem cells

Research plan

Task 2a: *In vitro* examination of human prostate cancer cell lines, both primary and established, for cells that express cancer stem cell surface markers. (months 6-24)

As noted in our last annual report, we have faced challenges in readily obtaining rSVM as a feeder layer for in vitro assays as we have previously described (Silvers et al, 2010). In the past year, we have focused attention on two alternative strategies: magnetic nanoparticles and human prostate fibroblasts serving as a feeder later.

Magnetic nanoparticles

Souza et al previously have shown that magnetic nanoparticles are able to passively diffuse into live cells, in an inert manner, and are capable of inducing 3D in vitro cell growth in a magnetic field.[1] This technique is based on the cellular uptake and magnetic levitation of a bioinorganic hydrogel (phage, magnetic iron oxide (MIO) and gold nanoparticles; see Figure 1). Notably, this technique has been observed to be useful in cultivating human primary cancer cell lines that are difficult to maintain in traditional cell culture. We obtained the magnetic nanoparticle reagents from n3D Biosciences (Houston, Texas).

Figure 1. Magnetic Levitation Based Three-Dimensional Tissue Culture

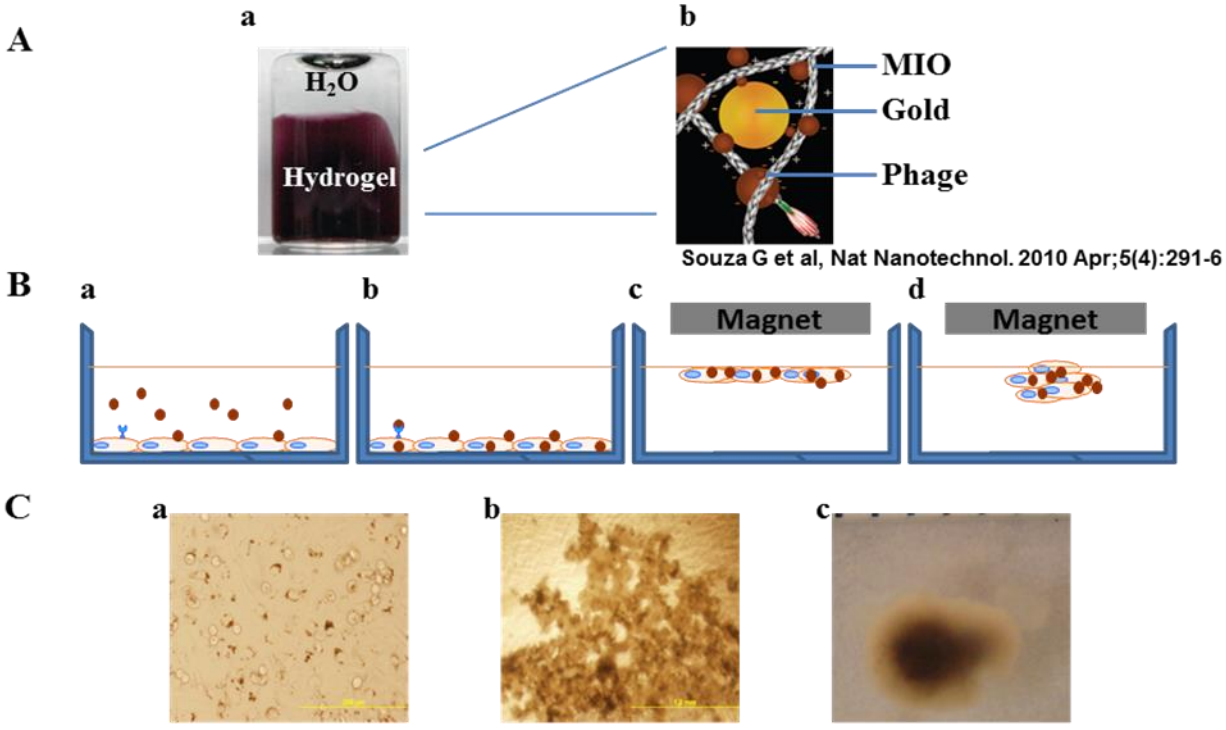

Figure 1. Magnetic Levitation Based Three-Dimensional Tissue Culture. A, Magnetic iron oxide-containing hydrogels. a, MIO-containing hydrogel in water. b, The scheme of hydrogel components with MIO, gold nanoparticles and phage. B. The strategy of cell levitation. a, Hydrogel is incubated with cells. b, hydrogel particles are uptaken by cells. c, magnetic pad raise cells to the air-medium interface. d, multicellular sphere structure forms. C. Prostate cancer cells were cultured with MIO. a, Brown colored hydrogel particle inside the cells after overnight incubation. b, 3 days after application of the magnetic force, cells levitated to the air-medium interface starting to form a three dimension structure. c, A sphere(LNCaP) like structure(~4mm in diameter) formed after 3 weeks culture.

Initially, we tested this technique with human prostate cancer cell lines. As shown in Figure 2, we were able to grow 3D clusters of LNCaP cells with this system that resembled 2D colonies with regards to PSA (+) and CD44 (-) expression.

Figure 2. Immunohistochemistry analysis of two dimensional and three dimensional culture with magnetic hydrogel

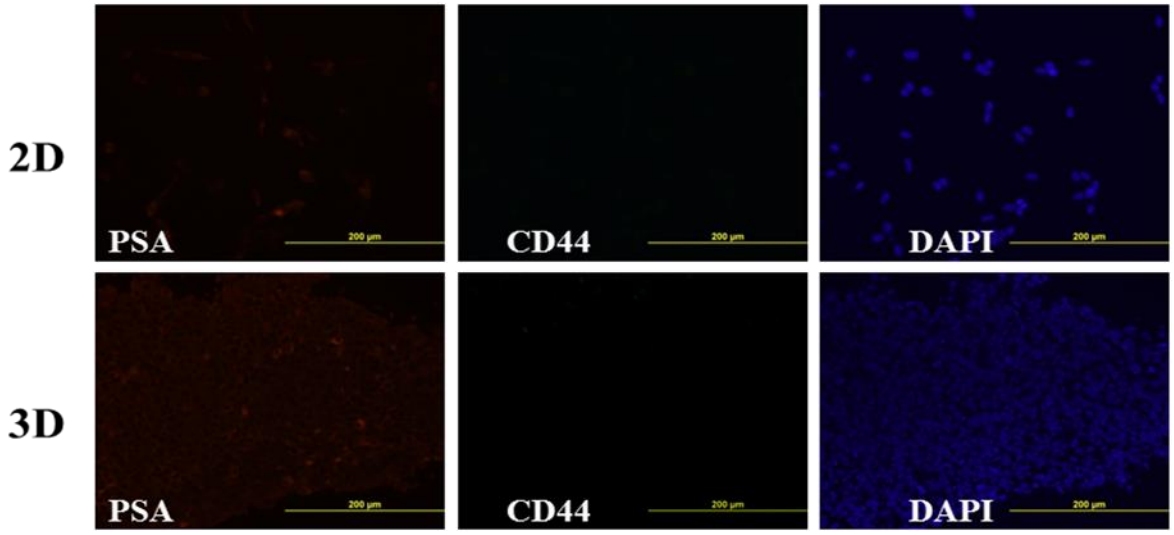

Figure 2. Immunohistochemistry analysis of two dimensional and three dimensional culture with magnetic hydrogel. Upper panels: LNCaP cells in the conventional two dimensional culture were fixed and Immunohistochemistry was performed with PSA antibody (red) and CD44 antibody (green) and DAPI (purple). Lower panels: LNCaP cells under three dimensional culture with magnetic hydrogel formed a sphere like structrue as showed in Figure 1, C(c). The sphere was paraffin-fixed and sectioned and after antigen retrieval, PSA antibody (red) and CD44 antibody (green) and DAPI (purple) were used for Immunohistochemistry.

We further evaluated this methodology with the xenograft prostate cancer cell line LAPC9, similar to what we had done before with rSVM (Figure 3).

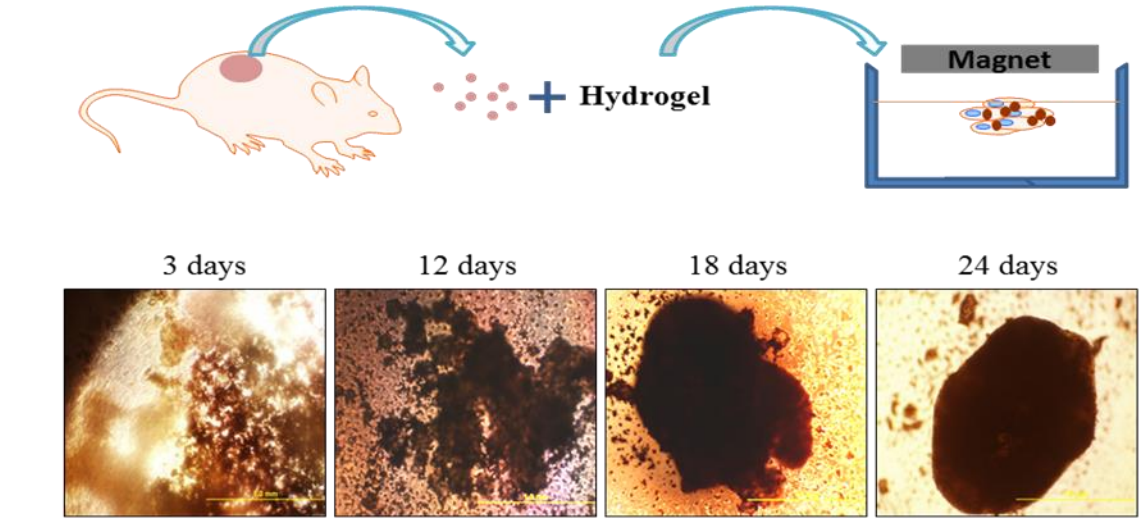

Figure 3. Three dimensional culture of xenograft prostate cancer cell line-LAPC9 with magnetic hydrogel. LAPC9 is a prostate xenograft cell line usually not growing in conventional two dimension conditions. Fresh LAPC9 tumor was dispersed into single cells and then incubated with MIO containing hydrogel, and the magnetic force was applied as showed in the upper panels. Cells levitated on the air-medium surface were analysed under the microscopy daily and the images at 3, 12, 18 and 24 days were taken as showed in the lower panels.

We then tested the capacity of this technique to grow 3D cultures from primary human prostate cancer patient samples (Figure 4). After 2-4 weeks, we observed 3D colony formation from 6 distinct patient samples; beyond 4 weeks the 3D structures began to break down and fragment. Single cells plated from these same samples in traditional 2D culture yielded no adherent epithelial cells (data not shown). We then attempted xenograft transplantation with matrigel in immunocompromised mice- none yielded viable tumor.

Figure 4. Three dimensional culture of fresh prostate cancer patient cells with magnetic hydrogel

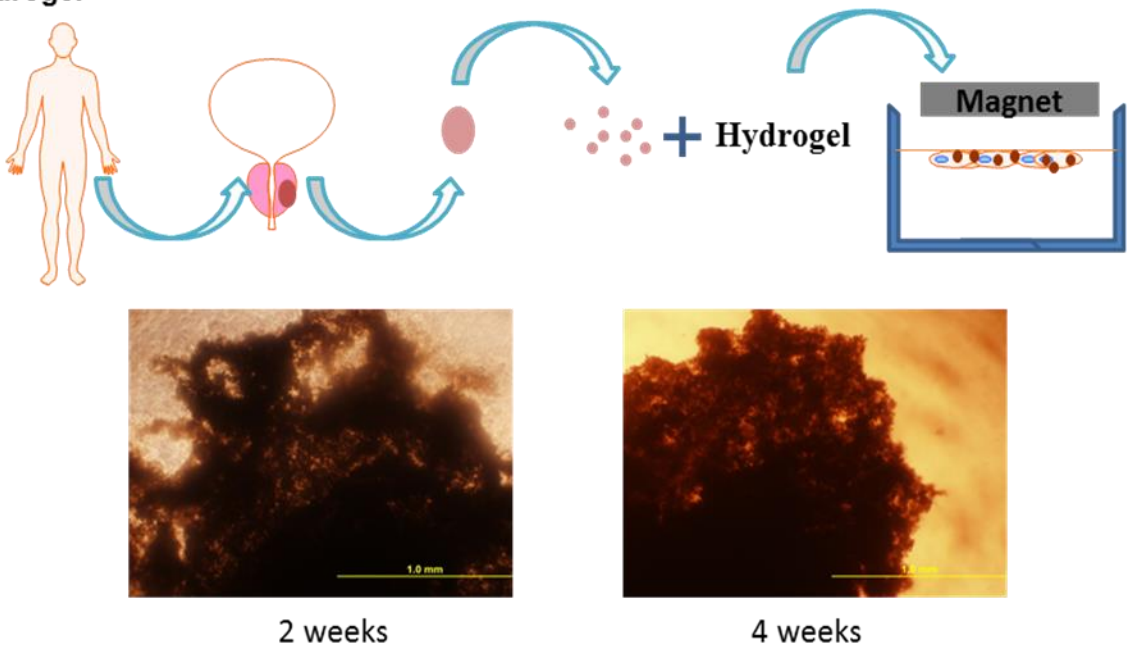

Figure 4. Three dimensional culture of fresh prostate cancer patient cells with magnetic hydrogel. Fresh prostate cancer patient samples were obtained in accordance with appropriate IRB protocols. Surgical resected prostate tissue was dispersed into single cells and then incubated with MIO containing hydrogel, then the magnetic force was applied as showed in the upper panels. Cells levitated on the air-medium surface were analyzed under the microscopy daily and the images at 2 weeks and 4 weeks were taken as showed in the lower panels.

Human prostate fibroblasts as a feeder layer

Through a collaboration with David Rowley, PhD at Baylor College of Medicine, we have obtained a human prostate fibroblast line (HPS 19I) from a 19 y/o motor vehicle accident victim. This line spontaneously immortalized and contains no gross chromosomal aberrations by spectral karyotype. Further, this line has been in culture for >2 years, has been passed >40 times and is non-tumorigenic. The Rowley lab has developed a co-culture system wherein 19I cells can co-mingle with prostate cancer epithelial cells to form 3D structures termed organoids (Figure 5). We have had initial success with cultivating prostate cancer lines in this system (Figures 6, 7).

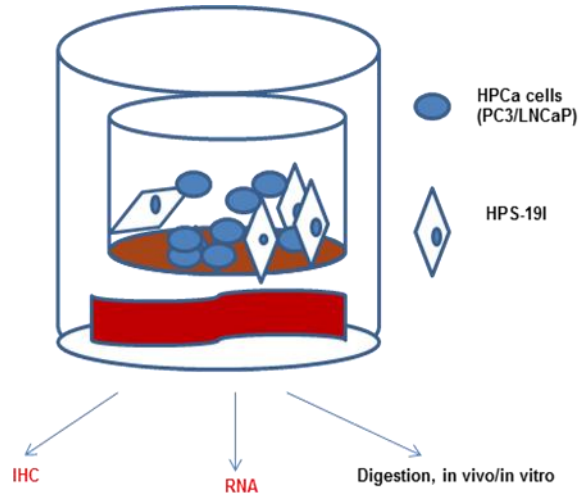

Figure 5. Stromal-epithelial co-culture system. In this system devised by the Rowley lab, epithelial cells (e.g., PC3, LNCaP) are mixed with HPS19I stromal cells in supportive media. A stirrer bar below helps circulate media in the chamber. Resultant 3D structures, organoids, can then be harvested for IHC, RNA or further studies.

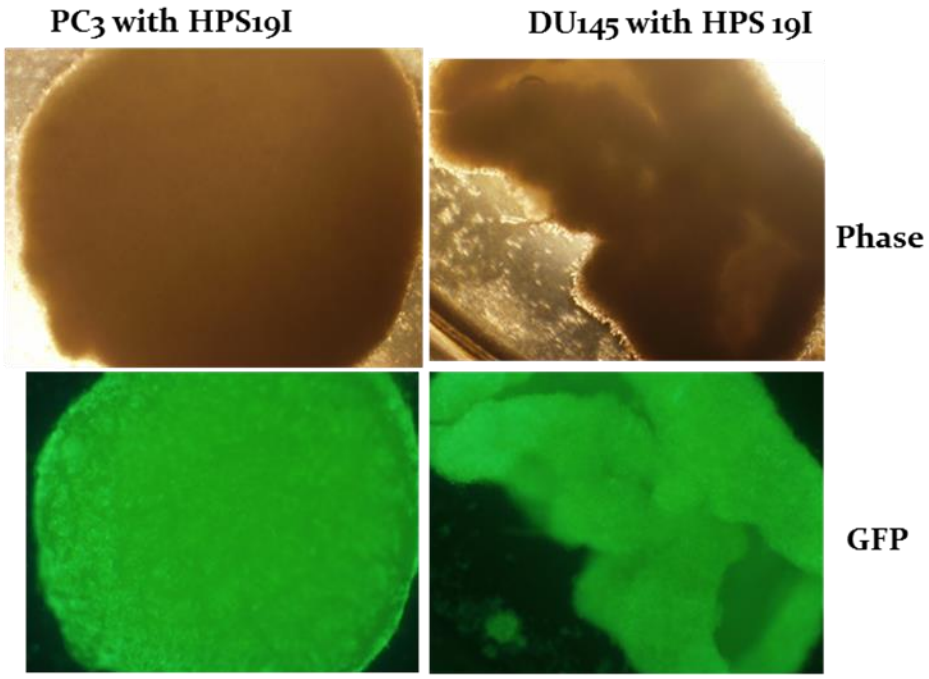

Figure 6. HPS191 and prostate cancer cell lines in vitro. After 2-3 weeks, organoids composed of stromal and epithelial cells (i.e., PC3 or DU145 transduced with GFP) are visible.

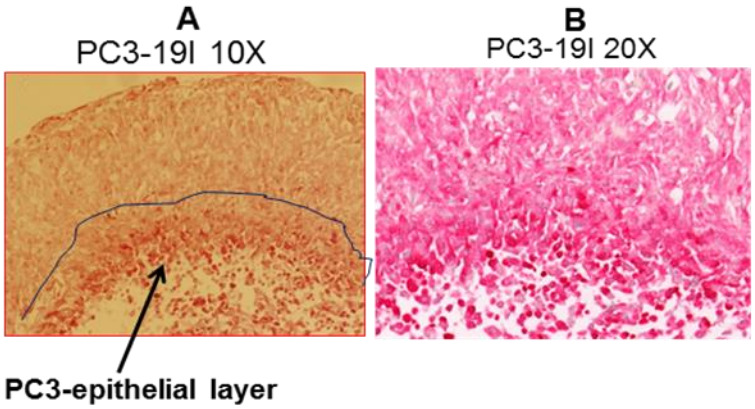

Figure 7. HPS191 and prostate cancer cell line organoids. After 2-3 weeks of co-culture, organoids form with stromal cells on the outside and epithelial cells on the inside. In panel A, line marks stromal-epithelial border. Panel B shows same border at higher magnification (H&E).

We are currently employing this stromal culture technique with primary patient samples with the goal of assaying resultant organoids for prostate cancer markers (IHC) and tumor initiation (xenograft studies).

Task 2b: Assessment of the ability of human prostate cancer cells that possess cancer stem cell surface antigen expression to determine therapy resistance *in vitro*. (months 14-28)

As noted, due to issues with developing an in vitro assay of tumor initiation no work on this sub-aim has been performed to date.

Task 3: Development of an *in vivo* model to assess human prostate cancer stem cell targeted therapy. (months 30-60)

No work on this aim has been completed to date. Given the difficulty of cultivating primary human prostate cancer cells in vitro/in vivo by us, and virtually investigators in the field, we may consider performing this aim with established cell lines (LNCaP, PC3 and DU-145). In this alternative approach, we may FACS cells by putative stem cell markers (e.g., CD44, CD144, side population) and establish xenografts from each line. Thereafter, we would treat with different therapies (hormone ablation, chemotherapy- as appropriate) once tumors became palpable (.5 cm x .5 cm).

2012-2013

The time period from 29 JAN 2012 - 28 JAN 2013 was a time of transition for our lab. In April of 2012 I was offered and accepted a position at the University of Michigan Medical School in the Department of Urology as Associate Professor, Chief of Urologic Oncology and The George F. and Sandy G. Valassis Professor of Urology. The DoD was made aware of my transition from The Methodist Hospital to the University of Michigan. From May 2012-June 2012 we prepared for transitioning our lab from Houston, Texas to Ann Arbor, Michigan. My official start date at the Univeristy of Michigan was October 1st, 2012. Upon starting, I began the process of setting up the lab. As of 28 JAN 2013 we were just getting personnel hired and starting the process of obtaining all necessary credentials to begin laboratory lab operations at the University of Michigan.

No significant work was completed on the proposed statement of work during this period.

We have received an extension to complete this award thru February 2015.

2013-2014

From 29 JAN 2013 - 28 JAN 2014 our lab was involved in i) hiring personnel, ii) procuring necessary equipment and iii) obtaining all necessary institutional approvals to conduct laboratory research. This included submitting a University of Michigan human subjects IRB protocol as well as an animal research protocol. Once these were obtained they were submitted to DoD for approval. The process to obtain DoD approval for our animal research protocol has been somewhat lengthy and at the end of this period is awaiting DoD approval. (approved obtained March 2014). An updated SOW was also submitted to the DoD and after several iterations was approved in September 2013.

Given that DoD approval of our animal protocol is still pending, no significant progress was made on animal studies during this grant period.

The functional definition of a cancer stem cell is a cell that is treatment resistant. To this end, we treated androgen receptor (AR+) prostate cancer cells VCaP and C4-2 with the potent anti-androgen enzalutamide (MDV3100) in vitro and examined the surviving populations by FACS for expression of the putative cancer stem cell marker CD44. Notably, C4-2 cells, while AR+ are not AR dependent, and hence are considered castrate resistant prostate cancer (CRPC) like.

VCaP DMSO

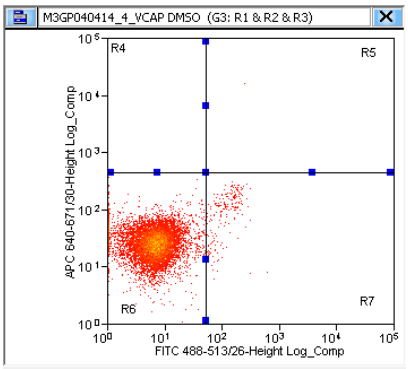

Region	Count	% Hist	% All
Total	10000	100.00	24.96
R4	0	0.00	0.00
R5	1	0.01	0.00
R6	9791	97.91	24.43
R7	208	2.08	0.52

CD44+ population: 2.08%

VCaP enza

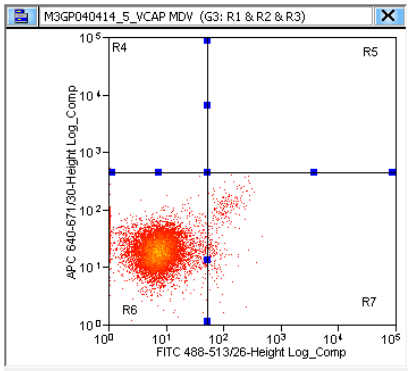

Region	Count	% Hist	% All
Total	10000	100.00	19.52
R4	1	0.01	0.00
R5	0	0.00	0.00
R6	9702	97.02	18.93
R7	297	2.97	0.58

2.97%

C4-2 DMSO

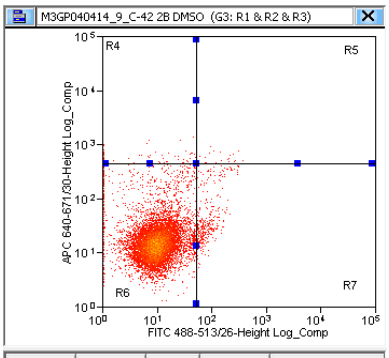

Region	Count	% Hist	% All
Total	10000	100.00	21.56
R4	55	0.55	0.12
R5	20	0.20	0.04
R6	9562	95.62	20.61
R7	363	3.63	0.78

CD44+ population: 3.36%

C4-2 enza

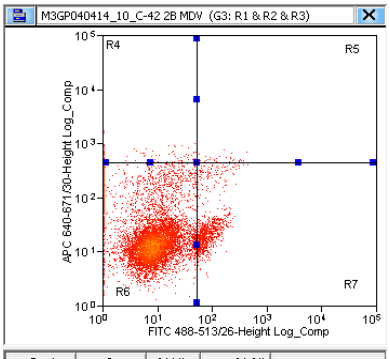

Region	Count	% Hist	% All
Total	10000	100.00	13.99
R4	80	0.80	0.11
R5	31	0.31	0.04
R6	8953	89.53	12.52
R7	936	9.36	1.31

9.63%

These early studies suggest that enzalutamide resistant cells appear enriched for CD44+, particularly in CRPC like cells. We are testing this observation in multiple other lines and plan to do in vivo studies as well to see if systemic treatment (enza and others) results disease that is enriched in CD44+ cells.

Given that we, and others, have had significant issues with taking fresh frozen tissues from radical prostatectomy specimens and generating tumors from single cell suspensions derived these samples, we are embarking on generating xenografts from chunks of tissue from radical prostatectomy specimens obtained from men with high grade disease (Gleason ≥8). After these have formed, we will treat animals with systemic therapies (e.g., enzalutamide) and examine refractory residual disease for stem cell markers. We will then validate our findings via correlation with treatment refractory samples in our vast tissue bank, inclusive of our warm autopsy cohort. We believe this approach will be more fruitful that our previous efforts.

Additionally, we have also begun testing the compound salinomycin.

Due to my changing of institutions twice during this award, please note that we have received an extension to complete this award thru February 2015.

2014-2015

Task 1. Due to certain technical difficulties we were unable to successfully isolate primary prostate cancer cells from human prostate tissues

Task 2a: *In vitro* examination of human cancer cell lines, both primary and established, for cells that express cancer stem cell surface markers.

We have previously discovered that treatment of androgen receptor positive (AR+) prostate cancer cells VCaP and C4-2 with a the anti-androgen enzalutamide (MDV3100) in vitro resulted in an enrichment of MDV3100 resistant cells. Examination of the surviving populations by FACS for expression of the putative cancer stem cell marker CD44 revealed that the drug-resistant cells expressed the CD44 on their surface. To further investigate whether this finding was specific to the tested cell lines and to anti-androgen therapy, we used another (AR+) cell line, LNCaP, which was treated with a common chemotherapeutic agent docetaxel for 24hrs. We found that all the surviving cells were expressing CD44+ protein on their surface as revealed by FACS (Figure 1 A). Cells were then FACS-sorted using the CD44 surface protein as a selection marker. Subsequent analyses of sorted cell behavior revealed that LNCaP_$CD44^{+}$ cells demonstrated increased proliferation (Figure 1 B), continued resistance to Docetaxel and MDV3100 (Figure 1 C) and increased migration (Figure 1 D). To our surprise, we were not able to detect AR in LNCaP $CD44^{+}$ cells, suggesting that these cells were no longer AR sensitive.

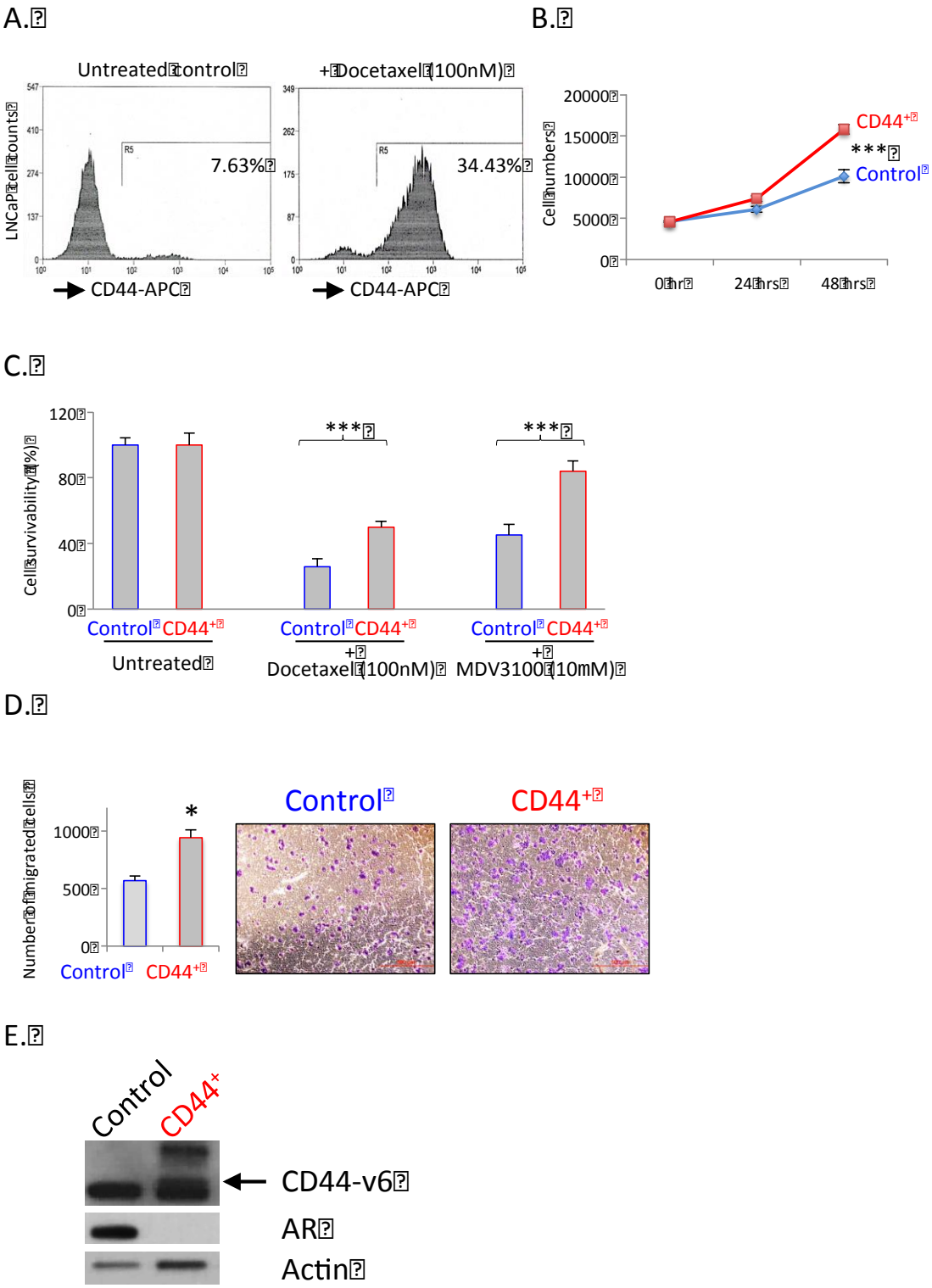

Figure 1. Drug resistant LNCaP cells express CD44 and demonstrate aggressive behavior. A. Only 7.63% of LNCaP cells express CD44. Treatment of LNCaP cells with 100nM of Docetaxel leads to an increase in the number of CD44+ cells (43.43%). B. Sorted by FACS CD44+ cells exhibit significantly accelerated proliferation in RPMI (supplemented with 10% FBS) over 48hrs. ***p<0.001. C. Treatment of CD44+ sorted cells with Docetexel and MDV3100 show increased resistance to these drugs by the CD44 expressing cells, as compared to control LNCaP cells. ***p<0.001. D. Boyden chamber migration assay demonstrates increased migration to 10% FBS supplemented RPMI media of the sorted CD44+ demonstrated. Upper chamber contained 1% FBS supplemented RPMI media. *p<0.05 E. Western blot analyses of LNCaP cells show increased expression of CD44-v6 in sorted CD44+ cells. Actin used as loading control.

To further investigate the significance of our findings, we examined CD44 and AR co-expression by examining the 260 RNA-seq libraries from the Michigan Center for Translational Pathology (MCTP) data set. The set included human tissues and several samples from human cell lines. Of the tissue libraries, 175 originated from primary tumor specimens, 31 originated from metastases and 56 originated from normal or benign, tumor-adjacent tissues.

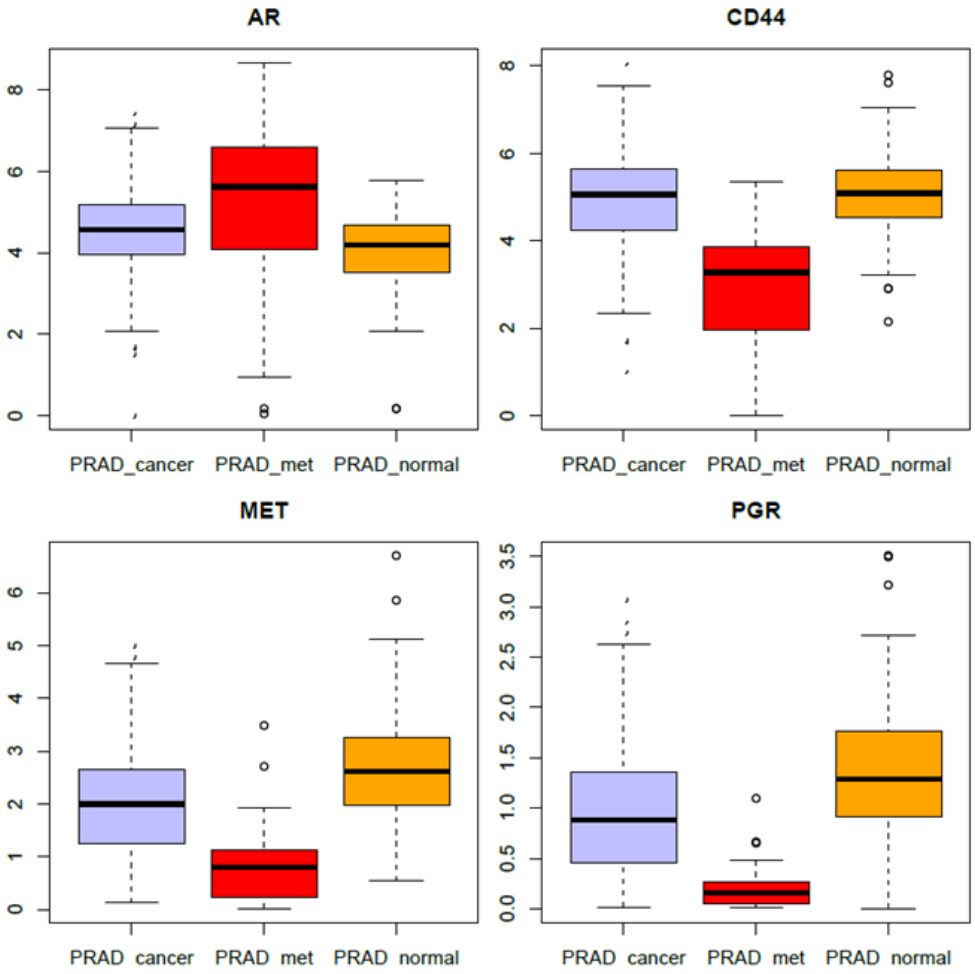

Figure 2. Analysis of the 260 RNA-seq libraries from the Michigan Center for Translational Pathology (MCTP) data set. A. Box plots comparing AR, CD44, MET and PGR across tissues. Relative to non-metastatic tissues, AR is overexpressed on average, and CD44 is underexpressed.

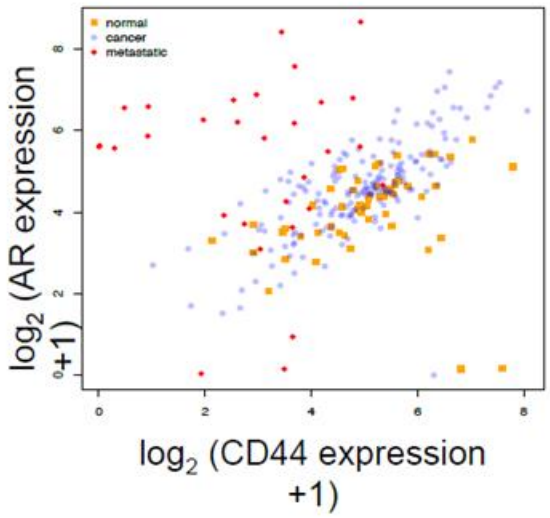

	cancer	metastatic	normal
cd44-ar#	0.73** (0.65, 0.79)	0.00 (-0.36, 0.36)	0.64** (0.45, 0.78)
cd44-met	0.76** (0.69, 0.82)	0.41* (0.06, 0.67)	0.84** (0.74, 0.90)
cd44-pgr	0.69** (0.61, 0.76)	0.38* (0.03, 0.65)	0.41** (0.17, 0.61)
ar-met#	0.60** (0.49, 0.68)	-0.34 (-0.62, 0.02)	0.65** (0.46, 0.78)
ar-pgr#	0.67** (0.57, 0.74)	-0.08 (-0.43, 0.29)	0.63** (0.44, 0.77)
met-pgr	0.76** (0.69, 0.82)	0.66** (0.40, 0.82)	0.42** (0.18, 0.62)

Two normal tissue samples have transformed AR expression below 1; these were removed as outliers when computing the correlations shown.

P-values are denoted by: * for $p < .05$ and ** for $p < .01$.

To summarize, all four genes are positively correlated in cancer and normal tissue. In metastatic tissue, only MET and PGR show strong evidence of correlation. There is weak evidence that CD44 is positively correlated with MET and PGR.

B. Scatter plot indicating positive correlation between all AR and CD44 genes in non-metastatic tissues. C Correlation coefficients for all gene pairs are shown in the table bellow. Values for normal tissue exclude two outliers with AR < 1. Relative to non-metastatic tissues, AR is overexpressed on average, and CD44 is underexpressed. Statistical analysis of the scatter plot indicating significance of gene co-expression in tissues from B. **C.** Heatmap showing expression (detectable vs. undetectable, as determined by qPCR, where Ct value of > 35 were filtered out) of AR and CD44 in two prostate tumor cell lines (i.e. VCAP, LNCaP), normal prostate epithelial cells (i.e. RWPE-1) and circulating tumor cells from men with high risk prostate cancer (High Risk) or from men with Castration resistant disease (CRPC).

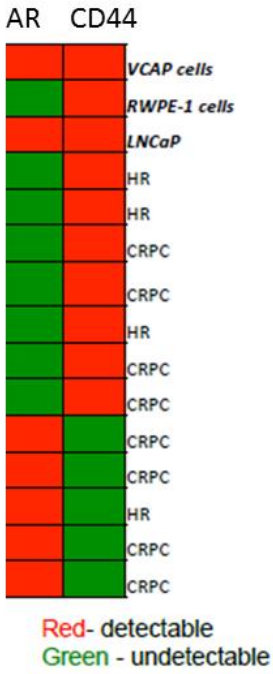

C. Heatmap showing expression (detectable vs. undetectable, as determined by qPCR, where Ct value of > 35 were filtered out) of AR and CD44 in two prostate tumor cell lines (i.e. VCAP, LNCaP), normal prostate epithelial cells (i.e. RWPE-1) and circulating tumor cells from men with high risk prostate cancer (High Risk) or from men with Castration resistant disease (CRPC).

Although we found a positive correlation between the expression of CD44 and AR in primary tumor and normal adjacent tissues, there was a strong inversed correlation between the AR and CD44 within the metastatic tissues. Specifically, we found that that overall, AR was significantly overexpressed on average in nearly all metastatic tissues in the data set, while the CD44 was significantly underexpressed (Figure 2 A-C). The expression of another marker of aggressive behavior by prostate cancer cells - cMET (MET) was also reduced in AR negative metastatic tissues, following similar expression trend as CD44 in the examined tissues.

Finally, we investigated the co-expression of CD44 and AR in circulating tumor cells isolated from peripheral blood samples from men with High Risk disease (n=4), defined as Gleason sum > 8, or PSA levels >20; and from men with castration resistant prostate cancer (n=8). DAPI and CD45 positive cells were excluded and all EpCAM (prostate cell specific antigen) positive cells were sorted with Flow Cytometer, followed by qPCR. The qPCR data was analysed using a comparative threshold cycle (ΔCT) method. To minimize potential noise, miRNAs with Ct value of > 35 were filtered out and the global normalization method was employed during analysis. As demonstrated in figure 2 D, we found that in all the samples that we tested (n=12), the negative correlation between the CD44 and AR expression remained true.

To reveal any potential link between the AR and CD44 expression, we artificially overexpressed *AR* in VCaP cells. We found that in cells overexpressing AR, the levels of CD44 protein were strongly reduced (Figure 3 A). Meanwhile, siRNA induced knockdown of AR in VCaP cells, resulted in CD44 protein levels increase (Figure 3 B).

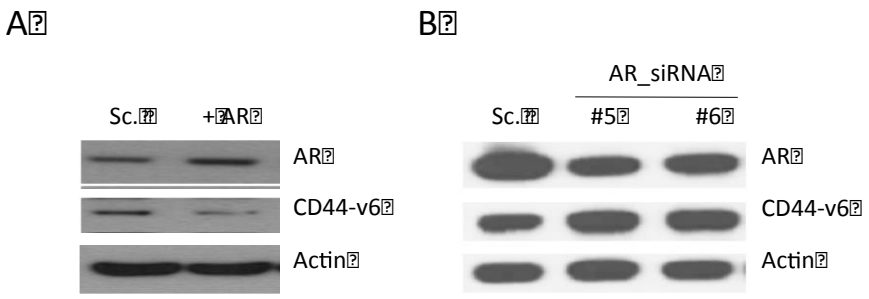

Figure 3. Overexpression and downregulation of androgen receptor in VCaP cells modulates CD44 expression. A. Western blot analyses of VCaP transiently transfected with empty vector (Sr.) or AR. Actin used as loading control. B. SiRNA knockdown of AR. SiRNA #5 and #6 are different siRNAs. (SC) Scrambled control. Actin used as loading control.

Task 2b: Assessment of the ability of human prostate cancer cells that possess cancer stem cell surface antigen expression to determine therapy resistance *in vitro*.

Sufficient body of evidence demonstrates that reactive oxygen species (ROS) are involved in regulation of drug-resistance-related proteins[1]. Therefore, we investigated whether there were any changes in the intracellular ROS levels in cells expressing CD44. We found that intracellular ROS levels in CD44+ cells that showed drug resistance were significantly reduced then in cells with low CD44 expression (Figure 4).

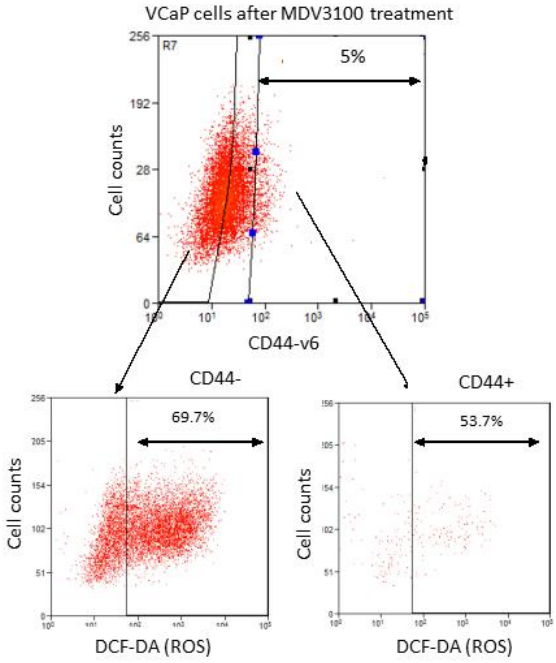

Figure 4. FACS analyses of cells after treatment with MDV3100 demonstrates lower ROS levels in drug resistant CD44 expressing VCaP cells. Only 5% of the cells demonstrate drug resistance. Intracellular

ROS levels, measured by DCF-DA expression, in cells following MDV3100 treatment is 69.7%. Intracellular ROS levels in drug resistant CD44+ cells is only 53.7%.

Task 3: Development of an in vivo model to assess human prostate cancer stem cell targeted therapy.
Due to technical challenges faced by our group and others in field, no substantial work was completed in this aim.

Key Research Accomplishments

Research accomplishments: description of an in vivo xenograft assay to assess prostate cancer progenitor/stem cell activity

Conclusion

From our work over the funded period we can conclude that treatment resistance in prostate cancer appears to enrich for CD44+ cells. Future work in this area may benefit from studying the regulation and mechanism of action of CD44 in this context.

Additionally, our work reinforces others' observations regarding the difficulty of cultivating primary human prostate cancer cells in a laboratory environment.

Over the past year, we can conclude that i) isolation of human prostate cancer stem cells from the primary tumor is not feasible due to low numbers of the potential stem cells and difficulties associated with culture of the isolated cells, ii) CD44 expression appears to be a marker of enzalutamide and docetaxel resistance in VCaP, C4-2 and LNCaP cells *in vitro*, iii) $CD44^{+}CD24^{-}$ LNCaP cells are highly aggressive (i.e. exhibit increased proliferation and migration *in vitro*), iv) CD44 and AR expression is inversely correlated in LNCaP cells, VCaP cells. The negative correlation remains true in clinical samples (i.e. circulating tumor cells from men with aggressive disease and in metastatic prostate tumor tissues).

Publications, Abstracts, and Presentations

Peer-reviewed publications:

Selective expression of CD44, a putative prostate cancer stem cell marker, in neuroendocrine tumor cells of human prostate cancer. **Palapattu GS**, Wu C, Silvers CR, Martin HB, Williams K, Salamone L, Bushnell T, Huang LS, Yang Q, Huang J. *Prostate*. 2009 May 15;69(7):787-98.

A novel in vitro assay of tumor-initiating cells in xenograft prostate tumors. Silvers CR, Williams K, Salamone L, Huang J, Jordan CT, Zhou H, **Palapattu GS**. *Prostate*. 2010 Sep 15;70(13):1379-87.

The PSA(-/lo) prostate cancer cell population harbors self-renewing long-term tumor-propagating cells that resist castration. Qin J, Liu X, Laffin B, Chen X, Choy G, Jeter CR, Calhoun-Davis T, Li H, **Palapattu GS**, Pang S, Lin K, Huang J, Ivanov I, Li W, Suraneni MV, Tang DG. *Cell Stem Cell*. 2012 May 4;10(5):556-69.

Inventions, Patents and Licenses

Nothing to report.

Reportable Outcomes

Nothing to report.

Other Achievements

By any measure, I would say my DoD PCRTF was highly successful. Because of this award,

1. I received an Astellas/AUA Foundation Rising Stars in Urology Award
2. I was offered/accepted a position at The Methodist Hospital/The Methodist Research Institute as Chief of Urologic Oncology with protected research time, ample lab space and generous start up package.
3. I was offered /accepted a position as Associate Professor (with tenure), Chief of Urologic Oncology at the University of Michigan
4. I was installed as the The George F. and Sandy G. Valassis Professor of Urology at the University of Michigan
5. I made critical scientific and professional collaborations that allowed my research work to flourish
6. I have been able to compete successfully for peer-reviewed funding. I am the PI on an NCI UO1 (prostate cancer health disparity), PI of an NCI T32, co-PI of DoD Prostate Cancer Health Disparity Award and co-PI of UM Prostate SPORE.

Training accomplishments:

- Attend prostate cancer research seminars bi-weekly
- Attend monthly prostate SPORE research meetings monthly
- Attend UM Cancer Center research seminars monthly
- Notably I am now the PI of a research training grant T32 from NCI

References

1. Seruga, Bostjan, Alberto Ocana, and Ian F. Tannock. "Drug resistance in metastatic castration-resistant prostate cancer." *Nature reviews Clinical oncology* 8.1 (2011): 12-23.

Appendix

None

Selective Expression of CD44, a Putative Prostate Cancer Stem Cell Marker, in Neuroendocrine Tumor Cells of Human Prostate Cancer

Ganesh S. Palapattu,[1,2,3] Chengyu Wu,[1] Christopher R. Silvers,[2] Heather B. Martin,[1] Karin Williams,[2] Linda Salamone,[2] Timothy Bushnell,[3] Li-Shan Huang,[4] Qi Yang,[1] and Jiaoti Huang[5]*

[1]*Department of Pathology, University of Rochester School of Medicine, Rochester, New York*
[2]*Department of Urology, University of Rochester School of Medicine, Rochester, New York*
[3]*Department of Oncology, University of Rochester School of Medicine, Rochester, New York*
[4]*Department of Biostatistics, University of Rochester School of Medicine, Rochester, New York*
[5]*Department of Pathology and Laboratory Medicine, David Geffen School of Medicine at UCLA, Los Angeles, California*

BACKGROUND. Hormonal therapy is effective for advanced prostate cancer (PC) but the disease often recurs and becomes hormone-refractory. It is hypothesized that a subpopulation of cancer cells, that is, cancer stem cells (CSCs), survives hormonal therapy and leads to tumor recurrence. CD44 expression was shown to identify tumor cells with CSC features. PC contains secretory type epithelial cells and a minor population of neuroendocrine cells. Neuroendocrine cells do not express androgen receptor and are quiescent, features associated with CSCs. The purpose of the study was to determine the expression of CD44 in human PC and its relationship to neuroendocrine tumor cells.

METHODS. Immunohistochemistry and immunofluorescence were performed to study CD44 expression in PC cell lines, single cells from fresh PC tissue and archival tissue sections of PC. We then determined if CD44 + cells represent neuroendocrine tumor cells.

RESULTS. In human PC cell lines, expression of CD44 is associated with cells of NE phenotype. In human PC tissues, NE tumor cells are virtually all positive for CD44 and CD44 + cells, excluding lymphocytes, are all NE tumor cells.

CONCLUSIONS. Selective expression of the stem cell-associated marker CD44 in NE tumor cells of PC, in combination with their other known features, further supports the significance of such cells in therapy resistance and tumor recurrence. *Prostate 69: 787–798, 2009.*

KEY WORDS: **prostate cancer; neuroendocrine cell; CD44; cancer stem cell**

INTRODUCTION

Prostate cancer (PC) is the most commonly diagnosed cancer and the second leading cause of cancer-related mortality [1]. Multiple options exist for the treatment of organ-confined PC. The primary treatment of choice for advanced/metastatic PC, however, is hormonal therapy [2], consisting of androgen ablation and/or inhibition of androgen action with anti-androgens. Although most patients initially respond to this therapy, the tumor commonly recurs and enters an

Grant sponsor: Department of Defense Prostate Cancer Research Program; Grant number: PC073121; Grant sponsor: AUA Foundation/Astellas Rising Stars in Urology Award; Grant sponsor: American Cancer Society; Grant number: RSG-07-092-01-TBE; Grant sponsor: Department of Defense Prostate Cancer Research Program; Grant number: PC061456

*Correspondence to: Jiaoti Huang, MD, PhD, Department of Pathology and Laboratory Medicine, David Geffen School of Medicine at UCLA, 10833 Le Conte Ave., A7-149 CHS, Los Angeles, CA 90095-1732.
E-mail: jiaotihuang@mednet.ucla.edu
Received 24 October 2008; Accepted 2 January 2009
DOI 10.1002/pros.20928
Published online 2 February 2009 in Wiley InterScience (www.interscience.wiley.com).

androgen-independent (hormone-refractory) stage for which no durable effective therapy is currently available.

Cancer cells within a given tumor were once considered homogeneous, a situation wherein each cell would have equal malignant potential. Data over the past decade, however, have challenged this hypothesis and established that a hierarchy often exists among tumor cells within a given cancer [3]. In vitro and in vivo assays in hematopoietic cancers as well as breast, brain and colon cancer have shown that only a minor subpopulation (typically 1–2%) of tumor cells possesses the ability to self-renew and recreate the entire tumor, inclusive of all cell types [4]. Such "tumor initiating" cells are termed cancer stem cells (CSCs) [5].

Unlike the bulk cancer cells, CSCs do not express differentiation markers and are typically quiescent. As a result, they may be resistant to traditional therapies that depend on continuous cell cycle activity, such as chemotherapy and radiation. The CSC model predicts that potential CSCs within PC are quiescent and do not express the luminal differentiation markers androgen receptor (AR) and prostate specific antigen (PSA) [6–8]. Therefore, these cells are likely androgen-independent and should survive androgen ablation therapy, leading to tumor recurrence [9]. To date, the critical experiment demonstrating the identification of prostate CSCs from primary human tissue with subsequent illustration that the proffered CSC is tumor-initiating in vivo has not been reported. Nonetheless, many groups have reported potential markers that may be associated with prostate CSCs, including the cell surface markers CD44, integrin α2β1, CD133, CXCR4 and breast cancer resistance protein (BCRP) [10–16] as well as cytokeratin 5/18 double positive intermediate cells [17,18] and the side population of cells [19].

In a comprehensive in vitro and in vivo study using cell lines and xenograft tumor models, Patrawala et al. [20] provided compelling evidence that CD44 expression is associated with stem/progenitor cells of PC. They found a general correlation between the proportion of CD44 + cells and tumorigenicity in PC cell lines, with the highly aggressive, androgen-independent PC3 cells and DU145 cells containing more CD44 + cells than the less aggressive, androgen-dependent LNCaP cells. CD44 + cells had higher clonogenicity and tumorigenicity and also expressed higher levels of stem cell-associated genes than CD44− cells. In addition, the authors noted that CD44 + cells did not express AR, while AR was exclusively detected in the CD44− cell population. Importantly, CD44 + , AR−, PC cells were capable of generating CD44−, AR + tumor cells in in vitro and in vivo assays [20]. These results have provided strong evidence that CD44 is associated with stem/progenitor cells in PC. Interestingly, in a landmark report, Leong et al. [21] showed that a single cell expressing CD44 as well as a few other stem cell markers can be used to generate mouse prostate. Expression of CD44, however, has not been studied in detail in human PC tissue. If CD44 expression is associated with human prostate CSCs, one might expect that CD44 + tumor cells would be scattered among the more abundant bulk tumor cells that possess features of luminal differentiation including expression of AR and PSA.

It is well established that PC is histologically heterogeneous. The majority of malignant cells are of the secretory type epithelial cells that express AR and secrete PSA. Notably, every case of PC also contains a minor population of cells that have neuron-like morphology and produce biogenic amines and neuropeptides. These cells have been termed neuroendocrine (NE) cells and they reside in the basal layer in benign prostate acini. We and others have characterized these NE cells in PC and shown that unlike the bulk secretory type tumor cells, the NE tumor cells are quiescent and do not express AR or PSA [22–24]. Several groups, including our own, have proposed that these NE cells may be resistant to hormonal therapy and therefore responsible for tumor recurrence following androgen ablation (reviewed in Refs. [25–27]). Here, we report our results showing that the putative CSC marker CD44 is selectively expressed in NE tumor cells of PC, further supporting the importance of such cells in therapy resistance and tumor recurrence and raising interesting questions about the relationship of the NE tumor cells to the elusive PC stem cell.

MATERIALS AND METHODS

Established Cell Lines

PC-3 (CRL-1435), DU145 (HTB-81), and LNCaP (CRL-1740) cells were obtained from American Type Culture Collection (ATCC; Manassas, VA). All cell lines were routinely maintained in RPMI 1640 (Invitrogen Corp., Carlsbad, CA) containing Penicillin-Streptomycin (Invitrogen Corp.) and 10% fetal bovine serum (FBS; Atlanta Biologicals, Atlanta, GA).

Fresh Human Surgical Samples

Fresh human prostate tissue was obtained from patients undergoing radical prostatectomy, in accordance with the protocol approved by the University of Rochester Research Subjects Review Board. Upon removal, fresh prostate tissue was cut into 1 mm cubes using sterile disposable scalpels. After washing in RPMI the tissue was incubated in a CO_2 tissue culture incubator overnight in 112 U/ml hyaluronidase (Sigma

H-3506) and 250 U/ml collagenase 1 (Worthington Biochemical MIE4816). The resultant single cell suspension was neutralized by repeated washing in RPMI/5% FBS followed by resuspension in FACS buffer (1% FBS in D-PBS [Invitrogen Corp.], 0.01% DNase, Sigma, St. Louis, MO). All samples were filtered through a 100 μm cell strainer prior to staining.

Tissue Microarray: Immunohistochemistry and Immunofluorescence

The prostate TMA was constructed as previously described [28]. Briefly, 73 prostatectomy specimens were reviewed and areas containing prostate adenocarcinoma were marked for sampling. Tumors ranged from Gleason patterns 2 to 5. Two to three cores per samples, measuring 0.6 mm in diameter, were obtained from selected regions in each donor paraffin block and transferred to a recipient paraffin block and the resulting block contained a total of 200 cores. A section was obtained from the TMA for H&E staining as quality control and unstained sections were used for immunohistochemical and immunofluorescence staining.

The procedure for immunohistochemical staining has been described in detail previously [28]. The TMA sections were stained with a mouse monoclonal antibody against chromogranin A (Chemicon International, Inc., Temecula, CA, Clone 2H10, used at 1:1,000), and a rat monoclonal antibody against CD44 (eBioscience, San Diego, CA., Clone IM7, used at 1:1,000). Paraffin embedded tissues were sectioned at 5 μm thickness and antigen retrieval was performed with pre-heated (95–99°C) Citrate Buffer, pH 6.1 (DakoCytomation, Carpinteria, CA) in a Black and Decker steamer (Shelton, CT, Model HS800) for 30 min. The sections were incubated with the primary antibodies at room temperature for 60 min (CD44) or 45 min (chromogranin A), followed by incubation for 30 min with the link antibody (rabbit or mouse) - labeled polymer-HRP (Envision Plus System, DakoCytomation). Slides were developed with AEC+ (DakoCytomation) and counterstained in Modified Mayers Hematoxylin.

For immunofluorescence staining of the TMA section, Antigen retrieval was performed as described above. Anti-CD44 (same source as above, used at 1:200), anti-CD45 (Dako North America, Inc., Carpinteria, CA; M0701, 1:100), and anti-chromogranin A (Dako; A0430, 1:1,000) antibodies were incubated with the TMA slide overnight at room temperature. The slide was then incubated with secondary antibodies (goat anti-rat IgG FITC [Invitrogen Corp.; 62-9511, 1:200], Alexa Fluor 546 goat anti-mouse [Invitrogen Corp.; A-11003, 1:200], and Alexa Fluor 633 $F(ab)_2$ fragment of goat anti-rabbit [Invitrogen Corp.; A-21072, 1:200]) for 40 min at room temperature. The slide was mounted with a coverslip using Vectashield HardSet Mounting Medium with DAPI (Vector; H-1500). Tissue cores were photographed individually with a Leica TCS SP Spectral Confocal microscope. Subsequently, the coverslip was removed and the TMA stained with H&E. The H&E-stained tissue cores were then photographed with a Leica DM5000 B microscope. Cancerous areas in each core were marked by a pathologist (JH) and the nuclei manually marked in each digital image and counted using the particle analysis feature of NIH ImageJ software (http://rsb.info.nih.gov/ij/). Marked cells in cancerous regions were examined for fluorescence in the corresponding confocal images, and the number of positive cells recorded.

Quantitative RT-PCR

Detailed method has been described previously [29]. Total RNA was isolated from cells with RNeasy® Kit (Qiagen) according to the manufacturers instructions. RNA was reverse transcribed by Transcriptor reverse transcriptase (Roche, Germany) with random hexamers (Promega). The following specific forward and reverse primers were used: for NSE, 5′-AGCTGC CCCTGCCTTAC-3′ and 5′-GAGACAAACAGCGTTA CTTAG-3′; for chromogranin A, 5′-GCGGTGGAAG AGCCATCAT-3′ and 5′-TCTGTGGCTTCACCACTT TTCTC-3′; for β-actin, 5′-GCGGGAAATCGTGCGT GACATT-3′ and 5′-GATGGAGTTGAAGGTAGTTTC GTG-3′.

Real time PCR was performed with iQ™ SYBR® Green Supermix in an iCycler iQ System (Bio-Rad) using the SYBR Green Detection protocol. Total reaction volume was 20 μl and a cycle consists of 95°C for 5 min, 95°C for 30 sec, 55°C for 30 sec, 72°C for 30 sec, for a total of 45 cycles followed by 72°C for 5 min.

Western Blotting

Detailed method has been described previously [29]. Briefly, cells were washed twice with cold PBS and lysed in RIPA lysis buffer for 30 min on ice. The cells were sheared twice through a 20 gauge needle and centrifuged at 14,000 rpm for 15 min at 4°C. The protein concentration in the supernatant was determined with the Bio-Rad Protein Assay kit. Equal amounts of protein were separated on 10% SDS–PAGE gels, transferred to nitrocellulose membrane with Semi-Dry Transfer Cell (Bio-Rad). The membrane was blocked with TBS containing 5% w/v nonfat dry milk, and hybridized with primary antibody in 2%w/v nonfat dry milk, followed by incubation with secondary antibody and detected with an ECL kit (BioRad).

Flow Cytometry

To minimize non-specific binding, single cells suspensions were treated with FC block before staining with PE-Cy5 labeled anti-human CD44 antibody for 20 min on ice. After washing with PBS containing 0.5% BSA, the cells were resuspended in the same solution and DAPI was added to a final concentration of 1 μg/ml. All flow-cytometry studies were performed using either a Becton Dickinson FACSAria or LSRII flow cytometer. For sorting experiments, the cells were maintained at 4°C during the sort, and an 85 μm nozzle was used. Cells were sorted into RPMI medium. Populations were analyzed post-sort to ensure purity of sorts before progressing with additional experiments. For cells that did not have a clear positive and negative distribution, the top 10% and bottom 10% of cells were sorted and designated as CD44 high and CD44 low.

Cytospin: Immunofluorescence Analysis

Cytospin preparations of PC cells were fixed in methanol for 10 min at −20°C, rehydrated in PBS (Sigma-Aldrich Corp., St. Louis, MO; D5773), and blocked in 5% normal goat serum (Rockland Immunochemicals, Inc., Gilbertsville, PA; B304) for 30 min. The slides were incubated with antibodies against CD44 (as above, used at 1:200) and neuron-specific enolase (NSE; Dako North America, Inc.; M0873, 1:50) overnight at 4°C followed by incubation with secondary antibodies (goat anti-rat IgG FITC and Alexa Fluor 546 goat anti-mouse, as described above) for 40 min at room temperature. For cell lines, the slides were mounted with coverslips using Vectashield HardSet Mounting Medium with DAPI. For cells derived from fresh prostatecomy specimens, the slides were stained with Hoechst 33258 (Sigma-Aldrich Corp.; 861405) for 10 min prior to coversliping. Fluorescence micrographs were obtained with a Leica DM5000 B microscope. Cellular co-expression of CD44 and NSE was quantified in fluorescence micrographs of PC3 and DU145 cytospin preparations. Total cell number was derived by counting nuclei in the DAPI images using the particle analysis feature of NIH ImageJ software (http://rsb.info.nih.gov/ij/). Cell masks were generated in ImageJ using a composite of the CD44 and NSE fluorescence signals; the masks were used to derive the mean pixel value of each fluorescence signal within individual cells.

Statistical Analysis

The analysis included calculation of the Pearson correlations and non-parametric Spearmans correlations between CD44 and NSE levels. Linear regression analysis was also implemented with an assessment of residuals as a check on the assumptions of normally distributed errors with constant variance. If the assumptions seemed to be violated, log-transformed values were used to produce more normally distributed residuals. Statistical outliers were defined as the standardized residuals values >3 or ≤ 3. Then the models were rerun without the outliers and the results with and without outliers were compared.

RESULTS

Expression of CD44 and NE markers in Human PC Cell Lines

Flow cytometric studies demonstrated that among the three well-characterized PC cell lines (LNCaP, DU145, and PC-3), PC3 cells were nearly 100% positive for CD44 expression, and ~60% of DU145 cells were positive for CD44. LNCaP cells were nearly entirely negative for CD44 (Fig. 1A). These results are consistent with the findings reported by Patrawala et al. [20] We then studied if CD44 expression correlates with NE phenotype in these cell lines. The most commonly used NE markers include chromogranin A and NSE [25]. As shown in Figure 1B,C, the largely CD44− LNCaP cell line did not express NE markers, while NE marker mRNA was detected, in varying degrees, in the CD44+ DU145 cells and PC3 cells. The observed expression pattern of chromogranin A and NSE mRNAs paralleled that of CD44 expression among the three cell lines (i.e., PC3 had the highest CD44 content and the highest NE marker mRNA concentration).

To further characterize the association of CD44 expression with NE markers, we used fluorescence activated cell sorting (FACS) to sort LNCaP, PC3 and DU145 cells into CD44 high and CD44 low expressing subpopulations. As shown in Figure 2A,B, within each cell line studied, NE marker expression was enriched in the CD44 high population versus unsorted and CD44 low cells. This finding was confirmed with Western blot analysis as depicted in Figure 2C.

We next examined the expression of CD44 and the NE marker NSE in the three cell lines by immunofluorescence after the cells were spun onto glass slides by the cytospin technique. The advantage of this technique is that the expression of multiple proteins can be simultaneously studied in the same cells. As shown in Figure 3A, LNCaP cells were essentially negative for both CD44 and NSE and PC3 cells were nearly all positive for both CD44 and NSE. DU145 cells displayed a wide range of staining, from totally negative to brightly positive for both CD44 and NSE. In general, CD44 negative DU145 cells were negative for NSE while CD44 positive DU145 cells were positive for NSE.

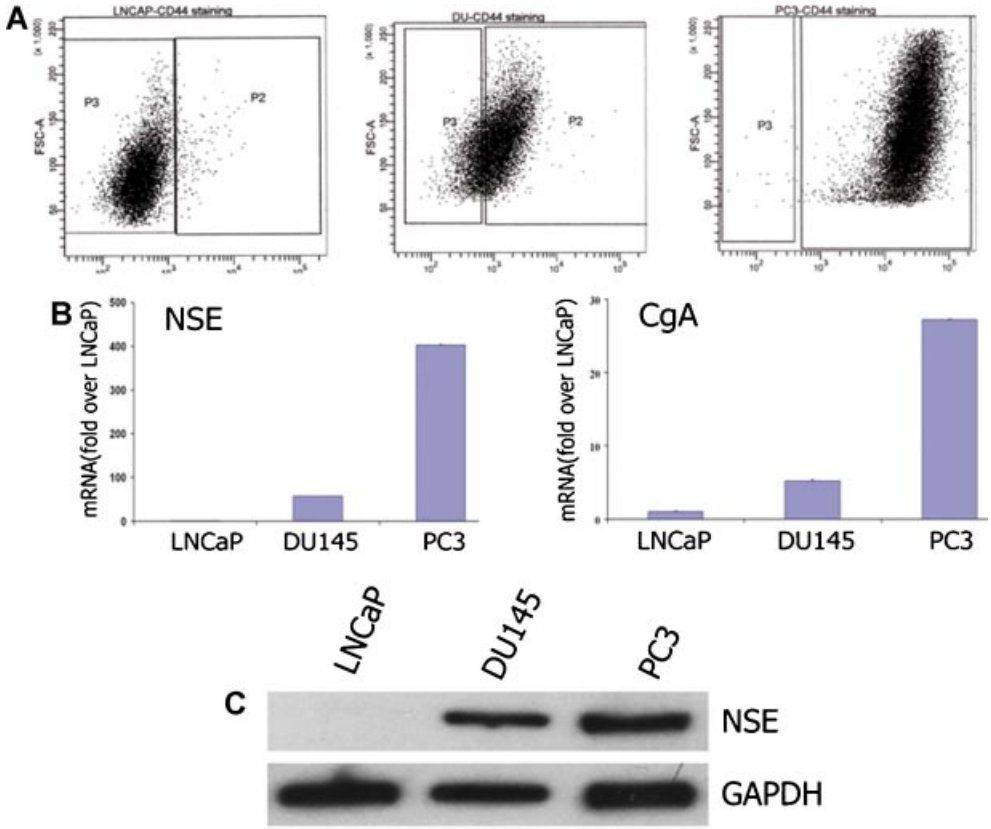

Fig. 1. Expression of CD44 and NE cell marker in human prostate cancer cell lines. **A**: Flow cytometry examining CD44 expression in LNCaP, DUI45, and PC3 cells. LNCaP cells are mostly negative for CD44. Approximately 60% of DUI45 cells are positive for CD44 while PC3 cells are mostly positive for CD44. **B**: RT-PCR analysis of the mRNA levels of NE cell markers in PC cell lines. Expression of NE cell markers neuron specific enolase (NSE) and chromogranin A (CgA) mirrored CD44 expression with LNCaP cells expressing lowest levels while PC3 cells expressed higher levels. **C**: Western blot analysis of the protein levels of NSE in PC cell lines. Similarly, NSE protein was undetectable in LNCaP cells and highest in PC3 cells. [Color figure can be viewed in the online issue, which is available at www.interscience.wiley.com.]

Statistical analysis was performed to study the correlation between CD44 and NSE expression after the image intensity of individual cells was captured, as described in Materials and Methods Section. The correlations between CD44 and NSE were 0.6901 in DU145 cells and 0.6518 in PC3 cells. The correlations based on log-transformed values were similar, 0.6860 and 0.6585 respectively. The non-parametric Spearman correlation was similar for DU145 cells (0.6764), and higher for PC3 cells (0.7516). The linear model for DU145 cells with CD44 as the predictor and NSE as the response had an R^2 of 0.4763, and for PC3 cells the R^2 was 0.4249. Both models were highly significant ($P < 0.0001$). The models identified 3 and 4 outliers for DU145 and PC3 cells respectively. After removing the outliers, the R^2 increased to 0.4944 and 0.5019, respectively. The residual plots showed that the assumption of normal error distribution was satisfactory. Nevertheless, the linear models for log-transformed values were explored and their R^2 values were similar to those without transformation, 0.4705 and 0.4336 respectively. Figure 3B shows the linear fits based on raw values (without log transformation). These data indicate that on cytospin examination, there is a strong correlation between the expression of CD44 and NSE, suggesting that CD44 expression is associated with NE phenotype in such cells.

Expression of CD44 and NE Markers in Primary Fresh Human PC Cells

To further establish the relationship between CD44 expression and NE markers in PC, we obtained fresh PC tissue from seven prostatectomy specimens immediately upon removal of the prostate. Single cell suspensions were obtained and flow-sorted into CD44 high and CD44 low cells. The small number of cells derived from the surgical specimens allowed only quantitative real-time PCR analysis. In every case, the levels of NE markers were much higher in the CD44 high cells than those in the CD44 low cells and the difference was statistically different in each case (Fig. 4A,B).

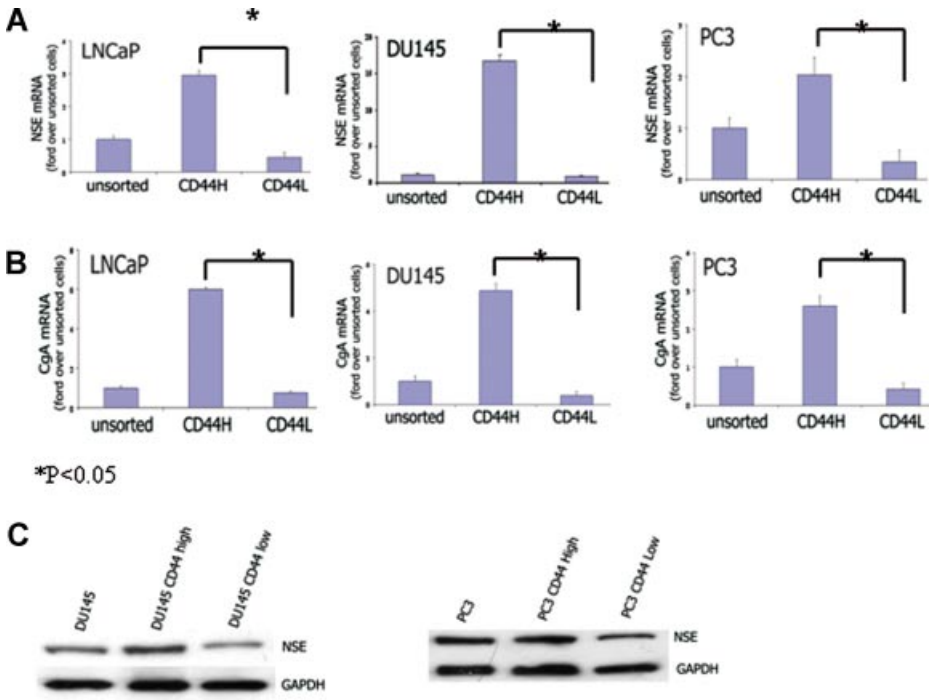

Fig. 2. Expression of NE markers in CD44 high and CD44 low fractions of human prostate cancer cell lines. RT-PCR for mRNA levels of NSE (**A**) and CgA (**B**) revealed enrichment for NE marker expression in CD44 high (CD44H) populations versus CD44 low (CD44L) and unsorted populations. This finding was confirmed at the protein level by Western blot for NSE (**C**). The low level of CD44 expression within LNCaP cells precluded accurate sorting and adequate protein extraction from CD44 + LNCaP cells for protein analysis. [Color figure can be viewed in the online issue, which is available at www.interscience.wiley.com.]

The single cell suspensions from fresh PC tissue were also spun onto slides by cytospin method and double-stained by immunofluorescence for the expression of CD44 and chromogranin A. As predicted, very few cells were NE cells. Similarly, in these single cell suspensions, CD44 expression was limited to NE tumor cells (Fig. 4C).

Expression of CD44 in Benign and Malignant ProstateTissue

We then performed immunohistochemistry to study the expression of CD44 in archival, formalin-fixed and paraffin-embedded sections of human PC. Positive staining was defined as strong membrane staining, consistent with CD44 being a cell surface protein. In benign prostate tissue, all basal cells expressed CD44, consistent with previous reports [30–32] (Fig. 5A). Lymphocytes and nerves were also positive for CD44 (Fig. 5B,C). PC is characterized by the absence of basal cells and the proliferation of luminal type malignant epithelial cells. Although the majority of cancer cells were negative for CD44, there were scattered individual cells or small nests of cells that displayed CD44 expression with a distinct membranous staining pattern. The distribution of the CD44 + cells was reminiscent of NE tumor cells of PC (Fig. 5D).

Co-Expression of CD44 and Chromogranin A in Human PC Tissue

We next performed experiments to confirm that CD44 + cells in PC tissues are in fact NE cells. We prepared adjacent sections of human PC tissue (5 μm apart) which contained virtually identical tumor cells. The first section was stained with an anti-CD44 antibody and the second section stained with an anti-chromogranin A antibody to highlight NE cells. Chromogranin A positive NE cells displayed cytoplasmic staining and were scattered among the more abundant cancerous epithelial cells. In the adjacent section, CD44 + cells demonstrated a membrane staining pattern and similarly appeared as single cells and small nests of cells surrounded by more abundant CD44− cells. When the same microscopic fields from the two adjacent sections were compared, cells that were positive for CD44 were also noted to be positive for chromogranin A and vice versa (for illustration, an area with abundant NE cells are shown in Fig. 6A).

In order to definitively prove the relationship of CD44 expression with NE cells in PC, we employed an immunofluorescence method so that multiple antibodies could be used to stain the same tumor cells. Our pilot studies indicated that NE cells within tumors were all positive for CD44 but CD44 positive cells were

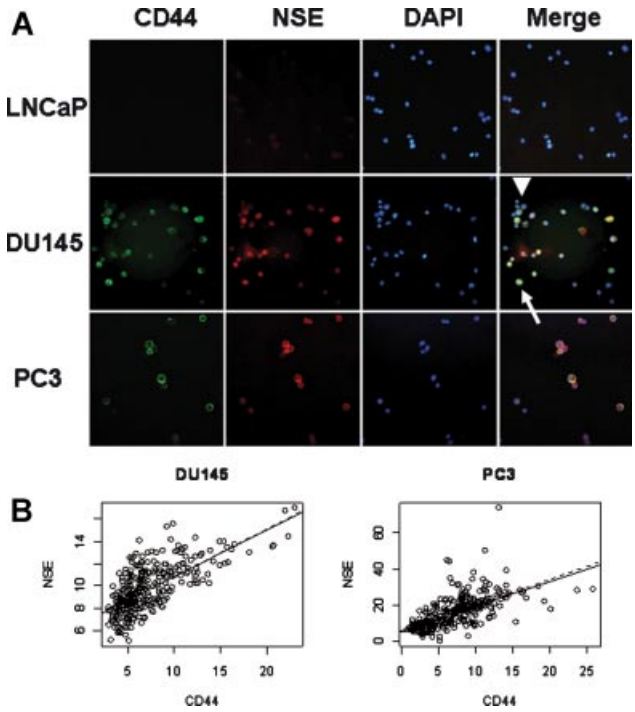

Fig. 3. Co-expression of NSE and CD44 in human prostate cancer cell lines. **A**: Immunofluorescence studies on cytospin samples with antibodies against CD44, NSE (with DAPI staining nuclei) show co-expression of CD44 and NSE in the same cells. LNCaP cells are double negative for the two markers and PC3 cells are double positive. The majority of DUI45 cells are double positive (arrow) but a minority are double negative (arrowhead) (magnification 400×). **B**: Linear fits of CD44 and NSE for DUI45 and PC3 cells. The linear model with CD44 as the predictor and NSE as the response for DUI45 cells yields an R^2 of 0.4763 and for PC3 cells 0.4249. Both models are highly significant ($P < 0.0001$). The dash line is the fit with outliers and the solid line without outliers. These data indicate that on cytospin examination, CD44 and NSE expressions were closely associated with each other in individual cells. [Color figure can be viewed in the online issue, which is available at www.interscience.wiley.com.]

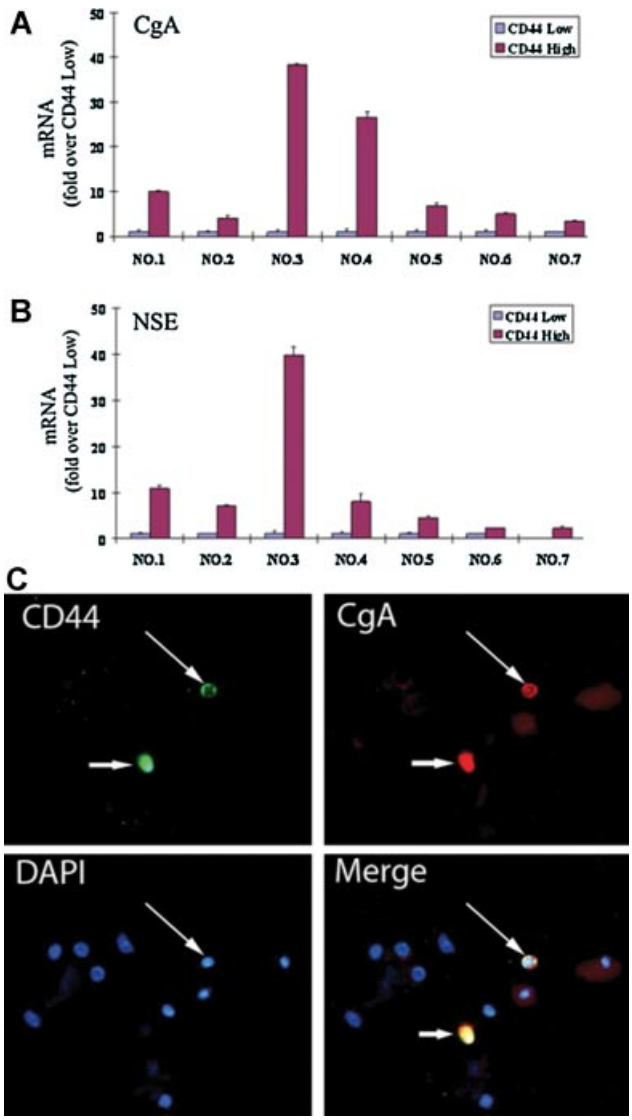

Fig. 4. Association of CD44 expression with NE cells in fresh primary human prostate cancer cells. **A**: Quantitative RT-PCR analysis performed on sorted single cell suspensions obtained from seven cases of fresh radical prostatectomy specimens revealed that NE markers CgA and NSE expression was significantly higher in the CD44 high versus the CD44 low population. **B**: Single cell suspension obtained from a case of fresh radical prostatectomy specimen was co-stained by immunofluorescence for the expression of CD44 and CgA (nuclei stained by Hoechst 33258). A single NE cell is the only CD44 + cell (long arrow). The other bright spot (short arrow) in the field is a contaminant as it is not associated with a nucleus (magnification 400×). [Color figure can be viewed in the online issue, which is available at www.interscience.wiley.com.]

composed of NE tumor cells and lymphocytes that commonly infiltrate PC. Therefore, we co-stained a section of a tissue microarray that contained 200 cores of PC tissue from 73 different radical prostatectomy cases for the expression of CD44, chromogranin A and CD45 (a marker of leukocytes including lymphocytes). The areas of cancer in each core were marked and the number of nuclei (stained by DAPI, including cancer cells + lymphocytes) in cancerous areas of each core counted manually, which ranged from 40 to 1,755 per core with a total of 61,070 cells surveyed in aggregate. Among them, 147 cells were positive for chromogranin A (NE cells) comprising 0.2% of all nuclei. Of these, 132 (89.8%) were CD44 +. Lymphocytes (CD45 +) comprised 0.8% (516 cells) of all nuclei (Table I). Approximately 10% (15 cells) of NE cells were negative for both CD44 and CD45. Among the 648 CD44 + cells counted, 132 (20.4%) were positive for chromogranin A, 516 (79.6%) were positive for CD45 and 2 (0.3%) were positive for both chromogranin A and CD45 (faint) (Table I). Of the 61,070 cells reviewed, 2 were faintly triple positive for CD44, CD45 and CgA. These two cells were not included in the above analysis. Therefore, with

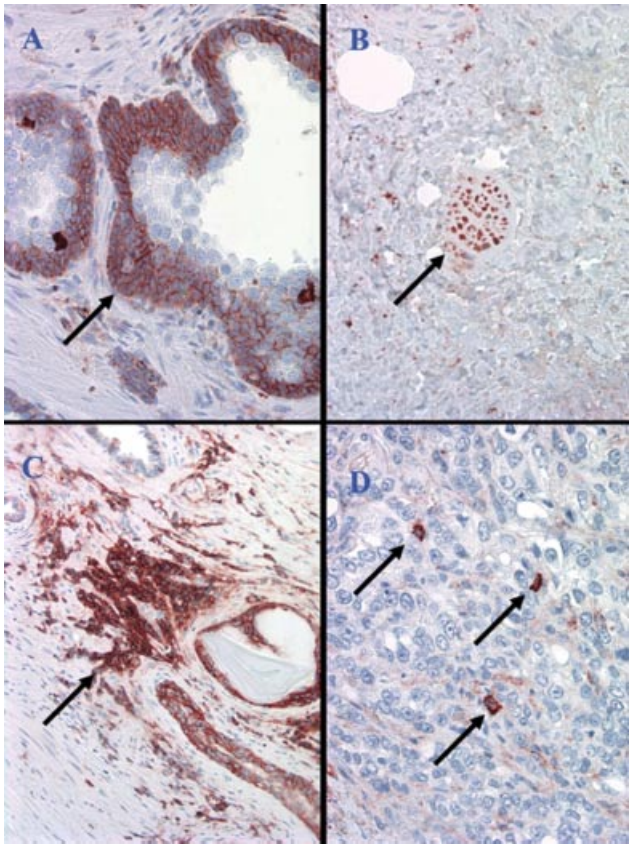

Fig. 5. Immunohistochemical study of the expression of CD44 in benign prostate and prostate cancer. In benign prostate, expression of CD44 is seen in (**A**) basal cells (arrow); (**B**) nerve (arrow); (**C**) lymphocytes (arrow). In prostate cancer (**D**), expression of CD44 is seen in scattered tumor cells, reminiscent of the distribution of neuroendocrine tumor cells (magnification 400×). [Color figure can be viewed in the online issue, which is available at www.interscience.wiley.com.]

few exceptions, NE tumor cells were CD44 + cells; and CD44 + cells, minus a population of lymphocytes, were all NE tumor cells (Fig. 6B). A representative area of PC with lymphocytes (CD45 + /CD44 + /CgA−) and an NE cell (CgA + CD44 + /CD45−) is shown in Figure 6C.

DISCUSSION

The mechanisms by which PC cells proliferate in an androgen-deprived environment remain unclear. Current hypotheses focus largely on altered AR signaling in tumor cells, including amplification of the AR gene, increased AR protein stability, AR hypersensitivity to low levels of androgen, AR mutation and activation of mutant AR by non-traditional ligands (reviewed by Scher and Sawyers [33]). An alternate theory that has gained significant attention recently involves CSCs. The hierarchical CSC model predicts that the putative PC stem cell, unlike the bulk tumor cells, is AR negative and androgen-independent. As a result, PC stem cells may be resistant to hormone ablation and responsible for tumor recurrence. Although many different markers have been reported to identify CSCs in PC [10–16,34–36], the comprehensive study by Patrawala et al. [20] as well as those by others, have provided convincing evidence that the CD44 + subpopulation of cells may demarcate the PC stem/progenitor cells.

PCs are composed mostly of secretory type epithelial tumor cells with a small population of morphologically and functionally distinct NE cells. NE cells are increased in high grade and high stage tumors, particularly in hormonally treated and hormone-refractory tumors [25]. The levels of circulating chromogranin A, a product of the NE cells, are increased in men with PC in comparison to patients with benign conditions. Furthermore, serum chromogranin A levels correlate with the stage of disease and is an independent prognostic factor in men with hormone-refractory disease [25]. An important feature of NE cells is that they do not express AR [22–24]. Thus, they may be resistant to androgen ablation and contribute to tumor recurrence after hormonal therapy. Animal studies using xenograft and genetic PC models support this view. Huss et al. reported that in the CWR22 human PC xenograft model, castration induces tumor regression followed by recurrence (androgen-independent tumor outgrowth). Notably, these investigators observed an increase in the number and proliferative activity of tumor NE cells after castration, suggesting that NE cells may promote tumor survival and resurgence [37]. Genetic animal models of PC also contain NE cells varying from very low in Pten−/− tumors [38] to high in tumors of TRAMP [39] and Rb-p53-mice [40]. Similarly, recurrent tumors in Pten−/− tumors after castration have been shown to be composed of significantly more NE cells than pre-castrate primary tumors [38].

In the current study, we have for the first time demonstrated unequivocally that NE cells are the only CD44 + tumor cells (i.e., non-lymphocyte/CD45−) in human PC tissue. In addition, we have ascertained an association of CD44 expression with cells expressing NE markers in three well-established human PC cell lines. Patrawala et al. [20] have shown that the AR− DU145 and PC3 cell lines, but not the AR + LNCaP cell line, express CD44. Leiblich et al. [41] found that NE markers are expressed in DU145 and PC3 cells, but not in LNCaP cells. Our results are consistent with these reports and indicate that in human PC cell lines, expression of the stem/progenitor cell marker CD44 is associated with cells with NE features. Furthermore, we confirmed the expression of NE markers from CD44 + cells in single cell suspensions obtained from fresh human surgical samples and human PC tissues at both the RNA and protein levels.

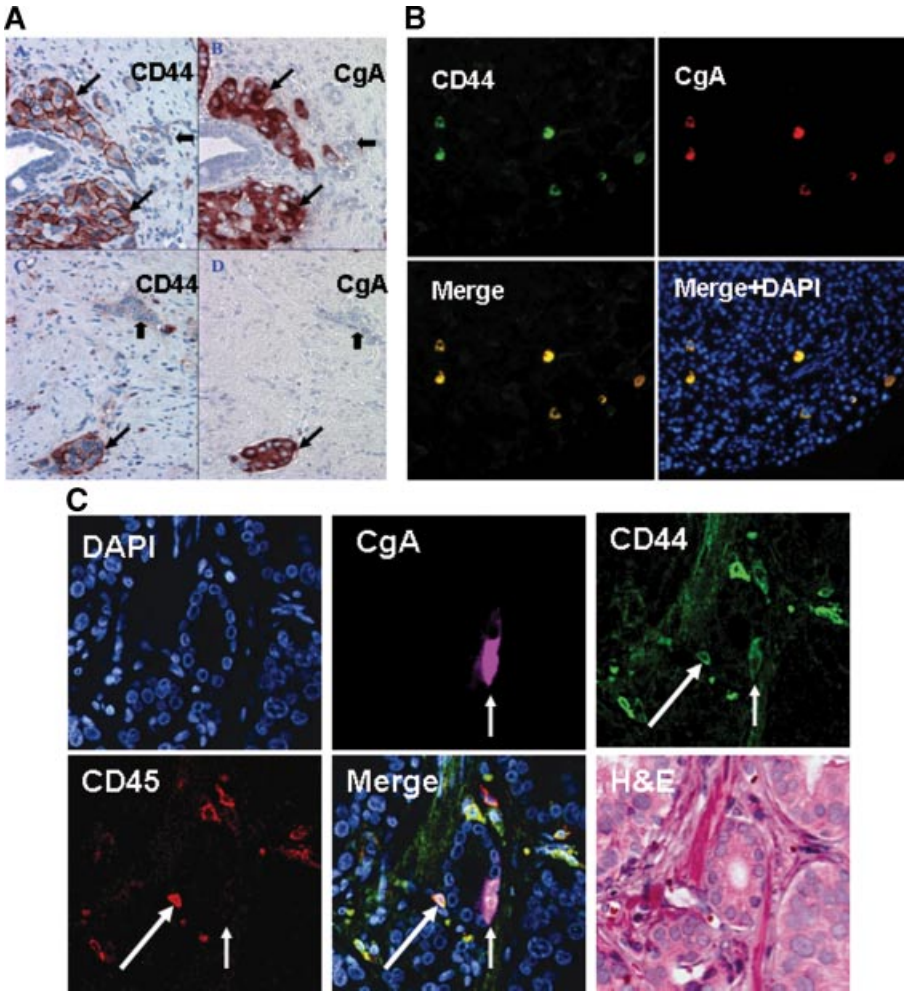

Fig. 6. Expression of CD44 is limited to NE tumor cells in human prostate cancer tissues. **A**: Immunohistochemical study of adjacent sections of a PC TMA for the expression of CD44 and CgA to show that NE tumor cells are CD44+ (long arrow) while non-NE tumor cells are CD44− (short arrow). **B**: A PC TMA slide was co-stained for the expression of CD44, CD45 and CgA by immunofluorescence study. In this field, there are no lymphocytes and all CD44+ cells are NE tumor cells (CgA+). **C**: In a different field, there is a single NE cell (CgA+) that is CD44+ and CD45− (short arrow). The other CD44+ cells are lymphocytes (CgA−, CD45+, long arrow) (magnification 400×). [Color figure can be viewed in the online issue, which is available at www.interscience.wiley.com.]

Using immunohistochemical and immunofluorescence studies of archival PC tissue in a tissue microarray, we showed that, excluding infiltrating lymphocytes (CD44 and CD45 double positive cells), expression of CD44, a putative CSC marker, is confined to NE tumor cells, an important observation that strengthens the hypothesis that NE cells within prostate tumors, being AR/PSA negative and normally quiescent [24,42], are possibly the therapy resistant cells responsible for tumor recurrence. These results are consistent with our recent finding that small cell carcinoma of the prostate, a tumor that is composed of pure malignant NE cells, consistently expresses CD44 [43].

TABLE I. Expression of CD44, CgA, and CD45 in Cancer Areas of Human PC TMA (Total Nucleated Cells = 61,070)

	CgA+ (NE cells) (n = 147)	CD44+ (NE cells + lymphocytes) (n = 648)	CD45+ (lymphocytes) (n = 516)
CgA− (n = 60,923)	—	516 (79.6%)	516 (100%)
CD44− (n = 60,407)	15 (10.2%)	—	0 (0%)
CD45− (n = 60,554)	147 (100%)	132 (20.4%)	—

A recent publication shows that p53 inhibits expression of the CD44 to allow an untransformed cell to respond to stress-induced, p53-dependent cytostatic and apoptotic signals. In the absence of p53 function, the resulting CD44 expression is essential for the growth and tumor-initiating ability of highly tumorigenic mammary epithelial cells [44]. Significant expression of CD44 in NE tumor cells of PC suggests that these cells may be highly tumorigenic, as has been proposed for CSCs, challenging the concept that NE tumor cells are terminally differentiated, post-mitotic and play no role in cancer progression. This hypothesis is also consistent with the observation by Patrawala et al. [20] that the CD44 +, AR− PC cells can give rise to CD44−, AR + cells.

The reverse analysis showed that approximately 90% of the NE cells express CD44 while the remaining 10% were CD44−. Although this suggests the possibility of heterogeneity within the NE population, we cannot rule out false negative CD44 staining in some NE cells due to a sample bias based upon technical issues. For example, tumor cells in tissue section may not have been uniformly sectioned and hence focal membrane staining for CD44 may be missed in rare cells.

The origin of NE cells in the prostate remains controversial. NE cells are present in benign prostate as well as all stages of prostatic carcinogenesis, from PIN [45] to invasive carcinoma to metastatic PC [46,47]. It has been proposed that they may be derived from the same stem cell or pluripotent cell that gives rise to luminal secretory cells [48,49]. A population of proliferating/transit amplifying intermediate cells has been identified and postulated to be a common precursor for NE cells and other epithelial cells of the benign prostate [50,51]. The same has been assumed for the NE cells in PC which are considered to share the same stem/precursor cells with the secretory type cancer cells; although no definitive experimental evidence has been reported. Alternatively, some investigators favor the trans-differentiation model of NE cell origin, which suggests that the tumor NE cells are derived from the non-NE secretory-type tumor cells. For example, in in vitro assays, LNCaP cells, an androgen-dependent cell line, can be induced to show NE-like phenotype by androgen deprivation [52] or agents that increase intracellular levels of cAMP [53]. Our results, in combination with recent publications, would suggest an entirely different view, that is, at least in cancer, NE cells may themselves represent the stem/progenitor cells for the bulk differentiated, secretory type cancer cells. This may have profound implications on the treatment of PC as it suggests that only therapies that target NE cells, in combination with hormonal therapy that target the bulk tumor cells, would have the potential of curing men with lethal PC.

The CSC concept may have different meanings in different contexts. As summarized by Jordan et al. [5] CSCs can (i) be the source of all tumor cells in a primary tumor, (ii) comprise the small reservoir of therapy-resistant cells that are responsible for tumor recurrence after therapy-induced remission, and/or (iii) give rise to metastatic tumors. Because of the difficulty associated with purifying NE cells from fresh human PC tissue, functional studies on NE cells have not been reported. However, current evidence suggests that they may represent the hormonal therapy-resistant cells that are responsible for tumor recurrence; thus fulfilling a functional definition of a CSC. Based upon the present study, further functional and mechanistic studies are warranted to establish the role of NE cells as the putative PC stem cell.

CONCLUSION

We have provided strong evidence that CD44, a marker that has been shown to be associated with increased tumorigenic potential in PC cell line and xenograft tumors, is expressed selectively in NE cells of human PC. This finding, in combination with the fact that such tumor cells do not express AR and are likely androgen-independent, further suggest their potential roles in tumor recurrence after hormonal therapy.

ACKNOWLEDGMENTS

G.S. Palapattu was supported by Department of Defense Prostate Cancer Research Program (PC073121) and AUA Foundation/Astellas Rising Stars in Urology Award. J. Huang was supported by grants from American Cancer Society (RSG-07-092-01-TBE) and Department of Defense Prostate Cancer Research Program (PC061456).

REFERENCES

1. Cooperberg MR, Park S, Carroll PR. Prostate cancer 2004: Insights from national disease registries. Oncology (Williston Park) 2004;18(10):1239–1247; discussion 1248–1250, 1256–1238.
2. Hussain A, Dawson N. Management of advanced/metastatic prostate cancer: 2000 update. Oncology (Williston Park) 2000; 14(12):1677–1688; discussion 1688, 1691–1674.
3. Wicha MS, Liu S, Dontu G. Cancer stem cells: An old idea—A paradigm shift. Cancer Res 2006;66(4):1883–1890; discussion 1895–1886.
4. Tan BT, Park CY, Ailles LE, Weissman IL. The cancer stem cell hypothesis: A work in progress. Lab Invest 2006;86(12): 1203–1207.
5. Jordan CT, Guzman ML, Noble M. Cancer stem cells. N Engl J Med 2006;355(12):1253–1261.
6. Nikitin AY, Matoso A, Roy-Burman P. Prostate stem cells and cancer. Histol Histopathol 2007;22(9):1043–1049.
7. Tang DG, Patrawala L, Calhoun T, Bhatia B, Choy G, Schneider-Broussard R, Jeter C. Prostate cancer stem/progenitor cells:

Identification, characterization, and implications. Mol Carcinog 2007;46(1):1–14.

8. Lawson DA, Witte ON. Stem cells in prostate cancer initiation and progression. J Clin Invest 2007;117(8):2044–2050.
9. Kasper S. Exploring the origins of the normal prostate and prostate cancer stem cell. Stem Cell Rev 2008;4(3):193–201.
10. Collins AT, Berry PA, Hyde C, Stower MJ, Maitland NJ. Prospective identification of tumorigenic prostate cancer stem cells. Cancer Res 2005;65(23):10946–10951.
11. Burger PE, Xiong X, Coetzee S, Salm SN, Moscatelli D, Goto K, Wilson EL. Sca-1 expression identifies stem cells in the proximal region of prostatic ducts with high capacity to reconstitute prostatic tissue. Proc Natl Acad Sci USA 2005;102(20): 7180–7185.
12. Gu G, Yuan J, Wills M, Kasper S. Prostate cancer cells with stem cell characteristics reconstitute the original human tumor in vivo. Cancer Res 2007;67(10):4807–4815.
13. Miki J, Furusato B, Li H, Gu Y, Takahashi H, Egawa S, Sesterhenn IA, McLeod DG, Srivastava S, Rhim JS. Identification of putative stem cell markers, CD133 and CXCR4, in hTERT-immortalized primary nonmalignant and malignant tumor-derived human prostate epithelial cell lines and in prostate cancer specimens. Cancer Res 2007;67(7):3153–3161.
14. Collins AT, Habib FK, Maitland NJ, Neal DE. Identification and isolation of human prostate epithelial stem cells based on alpha(2)beta(1)-integrin expression. J Cell Sci 2001;114(Pt21): 3865–3872.
15. Xin L, Lawson DA, Witte ON. The Sca-1 cell surface marker enriches for a prostate-regenerating cell subpopulation that can initiate prostate tumorigenesis. Proc Natl Acad Sci USA 2005; 102(19):6942–6947.
16. Huss WJ, Gray DR, Greenberg NM, Mohler JL, Smith GJ. Breast cancer resistance protein-mediated efflux of androgen in putative benign and malignant prostate stem cells. Cancer Res 2005; 65(15):6640–6650.
17. Tran CP, Lin C, Yamashiro J, Reiter RE. Prostate stem cell antigen is a marker of late intermediate prostate epithelial cells. Mol Cancer Res 2002;1(2):113–121.
18. Garraway LA, Lin D, Signoretti S, Waltregny D, Dilks J, Bhattacharya N, Loda M. Intermediate basal cells of the prostate: In vitro and in vivo characterization. Prostate 2003;55(3):206–218.
19. Bhatt RI, Brown MD, Hart CA, Gilmore P, Ramani VA, George NJ, Clarke NW. Novel method for the isolation and characterisation of the putative prostatic stem cell. Cytometry A 2003;54(2):89–99.
20. Patrawala L, Calhoun T, Schneider-Broussard R, Li H, Bhatia B, Tang S, Reilly JG, Chandra D, Zhou J, Claypool K, Coghlan L, Tang DG. Highly purified CD44 + prostate cancer cells from xenograft human tumors are enriched in tumorigenic and metastatic progenitor cells. Oncogene 2006;25(12):1696–1708.
21. Leong KG, Wang BE, Johnson L, Gao WQ. Generation of a prostate from a single adult stem cell. Nature 2008;456(7223):804–808.
22. Bonkhoff H, Stein U, Remberger K. Androgen receptor status in endocrine-paracrine cell types of the normal, hyperplastic, and neoplastic human prostate. Virchows Arch A Pathol Anat Histopathol 1993;423(4):291–294.
23. Krijnen JL, Janssen PJ, Ruizeveld de Winter JA, van Krimpen H, Schroder FH, van der Kwast TH. Do neuroendocrine cells in human prostate cancer express androgen receptor? Histochemistry 1993;100(5):393–398.
24. Huang J, Yao JL, di Santagnese PA, Yang Q, Bourne PA, Na Y. Immunohistochemical characterization of neuroendocrine cells in prostate cancer. Prostate 2006;66(13):1399–1406.
25. Huang J, Wu C, di SantAgnese PA, Yao JL, Cheng L, Na Y. Function and molecular mechanisms of neuroendocrine cells in prostate cancer. Anal Quant Cytol Histol 2007;29(3):128–138.
26. Yuan TC, Veeramani S, Lin MF. Neuroendocrine-like prostate cancer cells: Neuroendocrine transdifferentiation of prostate adenocarcinoma cells. Endocr Relat Cancer 2007;14(3):531–547.
27. Amorino GP, Parsons SJ. Neuroendocrine cells in prostate cancer. Crit Rev Eukaryot Gene Expr 2004;14(4):287–300.
28. Huang J, Yao JL, Zhang L, Bourne PA, Quinn AM, di SantAgnese PA, Reeder JE. Differential expression of interleukin-8 and its receptors in the neuroendocrine and non-neuroendocrine compartments of prostate cancer. Am J Pathol 2005;166(6):1807–1815.
29. Wu C, Huang J. Phosphatidylinositol 3-kinase-AKT-mammalian target of rapamycin pathway is essential for neuroendocrine differentiation of prostate cancer. J Biol Chem 2007;282(6): 3571–3583.
30. Alam TN, OHare MJ, Laczko I, Freeman A, Al-Beidh F, Masters JR, Hudson DL. Differential expression of CD44 during human prostate epithelial cell differentiation. J Histochem Cytochem 2004;52(8):1083–1090.
31. Paradis V, Eschwege P, Loric S, Dumas F, Ba N, Benoit G, Jardin A, Bedossa P. De novo expression of CD44 in prostate carcinoma is correlated with systemic dissemination of prostate cancer. J Clin Pathol 1998;51(11):798–802.
32. Kallakury BV, Yang F, Figge J, Smith KE, Kausik SJ, Tacy NJ, Fisher HA, Kaufman R, Figge H, Ross JS. Decreased levels of CD44 protein and mRNA in prostate carcinoma. Correlation with tumor grade and ploidy. Cancer 1996;78(7):1461–1469.
33. Scher HI, Sawyers CL. Biology of progressive, castration-resistant prostate cancer: Directed therapies targeting the androgen-receptor signaling axis. J Clin Oncol 2005;23(32):8253–8261.
34. Litvinov IV, De Marzo AM, Isaacs JT. Is the Achilles heel for prostate cancer therapy a gain of function in androgen receptor signaling? J Clin Endocrinol Metab 2003;88(7):2972–2982.
35. Richardson GD, Robson CN, Lang SH, Neal DE, Maitland NJ, Collins AT. CD133, a novel marker for human prostatic epithelial stem cells. J Cell Sci 2004;117(Pt16):3539–3545.
36. Lawson DA, Xin L, Lukacs RU, Cheng D, Witte ON. Isolation and functional characterization of murine prostate stem cells. Proc Natl Acad Sci USA 2007;104(1):181–186.
37. Huss WJ, Gregory CW, Smith GJ. Neuroendocrine cell differentiation in the CWR22 human prostate cancer xenograft: Association with tumor cell proliferation prior to recurrence. Prostate 2004; 60(2):91–97.
38. Liao CP, Zhong C, Saribekyan G, Bading J, Park R, Conti PS, Moats R, Berns A, Shi W, Zhou Z, Nikitin AY, Roy-Burman P. Mouse models of prostate adenocarcinoma with the capacity to monitor spontaneous carcinogenesis by bioluminescence or fluorescence. Cancer Res 2007;67(15):7525–7533.
39. Kaplan-Lefko PJ, Chen TM, Ittmann MM, Barrios RJ, Ayala GE, Huss WJ, Maddison LA, Foster BA, Greenberg NM. Pathobiology of autochthonous prostate cancer in a pre-clinical transgenic mouse model. Prostate 2003;55(3):219–237.
40. Zhou Z, Flesken-Nikitin A, Corney DC, Wang W, Goodrich DW, Roy-Burman P, Nikitin AY. Synergy of p53 and Rb deficiency in a conditional mouse model for metastatic prostate cancer. Cancer Res 2006;66(16):7889–7898.
41. Leiblich A, Cross SS, Catto JW, Pesce G, Hamdy FC, Rehman I. Human prostate cancer cells express neuroendocrine cell markers PGP 9.5 and chromogranin A. Prostate 2007;67(16): 1761–1769.

42. Bonkhoff H, Stein U, Remberger K. Endocrine-paracrine cell types in the prostate and prostatic adenocarcinoma are postmitotic cells. Hum Pathol 1995;26(2):167–170.
43. Simon RA, di Santagnese PA, Huang LS, Xu H, Yao JL, Yang Q, Liang S, Liu J, Yu R, Cheng L, Oh WK, Palapattu GS, Wei J, Huang J. CD44 expression is a feature of prostatic small cell carcinoma and distinguishes it from its mimickers. Hum Pathol 2009;40(2):252–258.
44. Godar S, Ince TA, Bell GW, Feldser D, Donaher JL, Bergh J, Liu A, Miu K, Watnick RS, Reinhardt F, McAllister SS, Jacks T, Weinberg RA. Growth-inhibitory and tumor- suppressive functions of p53 depend on its repression of CD44 expression. Cell 2008;134(1): 62–73.
45. Bostwick DG, Dousa MK, Crawford BG, Wollan PC. Neuroendocrine differentiation in prostatic intraepithelial neoplasia and adenocarcinoma. Am J Surg Pathol 1994;18(12):1240–1246.
46. Bostwick DG, Qian J, Pacelli A, Zincke H, Blute M, Bergstralh EJ, Slezak JM, Cheng L. Neuroendocrine expression in node positive prostate cancer: Correlation with systemic progression and patient survival. J Urol 2002;168(3):1204–1211.
47. Roudier MP, True LD, Vessella RL, Higano CS. Metastatic conventional prostatic adenocarcinoma with diffuse chromogranin A and androgen receptor positivity. J Clin Pathol 2004;57(3): 321–323.
48. Bonkhoff H, Remberger K. Differentiation pathways and histogenetic aspects of normal and abnormal prostatic growth: A stem cell model. Prostate 1996;28(2):98–106.
49. Rumpold H, Heinrich E, Untergasser G, Hermann M, Pfister G, Plas E, Berger P. Neuroendocrine differentiation of human prostatic primary epithelial cells in vitro. Prostate 2002;53(2):101–108.
50. Xue Y, Verhofstad A, Lange W, Smedts F, Debruyne F, de la Rosette J, Schalken J. Prostatic neuroendocrine cells have a unique keratin expression pattern and do not express Bcl-2: Cell kinetic features of neuroendocrine cells in the human prostate. Am J Pathol 1997;151(6):1759–1765.
51. Xue Y, Smedts F, Verhofstad A, Debruyne F, de la Rosette J, Schalken J. Cell kinetics of prostate exocrine and neuroendocrine epithelium and their differential interrelationship: New perspectives. Prostate Suppl 1998;8:62–73.
52. Burchardt T, Burchardt M, Chen MW, Cao Y, de la Taille A, Shabsigh A, Hayek O, Dorai T, Buttyan R. Transdifferentiation of prostate cancer cells to a neuroendocrine cell phenotype in vitro and in vivo. J Urol 1999;162(5):1800–1805.
53. Cox ME, Deeble PD, Lakhani S, Parsons SJ. Acquisition of neuroendocrine characteristics by prostate tumor cells is reversible: Implications for prostate cancer progression. Cancer Res 1999; 59(15):3821–3830.

Published in final edited form as:
Prostate. 2010 September 15; 70(13): . doi:10.1002/pros.21171.

A Novel In Vitro Assay of Tumor-Initiating Cells in Xenograft Prostate Tumors

Christopher R. Silvers[1], **Karin Williams**[1], **Linda Salamone**[1], **Jiaoti Huang**[2], **Craig T. Jordan**[3], **Haijun Zhou**[4], and **Ganesh S. Palapattu**[1,*]

[1]Department of Urology, University of Rochester School of Medicine, Rochester, New York

[2]Department of Pathology and Laboratory Medicine, David Geffen School of Medicine, University of California at Los Angeles, Los Angeles, California

[3]Department of Medicine, University of Rochester School of Medicine, Rochester, New York

[4]Department of Urology, The Methodist Hospital Research Institute, Houston, Texas

Abstract

BACKGROUND—The field of prostate cancer has been stymied by the difficulty of cultivating patient-derived samples in the laboratory. In order to help circumvent this challenge, we sought to develop an in vitro assay of human prostate cancer initiation employing a prostate-associated mesenchymal feeder layer.

METHODS—Rat seminal vesicle mesenchyme (rSVM) harvested from male neonatal rats was plated in 12-well plates and then irradiated with 30 Gy after ~75% confluence. Single-cell suspensions of two human non-adherent prostate cancer xenograft lines (TRPC and LAPC9) were then plated on irradiated rSVM. At 3–4 weeks, three-dimensional solid structures, termed glandoids, were harvested and analyzed or transplanted singly into the renal capsule of immunodeficient mice. Animals were assessed for tumor formation 8–12 weeks after engraftment. Finally, clonality assays were performed to determine whether glandoids usually arise from a single cell and are therefore clonal in origin.

RESULTS—Glandoids form with reliable frequency (1/~300 plated cells), are constituted by relevant cell types (CK8+, CK5–, PSA+) and after implantation into immunocompromised mice, give rise to tumors that recapitulate original xenograft histology and cell composition; defining a glandoid as a tumor-initiating unit. In addition, assessment of red fluorescent protein (RFP)-labeled glandoids revealed either all red or non-red structures, with few areas of fusion, suggesting glandoids are clonal in origin.

CONCLUSIONS—The above assay describes an adjunct technique to readily cultivate cells from prostate cancer xenografts in vitro and as such provides a platform on which tumor-initiating cell studies and high-throughput drug discovery may be performed.

Keywords

prostate cancer; seminal vesicle mesenchyme; xenograft; tumor-initiating cell; cancer stem cell

*Correspondence to: Dr. Ganesh S. Palapattu, MD, Chief of Urologic Oncology, Department of Urology, The Methodist Hospital Research Institute, 6560 Fannin, Suite 2100, Houston, TX 77030. gpalapattu@tmhs.org.

INTRODUCTION

Progress in the field of human prostate tumor-initiating cell biology has been stymied by various experimental challenges. Due to downward stage migration as a result of PSA screening, the vast majority of prostate cancers in prostatectomy specimens today are often of low grade and stage and are difficult to identify grossly, making cancer tissue harvest for research purposes challenging. In addition, given current treatment paradigms, access to potentially tumor-initiating cell-enriched areas, such as metastatic or treatment refractory tissues, is uncommon. Furthermore, primary human prostate cancer is notoriously difficult to maintain in a laboratory environment, in vitro or in vivo, for any prolonged period of time. Of the obstacles facing researchers in the field, these three specific hurdles have impeded advancement the most. Notably, these particular issues pose minimal barriers in brain [1], breast [2], and colon cancer [3] research, areas where considerable discoveries have been already made in tumor-initiating cell biology.

Nevertheless, several investigators have recently reported significant breakthroughs. Collins et al. [4] have described the ability to isolate a specific subset of human prostate cancer cells, from surgical specimens, that are capable of forming colonies in vitro that possess self-renewal properties and that are composed of a mixed population of cells. Kasper and coworkers have been able to generate serially transplantable prostate tumors that recapitulate the parent human tumor from a clonal population of experimentally transformed human prostate cancer cells [5]. And Tang and coworkers have observed that only a small subset of cells from established prostate cancer cell lines and xenografts possess tumor initiating ability [6,7]. At present, no group has established an in vitro prostate tumor-initiating cell functional assay utilizing primary human tissue.

In an effort to improve the efficiency of in vitro modeling of human prostate cancer, numerous groups have described the use of fibroblasts as a feeder layer [8]. Such reports have revealed the ability to grow primary prostate spheres in culture albeit with varying tumorigenicity. It is clear that in addition to tissue culture conditions, such as media and feeder layer composition, the cell source (i.e., grade, stage, treatment history of the tumor) is critical to growing tumor-initiating spheres in vitro. As a first step toward developing a functional in vitro assay for prostate cancer initiation based upon primary tissues, we sought to establish an in vitro assay employing non-adherent xenograft human prostate cancer cell lines. Such an assay has the potential to hasten the investigation of human prostate tumor-initiating cell biology and, further, provide a platform on which high-throughput drug discovery may be performed. Borrowing from the seminal work of Cunha and Chung [9] and adapting concepts introduced by Isaacs and coworkers [10] and Witte and coworkers [11], we hypothesized that a feeder layer reflective of prostate stroma would be conducive to human prostate cancer tissue culture. To this end, we employed a feeder layer composed of rodent seminal vesicle mesenchyme (rSVM) to cultivate non-adherent human prostate cancer cells in vitro. Resultant three-dimensional colonies of cells were assayed for cell composition, tumorigenicity, and clonality.

MATERIALS AND METHODS

Prostate Cancer Xenograft Tumor Lines

In accordance with the University of Rochester School of Medicine's Research Subject's Review Board and following informed consent, fresh tissue obtained at surgery from a man with Gleason sum 10 prostate cancer was placed into immunocompromised mice for xenograft establishment. The patient had previously received radiation therapy, hormone therapy, and docetaxel chemotherapy; however, subsequently developed locally progressive disease without overt metastasis. For palliation the patient underwent radical

cystoprostatectomy. Upon surgical removal of the tumor, a xenograft was established by placing 2–3 mm sections subcutaneously in castrated male severe combined immunodeficient mice (SCID; National Cancer Institute at Frederick). The resultant xenograft, treatment refractory prostate cancer (TRPC), has been maintained for more than 2 years and nine generations. A more detailed characterization of this line is being prepared in a separate manuscript. The LAPC9 xenograft was supplied by the Laboratory of Robert E. Reiter at UCLA.

Xenograft Tumor Dissociation

LAPC9 and TRPC xenograft tumors were excised and placed in Petri dishes containing 10% fetal bovine serum (FBS, Gibco, 10437) in RPMI 1640 (with GlutaMAX-l and phenol red, Gibco, 61870). Tumors were cut into 2–3 mm sections, resuspended in HBSS (Invitrogen, 14175) containing 200 U/ml collagenase type I (Worthington Biochemical, Lakewood, NJ, LS004197), and stirred at 37°C for 20 min. Dissociated cells were passed through a 40 μm nylon strainer and resuspended in 7.4% FBS in RPMI. Filtered cells were examined with an Olympus CKX31 inverted microscope to confirm total dissociation.

Primary Mesenchymal Cell Culture

Timed-pregnant female Sprague–Dawley rats were purchased from Harlan Laboratories. All animals used in this work were maintained according to the guidelines of the University Committee on Animal Resources at the University of Rochester. Seminal vesicles were excised from neonatal rats using a Leica MZ9.5 dissecting stereomicroscope and collected in RPMI containing 10% FBS. Seminal vesicles were resuspended in HBSS containing 10 BTEE units/ml trypsin (Sigma, T4799) for 1 hr at 4°C. The trypsin was then neutralized by resuspension of the seminal vesicles in RPMI containing 10% FBS and <0.5 mg/ml deoxyribonuclease I (Sigma, DN25-1G). Epithelium was teased away from each seminal vesicle with 25-gauge needles under the dissecting stereomicroscope. The remaining mesenchyme was resuspended in RPMI containing 200 U/ml collagenase type I and gently rocked at room temperature for 20 min. Dissociated cells were maintained in RPMI containing 10% FBS and 0.1 mg/ml Primocin (Invitrogen, ant-pm-1) and incubated at 37°C in humidified air containing 5% CO_2. Due to technical issues with cultivating and maintaining rodent urogenital mesenchyme (UGM) in vitro, UGM was not utilized in these studies as a feeder layer.

Glandoid Culture

Monolayers of rSVM cells were grown to ~75% confluence in 12-well culture plates (Corning, 3513), either directly or on cover glasses (VWR, 48380-046), and irradiated with 30 Gy of gamma radiation from a cesium-137 source. As controls, xenograft cells were also plated either directly on plastic or upon a STO cell (mouse embryonic fibroblast) feeder layer. The rSVM growth medium was replaced with RPMI containing 7.4% FBS and 0.1 mg/ml Primocin. Cells freshly dissociated from human prostate cancer xenograft tumors were plated at densities of 800–3,200 cells/cm^2 over the feeder layer. After 14 days of culture, the medium was replenished if acidification was noted (i.e., color change). Due to technical considerations, limiting dilution assays were not performed.

Lentiviral Infection of Dissociated Glandoid Cells

A pLentiRed plasmid containing the gene DsRed-N2, which encodes a red fluorescing protein, was transfected into 293FT cells using Lipofectamine 2000 according to manufacturer's instructions (Invitrogen, 11668). Cell culture medium containing the shed viral particles was harvested every 8 hr, filtered through a 0.45-μm filter, and stored at –80°C. Thawed medium was then used to replace the growth medium in 12-well culture

plates of irradiated rSVM feeder layer. To obtain cells, glandoids were collected one at a time with pipette tips of sufficient bore diameter to allow passage. Adherent glandoids were first dislodged from the substrate with a blunt glass probe. Each glandoid was removed to 200 μl of 37°C trypsin–EDTA (0.25%, Gibco, 25200) and pipetted vigorously for 3–6 min until completely dissociated. Resultant single cells from a number of TRPC glandoids were mixed, counted on a hemocytometer, and plated at a density of 800 cells/cm^2 over the feeder layer, and the medium containing lentivirus served as the growth medium until red fluorescing glandoids appeared. Culture wells were subsequently photographed with an Olympus IX70 inverted microscope.

Engraftment of Glandoids Into Immunocompromised Mice

Glandoids were engrafted beneath the murine renal capsule using the method described at the following website: http://mammary.nih.gov/tools/mousework/Cunha001. Each glandoid remained intact during handling and was positioned beneath the renal capsule with a blunt glass probe, two to four glandoids per kidney in distinct locations. Glandoid position was easily observed using a Leica MZ9.5 dissecting stereomicroscope. TRPC glandoids were engrafted into castrated male SCID mice. LAPC9 glandoids were engrafted into intact non-obese diabetic/SCID (NOD/SCID; National Cancer Institute at Frederick) males supplemented with 9 mg testosterone pellets placed subcutaneously. Grafts were harvested at 6 or 8 weeks.

Immunofluorescent and Histological Analysis

Harvested xenografts were fixed in 10% neutral-buffered formalin and embedded in paraffin. Glandoids were prepared for paraffin processing by fixation in 10% neutral-buffered formalin for 1 hr and resuspension in 100 μl of type I rat tail collagen. The collagen was pipetted as a round button into a Petri dish, allowed to polymerize for 30 min at 37°C, and immersed in formalin overnight before paraffin embedding. Sections were cut on a microtome and mounted on microscope slides (VWR, 48311). For staining of intact structures, glandoids were left adherent to their culture wells or cover glasses and fixed in –20°C methanol for 10 min.

Conventional hematoxylin and eosin staining was performed for histological analysis. For indirect immunofluorescent analysis of sections, antigen unmasking was performed with pre-heated (95–99°C) citrate buffer (Vector, H-3300) in a Black and Decker steamer (HS800) for 30 min. Sections were permeabilized in 0.2% Triton X-100 (Sigma, T9284) in 2% normal goat serum for 30 min, and all materials were blocked with 5% normal goat serum in PBS for 2 hr to bind nonspecific sites. A monoclonal mouse antibody raised against cytokeratin 8 (Santa Cruz, sc-8020, 1:200) was used in combination with rabbit polyclonal antibodies raised against cytokeratin 5 (Santa Cruz, sc-66856, 1:200) or prostate-specific antigen (PSA) (Genetex, GTX72905, 1:100) in 5% normal goat serum and incubated overnight at room temperature. Secondary antibodies Alexa Fluor 546 goat anti-mouse IgG (Invitrogen, A-11003, 1:200) and Alexa Fluor 488 donkey anti-rabbit IgG (Invitrogen, A-21206, 1:200) diluted in PBS were then conjugated to the primary antibodies in a 40-min incubation at room temperature. DAPI staining was performed separately or with Vectashield HardSet Mounting Medium (Vector; H-1500). Sections were photographed with a Leica DM5000 B microscope. Glandoids stained in the culture wells were photographed with an Olympus IX70 inverted microscope.

A rabbit polyclonal antibody raised against chromogranin A (Dako, A0430, 1:1,000) was used in combination with mouse monoclonal anti-human nuclear antigen (Chemicon, MAB1281, 1:50) and incubated overnight at room temperature on the original cover glasses. Secondary antibodies Alexa Fluor 546 goat anti-mouse IgG and Alexa Fluor 633 F(ab)2

fragment of goat anti-rabbit IgG (Invitrogen, A-21072, 1:200) were then conjugated to the primary antibodies in a 40-min incubation at room temperature. This stain was photographed with a Leica TCS SP confocal microscope.

Conventional immunohistochemical staining was performed on glandoids adherent to their culture wells. Endogenous peroxidase activity was blocked with 0.3% hydrogen peroxide in methanol for 30 min; nonspecific sites were blocked with 5% normal swine serum in PBS for 2 hr. Anti-PSA antibody was diluted in 5% normal swine serum, and glandoids were incubated overnight at 4°C. Biotinylated polyclonal swine anti-rabbit secondary antibody (Dako, E0353, 1:500) was diluted in 5% normal swine serum, and the culture wells were incubated for 40 min at room temperature. Subsequently, the material was incubated with avidin–biotin complex (Vector, PK-6100) for 30 min at room temperature. Immunoreactivity was visualized with diaminobenzidine (DAB) (Dako, K3465); the material was lightly counterstained with hematoxylin.

RESULTS

In Vitro Assay: Technique

We obtained rSVM from male neonatal rats (day of life 1–4) via microdissection (see Fig. 1), as previously described. After harvest, rSVM was plated in 12-well plates and allowed to adhere and grow. At ~75% confluence, rSVM was irradiated with 30 Gy to prevent overgrowth. This radiation dose is enough to halt cell proliferation without causing cell death. Single-cell suspensions of human prostate cancer cells were then applied on top of this feeder layer to create a floating co-culture system. At 21–28 days, three-dimensional colonies we have termed glandoids are grossly visible (Fig. 1, panel F). No glandoids were visualized when xenograft cells were plated either alone or upon an STO cell feeder layer (data not shown).

Non-Adherent Xenograft Prostate Cancer Cell Lines: TRPC and LAPC9

The non-adherent xenograft cell lines TRPC and LAPC9 were utilized for our studies. TRPC was isolated by our lab from a patient who had locally recurrent/progressive disease despite radiation therapy, hormone ablation, and docetaxel chemotherapy (see the Materials and Methods Section). Efforts to cultivate this line in vitro alone or with a fibroblast feeder layer (STO cells) have been unsuccessful (data not shown). LAPC9 is a well-established human prostate cancer xenograft cell line derived from a hormone refractory metastatic lesion [12]. Due to the difficulty of maintaining it in cell culture, it has largely been studied in vivo as a xenograft. Notably, some have reported in vitro colony-forming ability when LAPC9 is plated upon a feeder layer of fibroblasts [6]. Based upon the relatively poor performance of TRPC and LAPC9 in cell culture, we elected to use these non-adherent xenograft lines to test the efficacy of our in vitro assay of prostate tumor initiation. Cell composition and histology of the xenograft lines are shown in Figure 2.

TRPC and LAPC9 Form Glandoids In Vitro

TRPC and LAPC9 glandoids were grossly visible by ~21 days in culture (see Figs. 3 and 4). TRPC-derived glandoids were observed to be more rounded while LAPC9 glandoids tended to be more flattened. Overall, we detected a relatively consistent glandoid forming rate for each cell line: TRPC 300–600 plated cells/glandoid and LAPC9 200–300 plated cells/glandoid. Glandoids were found to be composed of all cell types found in the parent xenograft (see Figs. 3 and 4). No cytokeratin-5-positive cells (basal cells) were detected in the TRPC xenograft or in TRPC glandoids that were examined. While cytokeratin-5-positive cells were not observed in the LAPC9 xenograft, one LAPC9 glandoid was found to have a small cytokeratin 5 positive population (data not shown).

TRPC and LAPC9 Glandoids Are Tumorigenic

To assess tumorigenicity, we micro-surgically transplanted single glandoids without rSVM into the renal capsule of immunodeficient mice. At 6 or 8 weeks, engrafted kidneys were harvested and analyzed. Gross tumors developed in 6/9 TRPC and 9/9 LAPC9 glandoids implanted (see Fig. 5, panel A). No obvious evidence of metastasis was noted on harvest. Immunocytochemical analysis of glandoid-induced tumors (GITs) revealed cell composition similar to that of the parent glandoid and xenograft cell line (see Fig. 5, panel B). Moreover, GITs and the parental xenograft appeared histologically similar.

Glandoids Show Evidence of Clonality

One possible way by which glandoids form is simply through aggregation of input cells. This type of event would yield heterogeneous populations, but would not represent a true tumor-initiating cell assay, which is a central goal of our work. To begin to evaluate whether glandoids arise from a single-initiating cell versus a cellular aggregate, we employed a cell autonomous marking strategy. Specifically, primary TRPC glandoids were harvested, pooled together, and gently treated with trypsin to create a single-cell suspension. The cells were then transduced with a lentivirus vector encoding the red fluorescent protein (RFP), and plated in the glandoid assay. As shown in Figure 6 resultant glandoids were observed to be one of three kinds: (i) all red, (ii) completely colorless, or (iii) composed of a small pocket of a minority color of cells (either red or colorless depending on the majority cell color). Isolated clusters of uniformly colored cells within glandoids are thought to have occurred via glandoid fusion. The fact that the no red speckled or polka dot appearing glandoids were detected suggests that glandoids are clonal and not the result of cell aggregation.

DISCUSSION

Methodologies that enable laboratory modeling of primary prostate cancer are desperately needed. Such systems would allow the interrogation of tumor-initiating cell biology as well as drug discovery, among other things, from clinically relevant tissue samples. In this report, we describe an in vitro functional assay of prostate cancer initiation that utilizes rSVM as a feeder layer. Employing this technique with non-adherent human prostate cancer cells plated on the surface, we observed the formation of clusters of dense cellular spheres that we have termed glandoids, at a reproducible frequency. Additionally, we have shown that glandoids share cell composition with the parent xenograft and are tumorigenic, an important observation that defines glandoids as tumor initiating units. Furthermore, we have presented evidence suggesting that glandoids are clonal; thus, demonstrating a way the presented technique may be used to gain insights into prostate tumor-initiating cell biology.

For decades investigators have sought to develop in vitro culture systems that are conducive to studying non-adherent patient-derived human prostate cancer cells. To be sure, the concept of an in vitro feeder layer is not new and has been used widely in other organ systems to facilitate primary cell culture [13–16]. In the prostate, the mouse embryonic fibroblast cell line 3T3 has been employed and has met with some success vis-à-vis supporting in vitro growth of primary or xenograft prostate cancer cell lines [6,8]. Immortalized 3T3 cells (STO cells) and mesenchymal stem cells have been used to cultivate primary epithelial cells from other organs but have not been fully explored in the prostate [17,18]. We elected to utilize rSVM as a mesenchymal feeder layer given the tremendous success of this tissue to support modeling of human prostate tissue in vivo with tissue recombination. To our knowledge, this is the first report of using rSVM to facilitate in vitro culture of non-adherent human prostate cancer cells.

Human prostasphere forming assays utilizing non-adherent cell culture conditions derived from primary surgical specimens have been reported. These studies have been able to demonstrate that prostaspheres cultivated in this manner possess phenotypic characteristics (e.g., PSA expression, cytokeratin 8 expression, *TMPRSS/ERG* gene fusion) of cancer and functional attributes (e.g., self-renewal) of tumor-initiating cells in vitro [19]. Importantly, to date, no one has reported the ability to form prostaspheres directly from patient samples that are themselves tumorigenic in vivo. The reasons for this are likely multifold and may be related to (i) the tissue source (i.e., grade/stage, treatment history), (ii) tissue/cell handling (i.e., pathological manipulation, cell separation techniques), (iii) in vitro culture conditions (i.e., feeder layer, media, growth factors), and (iv) the immunodeficient animal used (i.e., nude vs. NOD vs. NOD/SCID vs. NOD/SCID gamma vs. Rag2 knockout mice). As an initial attempt to circumvent these obstacles we tested the ability of rSVM to act as a feeder layer to non-adherent human prostate cancer xenograft lines in vitro and found that the resultant sphere-like structures (“glandoids”) were tumorigenic.

Based on these findings, we propose that rSVM may serve as a viable feeder layer for primary human prostate cancer cells in vitro, perhaps owing to either a secreted or cell surface factor. Further studies that seek to understand the precise mechanisms by which rSVM can support human prostate cancer cell growth in vitro are needed. In addition, experiments that aim to grow glandoids directly from patient samples and that assay glandoids for tumorigenicity need to be performed to validate this technique for use with primary patient samples. Nevertheless, the assay as presently described has potential to interrogate tumor-initiating cell properties and explore therapeutic targets in xenograft prostate cancer cell lines.

CONCLUSION

Here, we report on the capacity of rSVM to serve as a feeder layer to non-adherent human prostate cancer cells in vitro. Xenograft maintained cells that are grown in this way form three-dimensional structures that (i) comprised all relevant cell types, (ii) give evidence for clonality, and (iii) are tumorigenic. The described methodology may prove useful in studying tumor-initiating cell biology and drug susceptibility of xenograft maintained cancer cell lines and if validated with primary cells, may dramatically improve our ability to model human prostate cancer in the laboratory.

Acknowledgments

G.S.P. is funded by Department of Defense award W81XWH-08-1-0508, AUA Foundation Rising Stars in Urology award, NE section-AUA Young Investigators award, and the Prostate Cancer Foundation. J.H. is supported by grants from American Cancer Society (RSG-07-092-01-TBE), Department of Defense Prostate Cancer Research Program (PC061456), a developmental research award from UCLA SPORE in prostate cancer, and a challenge award from the Prostate Cancer Foundation.

Grant sponsor: Prostate Cancer Foundation; Grant sponsor: American Cancer Society; Grant number: RSG-07-092-01-TBE; Grant sponsor: Department of Defense Prostate Cancer Research Program; Grant number: PC073121, PC061456.

REFERENCES

1. Singh SK, Hawkins C, Clarke ID, Squire JA, Bayani J, Hide T, Henkelman RM, Cusimano MD, Dirks PB. Identification of human brain tumour initiating cells. Nature. 2004; 432(7015):396–401. [PubMed: 15549107]
2. Ginestier C, Hur MH, Charafe-Jauffret E, Monville F, Dutcher J, Brown M, Jacquemier J, Viens P, Kleer CG, Liu S, Schott A, Hayes D, Birnbaum D, Wicha MS, Dontu G. ALDH1 is a marker of

normal and malignant human mammary stem cells and a predictor of poor clinical outcome. Cell Stem Cell. 2007; 1(5):555–567. [PubMed: 18371393]

3. O'Brien CA, Pollett A, Gallinger S, Dick JE. A human colon cancer cell capable of initiating tumour growth in immunodeficient mice. Nature. 2007; 445(7123):106–110. [PubMed: 17122772]
4. Collins AT, Berry PA, Hyde C, Stower MJ, Maitland NJ. Prospective identification of tumorigenic prostate cancer stem cells. Cancer Res. 2005; 65(23):10946–10951. [PubMed: 16322242]
5. Gu G, Yuan J, Wills M, Kasper S. Prostate cancer cells with stem cell characteristics reconstitute the original human tumor in vivo. Cancer Res. 2007; 67(10):4807–4815. [PubMed: 17510410]
6. Patrawala L, Calhoun T, Schneider-Broussard R, Li H, Bhatia B, Tang S, Reilly JG, Chandra D, Zhou J, Claypool K, Coghlan L, Tang DG. Highly purified CD44+ prostate cancer cells from xenograft human tumors are enriched in tumorigenic and metastatic progenitor cells. Oncogene. 2006; 25(12):1696–1708. [PubMed: 16449977]
7. Patrawala L, Calhoun-Davis T, Schneider-Broussard R, Tang DG. Hierarchical organization of prostate cancer cells in xenograft tumors: The CD44+alpha2beta1+ cell population is enriched in tumor-initiating cells. Cancer Res. 2007; 67(14):6796–6805. [PubMed: 17638891]
8. Miki J, Rhim JS. Prostate cell cultures as in vitro models for the study of normal stem cells and cancer stem cells. Prostate Cancer Prostatic Dis. 2008; 11(1):32–39. [PubMed: 17984999]
9. Cunha GR, Chung LW. Stromal-epithelial interactions—I. Induction of prostatic phenotype in urothelium of testicular feminized (Tfm/y) mice. J Steroid Biochem. 1981; 14(12):1317–1324. [PubMed: 6460136]
10. Litvinov IV, Vander Griend DJ, Xu Y, Antony L, Dalrymple SL, Isaacs JT. Low-calcium serum-free defined medium selects for growth of normal prostatic epithelial stem cells. Cancer Res. 2006; 66(1):8598–8607. [PubMed: 16951173]
11. Lawson DA, Xin L, Lukacs RU, Cheng D, Witte ON. Isolation and functional characterization of murine prostate stem cells. Proc Natl Acad Sci USA. 2007; 104(1):181–186. [PubMed: 17185413]
12. Craft N, Chhor C, Tran C, Belldegrun A, DeKernion J, Witte ON, Said J, Reiter RE, Sawyers CL. Evidence for clonal outgrowth of androgen-independent prostate cancer cells from androgen-dependent tumors through a two-step process. Cancer Res. 1999; 59(19):5030–5036. [PubMed: 10519419]
13. Matouskova E, Dudorkinova D, Krasna L, Vesely P. Temporal in vitro expansion of the luminal lineage of human mammary epithelial cells achieved with the 3T3 feeder layer technique. Breast Cancer Res Treat. 2000; 60(3):241–249. [PubMed: 10930112]
14. Tenchini ML, Ranzati C, Malcovati M. Culture techniques for human keratinocytes. Burns. 1992; 18(Suppl 1):S11–S16. [PubMed: 1554417]
15. Paraskeva C, Buckle BG, Sheer D, Wigley CB. The isolation and characterization of colorectal epithelial cell lines at different stages in malignant transformation from familial polyposis coli patients. Int J Cancer. 1984; 34(1):49–56. [PubMed: 6746117]
16. Whitehead RH, Brown A, Bhathal PS. A method for the isolation and culture of human colonic crypts in collagen gels. In Vitro Cell Dev Biol. 1987; 23(6):436–442. [PubMed: 3597283]
17. Park SP, Lee YJ, Lee KS, Ah Shin H, Cho HY, Chung KS, Kim EY, Lim JH. Establishment of human embryonic stem cell lines from frozen-thawed blastocysts using STO cell feeder layers. Hum Reprod (Oxford, Engl). 2004; 19(3):676–684.
18. Shamblott MJ, Axelman J, Wang S, Bugg EM, Littlefield JW, Donovan PJ, Blumenthal PD, Huggins GR, Gearhart JD. Derivation of pluripotent stem cells from cultured human primordial germ cells. Proc Natl Acad Sci USA. 1998; 95(23):13726–13731. [PubMed: 9811868]
19. Guzman-Ramirez N, Voller M, Wetterwald A, Germann M, Cross NA, Rentsch CA, Schalken J, Thalmann GN, Cecchini MG. In vitro propagation and characterization of neoplastic stem/progenitor-like cells from human prostate cancer tissue. Prostate. 2009; 69(15):1683–1693. [PubMed: 19644960]

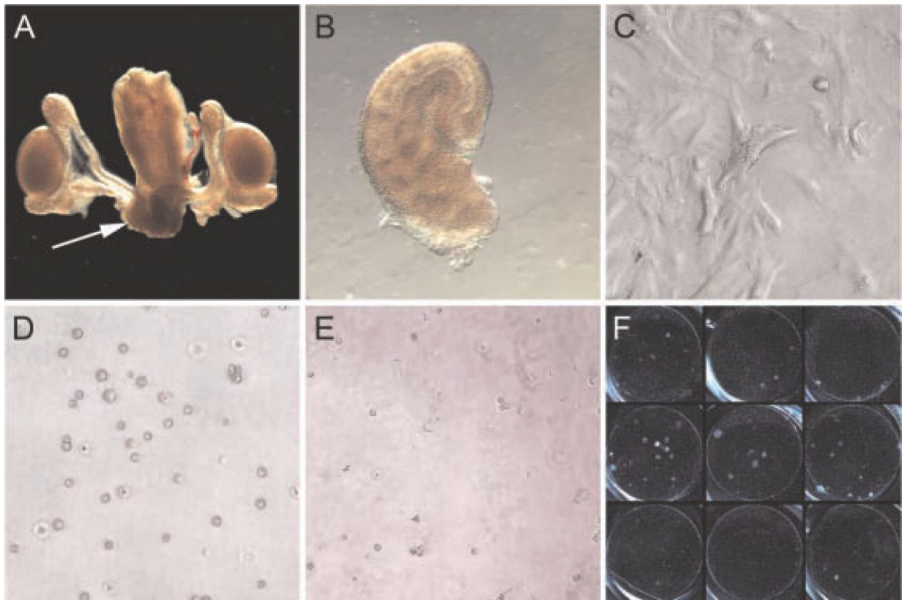

Fig. 1.

In vivo assay technique. Urogenital tract from a neonatal rat male pup (day of life1) is shown in **panel A** with arrow pointing to seminal vesicle mesenchyme (SVM). Microdissected rat SVM (**panel B**) is then plated in a 12-well plate and allowed to reach ~75% confluence (**panel C**) at which point 30 Gy is administered to prevent further outgrowth. A single-cell suspension of human prostate cancer cells (**panel D**) is then placed on top of the irradiated rSVM feeder layer (**panel E**). Approximately 21–28 days later, three-dimensional colonies (“glandoids”) are grossly visible (**panel F**).

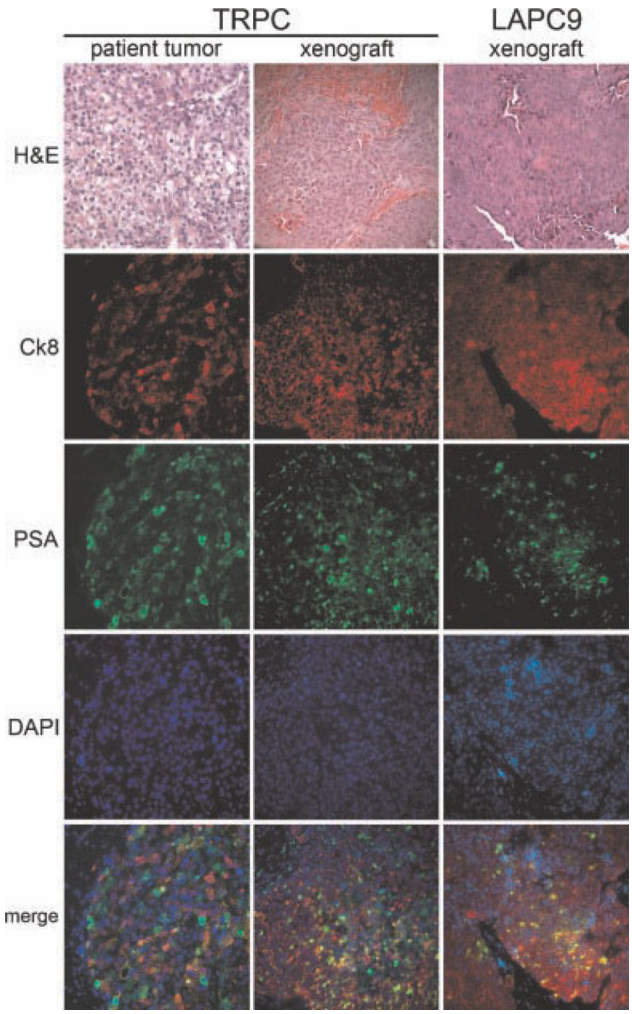

Fig. 2.

Non-adherent xenograft celllines TRPC and LAPC9. Treatment refractory prostate cancer (TRPC) and LAPC-9 histology and cell composition demonstrate xenografts that express cytokeratin 8 and PSA in the majority of cells. Cytokeratin 5 expression was not observed in either the TRPC xenograft or in TRPC glandoids; one LAPC9 glandoid was observed to have a small population of cytokeratin-5-positive cells (data not shown). Consistency of cell composition between TRPC directly from the patient and from a xenograft >8 generations later is alsonoted. DAPI = nuclear stain.

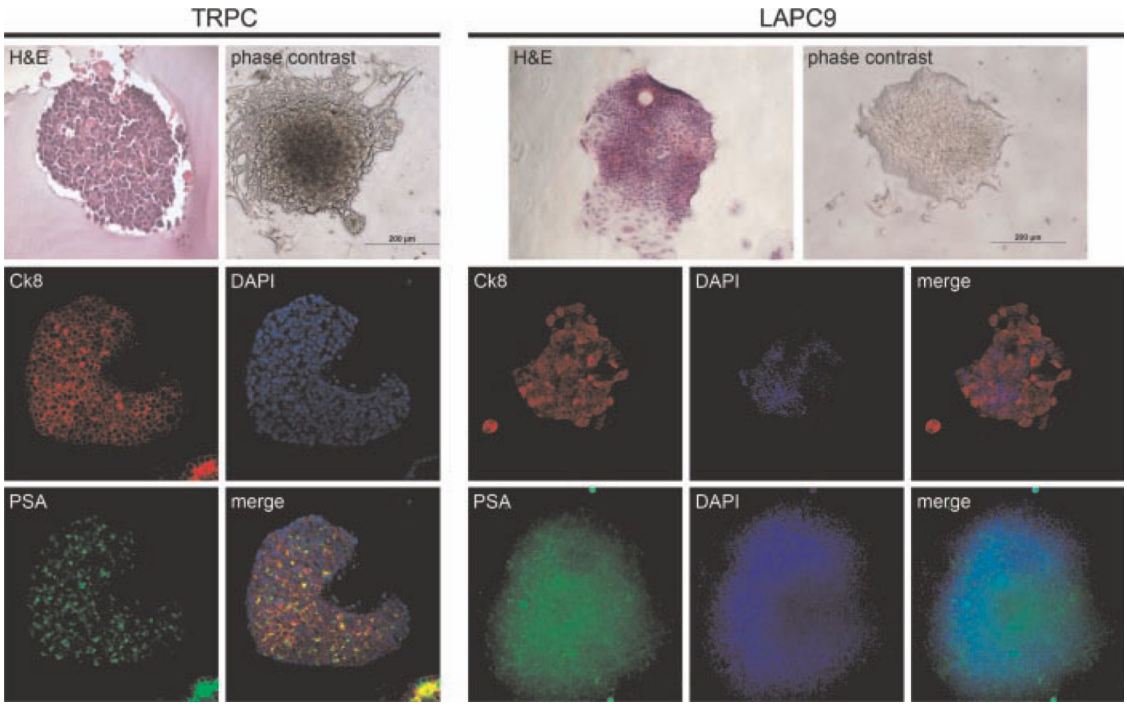

Fig. 3.

TRPC- and LAPC9-derived glandoids. Characterization of glandoids obtained from TRPC demonstrates fidelity with regard to H&E (glandoid embedded in collagen after retrieval from plate to facilitate handling), cytokeratin 8, and PSA staining when compared to thexenograft line. Cytokeratin 5 expression was not observed (data not shown). Similarly, characterization of glandoids obtained from LAPC9 demonstrate uniformity with regard to H&E, cytokeratin 8, and PSA staining when compared to the xenograft line.

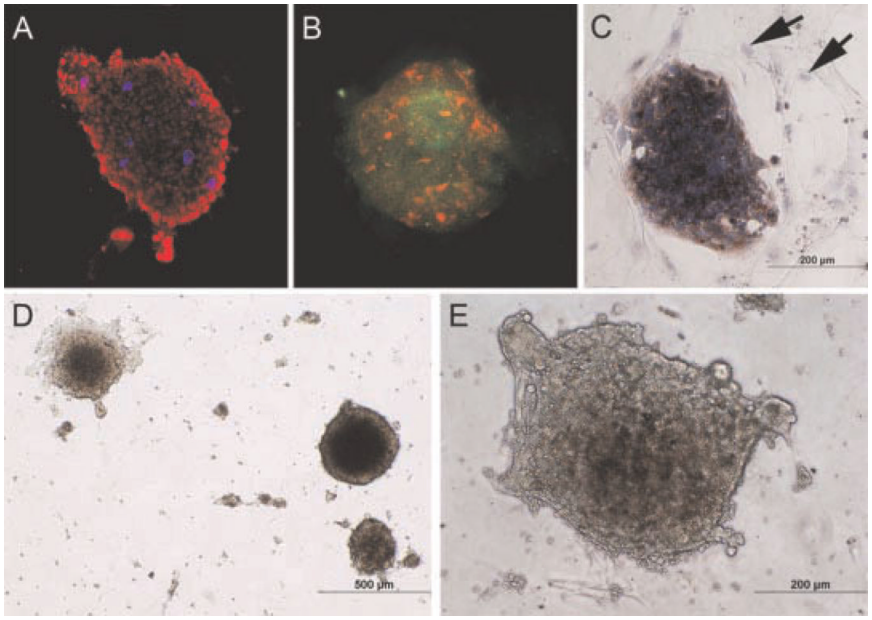

Fig. 4.

Additional glandoid characterization.**Panel A** depicts human nuclear antigen staining (red) and chromogranin A expression (blue) within a TRPC-derive dglandoid. **Panels B** and **C** demonstrate glandoids obtained directly from the patient whose tumor became TRPC (panel B: green = PSA,red = cytokeratin 8; Panel C: brown = PSA, blue = hematoxylin counter stain, arrows denoter SVM stromal cells). **Panels D** (low power) and **E** (high power) show phase-contrast images of TRPC glandoids in culture.

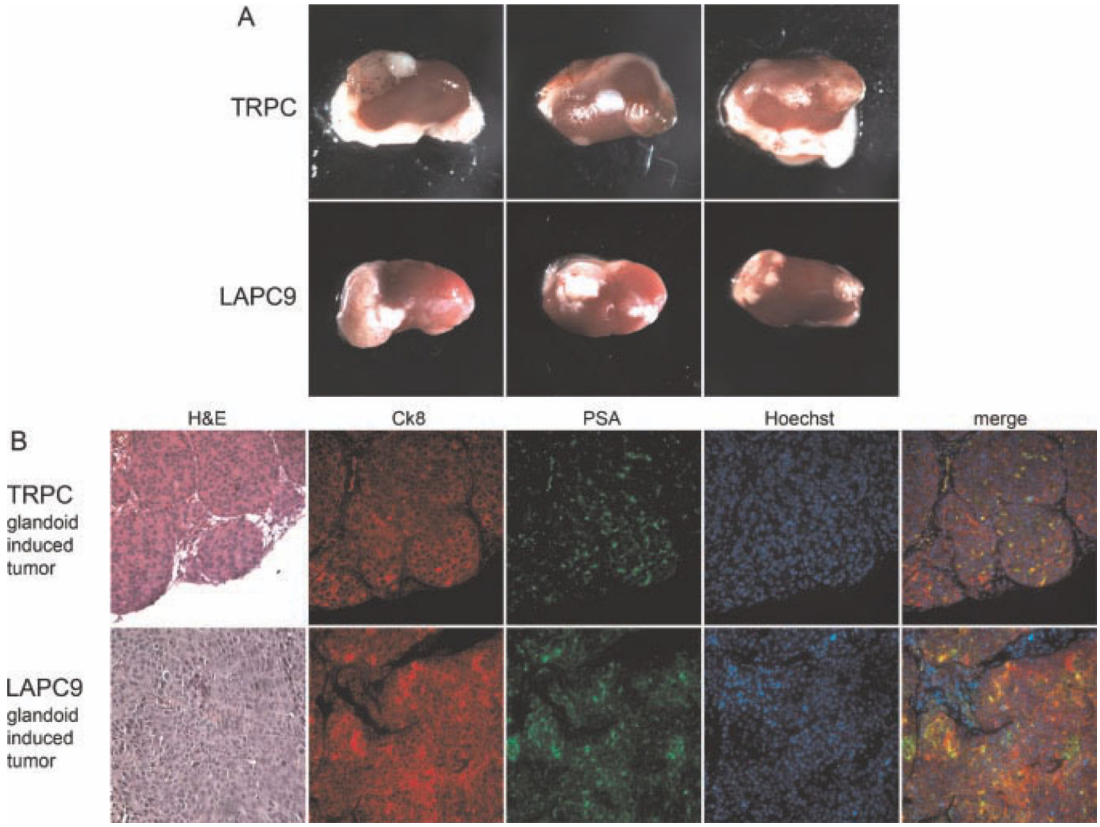

Fig. 5.

Glandoids induce in vivo tumors. Singly implanted (without rSVM) TRPC and LAPC9 glandoids generate gross tumors within the renal capsule of immunodeficient mice by 8 weeks (**panel A**). Glandoid-induced tumors (GITs) derived from both TRPC and LAPC9 demonstrate identical histology and expression of cytokeratin 8 and PSA as that seen in the parent xenograft (**panel B**). DAPI = nuclear stain.

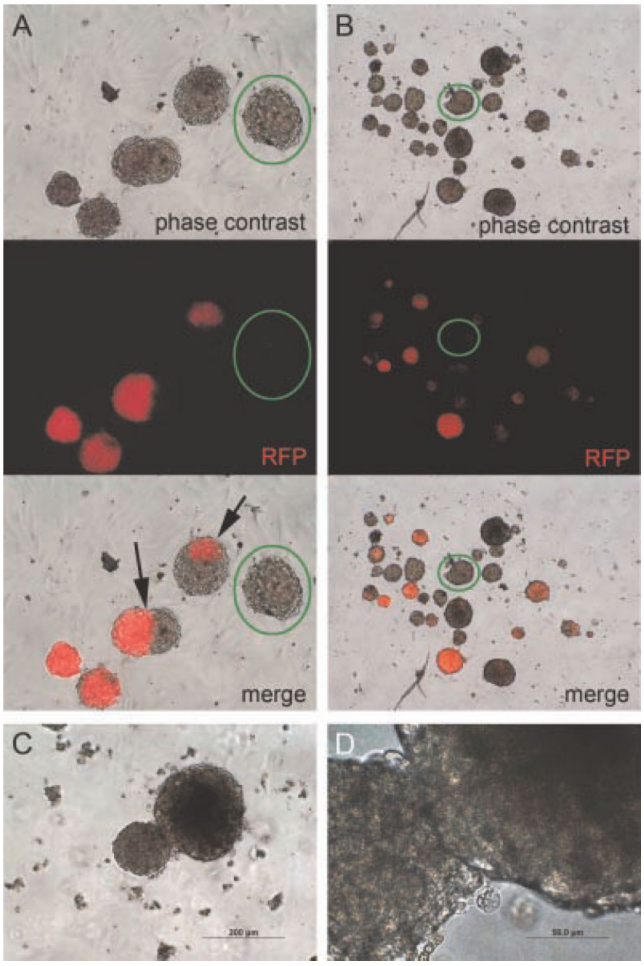

Fig. 6.

Glandoids and clonality. RFP (red fluorescent protein) lenti-virus-treated TRPC cells generated glandoids that were either all red or all not red (**columns A** and **B**). Arrows point to clustered areas of red cells suggesting fusion of separate glandoids. Green circles denote RFP negative glandoids.The lack of red speckled or red polka dot appearing glandoids suggests that cell aggregation is not likely to account for glandoid formation and provides evidence in support of glandoid clonality. **Panels C** (10X) and **D** (40×) depict the adhesion of two neighboring glandoids.

Published in final edited form as:
Cell Stem Cell. 2012 May 4; 10(5): 556–569. doi:10.1016/j.stem.2012.03.009.

The PSA$^{-/lo}$ prostate cancer cell population harbors self-renewing long-term tumor-propagating cells that resist castration

Jichao Qin[1,2,*], **Xin Liu**[1,3,*], **Brian Laffin**[1], **Xin Chen**[1,4], **Grace Choy**[1], **Collene Jeter**[1], **Tammy Calhoun-Davis**[1], **Hangwen Li**[1,3], **Ganesh S. Palapattu**[5], **Shen Pang**[6], **Kevin Lin**[1], **Jiaoti Huang**[7], **Ivan Ivanov**[8], **Wei Li**[9], **Mahipal V. Suraneni**[1], and **Dean G. Tang**[1,4,10,11]

[1]Department of Molecular Carcinogenesis, University of Texas M.D. Anderson Cancer Center, Science Park, Smithville, TX 78957, USA

[2]Department of Surgery, Tongji Hospital, Tongji Medical College, Huazhong University of Science and Technology, Wuhan 430030, China

[3]Department of Nutritional Science, University of Texas at Austin, Austin, TX 78712, USA

[4]Program in Molecular Carcinogenesis, University of Texas Graduate School of Biomedical Sciences (GSBS), Houston, TX 77030, USA

[5]Department of Urology, The Methodist Hospital, Houston, TX 77030, USA

[6]UCLA Dental Research Institute and UCLA School of Dentistry, 10833 Le Conte Avenue, Los Angeles, CA 90095, USA

[7]Department of Pathology and Laboratory Medicine, David Geffen School of Medicine, UCLA, Los Angeles, CA 90095, USA

[8]Department of Veterinary Physiology and Pharmacology, Texas A&M University, College Station, TX 77843, USA

[9]Department of Molecular and Cellular Biology, Baylor College of Medicine, Houston, TX 77030

[10]Centers for Cancer Epigenetics, Stem Cell and Developmental Biology, RNA Interference and Non-coding RNAs, and Molecular Carcinogenesis, University of Texas M.D. Anderson Cancer Center, Houston, TX 77030, USA

[11]Cancer Stem Cell Institute, Research Center for Translational Medicine, East Hospital, Tongji University, Shanghai 200120, China

SUMMARY

Correspondence: Dean Tang, Department of Molecular Carcinogenesis, The University of Texas M.D. Anderson Cancer Center, Science Park, 1808 Park Rd. 1C, Smithville, TX 78957, USA. Tel: (512) 237-9575; Fax: (512) 237-9510; dtang@mdanderson.org.
*These authors contributed equally to this work

SUPPLEMENTAL INFORMATION
Supplemental Information includes Supplemental Results, eight figures, four tables, six movies, Extended Experimental Procedures, and Supplemental References and can be found with this article online.

Prostate cancer (PCa) is heterogeneous and contains both differentiated and undifferentiated tumor cells, but the relative functional contribution of these two cell populations remains unclear. Here we report distinct molecular, cellular, and tumor-propagating properties of PCa cells that express high (PSA^+) and low ($PSA^{-/lo}$) levels of the differentiation marker PSA. $PSA^{-/lo}$ PCa cells are quiescent and refractory to stresses including androgen deprivation, exhibit high clonogenic potential, and possess long-term tumor-propagating capacity. They preferentially express stem cell genes and can undergo asymmetric cell division generating PSA^+ cells. Importantly, $PSA^{-/lo}$ PCa cells can initiate robust tumor development and resist androgen ablation in castrated hosts, and harbor highly tumorigenic castration-resistant PCa cells that can be prospectively enriched using $ALDH^+CD44^+\alpha2\beta1^+$ phenotype. In contrast, PSA^+ PCa cells possess more limited tumor-propagating capacity, undergo symmetric division and are sensitive to castration. Together, our study suggests $PSA^{-/lo}$ cells may represent a critical source of castration-resistant PCa cells.

Keywords

prostate cancer; PSA; cancer stem cells; differentiation; asymmetric cell division; castration resistance

INTRODUCTION

PCa is heterogeneous manifesting variegated cellular morphologies and histopathological presentations. PCa also exhibits great intra-tumor histological and immunophenotypic heterogeneities, with low-grade tumors often harboring poorly differentiated areas and high-grade tumors containing relatively differentiated foci. The cellular basis for the histological and cellular heterogeneity of PCa remains unclear.

Androgen and androgen receptor (AR) signaling has been implicated in PCa. Androgen-deprivation therapy (ADT) blocks androgen production or AR signaling and is the mainstay treatment for advanced and recurrent PCa but such interventions only achieve short-term efficacy due to the emergence of castration-resistant disease (i.e., CRPC). Although many mechanisms, mostly centered on AR, have been proposed for CRPC development (Shen and Abate-Shen 2010; Wang Q et al., 2009), the cell-of-origin and molecular identity of CRPC cells remain undefined.

Numerous studies have demonstrated that PSA (prostate-specific antigen) protein expression in PCa positively correlates with its overall degree of differentiation (e.g., Abrahamsson et al., 1988; Feiner and Gonzales, 1986; Gallee et al., 1990). At the cellular level, PCa contains differentiated cancer cells expressing high levels of PSA (i.e., PSA^+) as well as PCa cells that express little or no PSA (i.e., $PSA^{-/lo}$). The $PSA^{-/lo}$ cells appear to be rare in early-stage tumors but become more abundant in high-grade and locally advanced tumors and some cases of PCa may completely lack PSA expression. PCa patients with their tumors containing >50% PSA^+ PCa cells tend to have longer survival (Roudier et al., 2003; Shah et al., 2004). These clinical observations raise a fundamental question: could $PSA^{-/lo}$ PCa cells be intrinsically distinct from PSA^+ cells and thus play differential roles in tumor maintenance and progression to CRPC? Herein, we address this clinically relevant question using a PSA promoter-driven lentiviral reporter system to separate bulk PCa cells into $PSA^{-/lo}$ and PSA^+ subpopulations.

RESULTS

Increased PSA$^{-/lo}$ Cells and Reduced *PSA* mRNA in High-Grade Primary Tumors and Recurrent PCa

We first performed a semi-quantitative PSA immunohistochemical (IHC) analysis in cohorts of untreated Gleason 7 (GS7, $n = 10$), Gleason 9 or 10 (GS9/10, $n = 10$), and treatment-failed ($n = 23$) PCa (Figure S1; Table S1). Most tumor glands in GS7 tumors stained strongly for PSA but there existed poorly differentiated areas of PSA$^{-/lo}$ cells (Figure S1A). In contrast, in GS9/10 tumors, the main histological pattern was undifferentiated tumor mass in which most tumor cells were PSA$^{-/lo}$ with PSA^{+} foci only occasionally present (Figure S1B). In 23 recurrent PCa cases (mainly CRPC), some tumors resembled untreated GS9/10 tumors but most tumors completely lacked PSA^{+} PCa cells (Figure S1C–F). Quantification revealed significantly increased numbers of PSA$^{-/lo}$ PCa cells in untreated GS9/10 and treatment-failed PCa compared to untreated GS7 tumors (Figure 1A).

Consistent with the IHC results, analysis of multiple microarray data sets in *Oncomine* revealed that tumor *PSA* mRNA levels were significantly decreased in high-grade primary tumors and in recurrent and metastatic PCa (Figure S2; data not shown). Importantly, reduced tumor *PSA* mRNA levels correlated with lymph node positivity, tumor recurrence, metastasis, and shortened patient survival (Figure S2; data not shown; also see Figure 7A). Together, the PSA IHC and mRNA analysis indicates that advanced and recurrent PCa have lower *PSA* mRNA and more undifferentiated PSA$^{-/lo}$ cells.

A Lentiviral Reporter System that Separates PSA$^{-/lo}$ PCa Cells from PSA^{+} Cells

To separate PSA$^{-/lo}$ from PSA^{+} PCa cells, we employed the PSAP-GFP lentivector, in which the PSA promoter (PSAP) drives eGFP expression (Yu et al., 2001) (Figure S3A). The PSAP was originally isolated from a PCa patient with high serum PSA and was highly specific and sensitive for PSA-positive prostate (cancer) cells. We also generated two modified PSAP-GFP vectors (Figure S3A).

Using the PSAP-GFP vector, we infected LNCaP cells at an MOI of 25 (Figure 1B), at which virtually all cells were infected as evidenced by PCR detection of the GFP sequence in genomic DNA of randomly picked clones (Figure 1C). We then used fluorescence-activated cell sorting (FACS) to purify out the top 10% GFP-bright (GFP^{+}) and bottom 2–6% GFP-negative/GFP-dim (i.e., GFP$^{-/lo}$) LNCaP cells. The purity of GFP$^{-/lo}$ and GFP^{+} cells was 98–100% and ≥97%, respectively (e.g., Figure S3B). LNCaP cells routinely cultured in RPMI-7% FBS contained 2.7 ± 1.8% (0.3 – 6.0%; $n = 15$) GFP$^{-/lo}$ cells. When LNCaP cells were infected with PSAP-GFP-Psv40-neo (Figure S3A) followed by G418 selection for several weeks, we observed 2.7 ± 1.7 % ($n = 7$) GFP$^{-/lo}$ cells.

The percentage of GFP$^{-/lo}$ LNCaP cells was very close to that of PSA$^{-/lo}$ cells in LNCaP cultures (2.2 ± 1.5%; $n = 4$). Real-time (qPCR; Figure 1D) and semi-quantitative (Figure S3C) RT-PCR revealed lower *PSA* mRNA levels in GFP$^{-/lo}$ LNCaP cells compared to the corresponding GFP^{+} cells. Also, most purified GFP^{+} LNCaP cells stained strongly positive for PSA protein whereas GFP$^{-/lo}$ cells were weak or negative for PSA (Figure 1E). GFP$^{-/lo}$ LNCaP cells also expressed lower levels of AR mRNA (Figure 1D; Figure S3C) and protein (Figure 1F–G) compared to GFP^{+} cells. These results indicate that the PSAP-GFP lentiviral system faithfully reports endogenous PSA expression. Hence, in many forgoing experiments we refer to GFP^{+} and GFP$^{-/lo}$ cells as PSA^{+} and PSA$^{-/lo}$ cells, respectively.

AR staining revealed ~82% and 18% GFP^{+} LNCaP cells showing strong and intermediate nuclear AR, respectively, and no GFP^{+} LNCaP cells were negative for AR (Figure 1F). In contrast, 46% of the PSA$^{-/lo}$ LNCaP cells were completely negative for AR whereas 41%

and 13% $PSA^{-/lo}$ LNCaP cells had weak and strong AR, respectively (Figure 1F). These results suggest that the majority of PSA^{+} PCa cells are high in AR whereas $PSA^{-/lo}$ cells express a gradient of AR, from completely negative to strong nuclear staining.

$PSA^{-/lo}$ LNCaP Cells Preferentially Express Anti-Stress Genes and Are Resistant to Androgen Deprivation, Chemotherapeutics, and Pro-oxidants

When PSAP-GFP infected LNCaP cells were cultured in androgen-deprived conditions, i.e., using charcoal dextran-stripped serum (CDSS) or with bicalutamide (an antiandrogen), PSA^{+} cells dramatically decreased with a concomitant expansion of $PSA^{-/lo}$ cells (Figure S3D). Purified $PSA^{-/lo}$ LNCaP cells also displayed higher survival and holoclone (Li et al., 2008) forming capacity in the absence of androgen (Figure S3E). These results suggest that $PSA^{-/lo}$ PCa cells are resistant to androgen deprivation.

Whole-genome transcriptome profiling in purified $PSA^{-/lo}$ and PSA^{+} LNCaP cells revealed distinct gene expression patterns in the two isogenic subpopulations (Figure 1H). A total of 726 probes representing 561 unique genes were significantly overexpressed whereas 557 probes representing 403 genes were under-expressed (fold change [F.C] ≥1.4, P <0.05) in $PSA^{-/lo}$ LNCaP cells (Figure S3F; Figure S3G shows qPCR of several genes). A combination of Gene Ontology (GO) analysis and literature-based curation put many of these differentially expressed genes into distinct functional categories (Figure 1H; Table S2). Strikingly, as many as 10% of the genes overexpressed in $PSA^{-/lo}$ LNCaP cells were involved in anti-stress responses, which included detoxification (metallothioneins, GSTT2, etc), hypoxia-responsive (HIF1α, THBS1, PLAU, APLN), p53 signaling (e.g, ZBTB7A, PSME3), and DNA-damage sensing/repair (e.g., MSH6, XPA, REV1) genes (Figure 1H–I; Table S2). The $PSA^{-/lo}$ LNCaP cells also overexpressed Bcl-2 and under-expressed many proapoptotic genes (Table S2).

Differential expression of anti-stress and proapoptotic genes suggests that the $PSA^{-/lo}$ cells would be more resistant to not only androgen deprivation but also other stresses. Indeed, when LNCaP cells infected with PSAP-GFP were treated with CDSS plus bicalutamide, etoposide, paclitaxel (taxol), or H_2O_2, $PSA^{-/lo}$ cells expanded with concomitant decreases in PSA^{+} cells (Figure 1J). FACS analysis indicated that these treatments preferentially induced apoptosis in PSA^{+} LNCaP cells (not shown).

$PSA^{-/lo}$ LNCaP Cells Under-Express Genes Associated with Cell-Cycle Progression and Mitosis, Are Quiescent, and Possess Stem Cell Gene Expression Profiles

The $PSA^{-/lo}$ LNCaP cells under-expressed dozens of cell cycle and mitosis-related genes (Figure 1H; Figure S3H; Table S2), suggesting that $PSA^{-/lo}$ PCa cells may be more quiescent than PSA^{+} cells. Several lines of evidence supported this suggestion. *First*, cell-cycle analysis revealed a smaller percentage of $PSA^{-/lo}$ LNCaP cells in S and G2/M phases (Figure 1K). *Second*, the $PSA^{-/lo}$ and PSA^{+} LNCaP populations had 4.2% and 12%, respectively, of $Ki\text{-}67^{+}$ cells (P <0.0001). *Third*, BrdU label-retaining experiments demonstrated that many more $PSA^{-/lo}$ LNCaP cells retained the BrdU label upon an 11-d chase (Figure 1L).

The observations that $PSA^{-/lo}$ LNCaP cells are quiescent and resist stress stimulations suggest that the population may be enriched in stem cells (SCs) (Laffin and Tang, 2010). In support, the $PSA^{-/lo}$ LNCaP cells, in androgen/serum-free medium, possessed higher capacity to establish holoclones (Figure S3E) and anchorage-independent prostaspheres (Figure 2A). The $PSA^{-/lo}$ cell-derived spheres were much larger (Figure 2A, *insets*) and generated significantly more secondary spheres than the PSA^{+} cell-originated spheres (Figure 2B). $PSA^{-/lo}$ LNCaP cells also preferentially expressed many SC and developmental

genes such as ASCL1, CTED2, GATA6, IGF-1R, KLF5, LRIG1, NKX3.1, and TBX15 (Figure 1H; Figure 2C; Table S2). We employed tetracycline inducible pTRIPZ lentiviral shRNAmir system to knock down three representative SC molecules, i.e., ASCL1 (Jiang et al., 2009), NKX3.1 (Wang X. et al., 2009), and IGF-1R (Chan et al., 1998) (Figure S3I) in $PSA^{-/lo}$ LNCaP cells. Knocking down each of these molecules reduced sphere formation of $PSA^{-/lo}$ LNCaP cells (Figure 2D) without affecting the inherently low sphere-forming activity in PSA^{+} LNCaP cells (not shown). Furthermore, ASCL1 knockdown significantly inhibited ($P<0.05$) whereas IGF-1R or NKX3.1 knockdown partially reduced the expansion of $PSA^{-/lo}$ cells caused by androgen-deprivation and etoposide (Figure 2E). These results suggest that at least some of the 'stemness' genes over-expressed in the $PSA^{-/lo}$ LNCaP cells are functionally important.

Interestingly, $PSA^{-/lo}$ LNCaP cells, compared to PSA^{+} cells, overexpressed some (e.g., EED, HDAC4, PHF8) whereas under-expressed other (e.g., DNMT3B, PHF19) chromatin modifiers/epigenetic regulators (Figure S3J; Table S2). The functional significance of these changes in regulating the epigenetic landscape of $PSA^{-/lo}$ PCa cells is currently explored by genome-wide ChIP-Seq analysis.

$PSA^{-/lo}$ LNCaP Cells Can Undergo Asymmetric Cell Division (ACD) and Regenerate PSA^{+} Cells

LNCaP cultures in RPMI-7% FBS contained ~1.4% of $GFP^{-/lo}$ cells with the bulk being GFP^{+} (Figure S4A). When purified cells were cultured continuously for ~3 weeks, GFP^{+} LNCaP cells remained all GFP^{+} (Figure S4B) whereas GFP^{-} cultures became heterogeneous containing 1.8% GFP^{-} cells and ~75% GFP-bright cells (Figure S4C). The 2^0 GFP^{+} LNCaP cultures derived from 1^0 GFP^{-} cells continued to remain all GFP^{+} after an additional 17-day culture (Figure S4D) whereas the 2^0 GFP^{-} cultures continued to regenerate both GFP^{-} and GFP^{+} cells (not shown). Clonal development assays (Patrawala et al., 2005, 2006) revealed that cells in the clones derived from single GFP^{+} LNCaP cells remained 100% GFP^{+} at 2 (Figure S4E) and 4 (not shown) weeks. In contrast, single $GFP^{-/lo}$ LNCaP cells developed into 3 distinct types of clones: type I with all cells being GFP^{+}, type II containing both GFP^{+} and $GFP^{-/lo}$ cells, and type III containing all $GFP^{-/lo}$ cells (Figure S4F–H). Quantitative analysis demonstrated that by 2 weeks, 70–80% of all clones derived from single $GFP^{-/lo}$ LNCaP cells were type I and ~20% were type II whereas the rest were type III (Figure S4, I and J). Type I clones were likely derived from the cells that at the sorting, had already committed to differentiation. Type III clones might all be $PSA^{-/lo}$ cells that underwent symmetric self-renewal based on PCR exclusion of non-infection (Figure 1C). Regardless, the emergence of type II clones indicated that ~20% $PSA^{-/lo}$ LNCaP cells were able to undergo ACD regenerating $PSA^{-/lo}$ and giving rise to PSA^{+} cells.

Since ACD is *the* cardinal feature of SCs (Knoblich, 2008), we used time-lapse videomicroscopy to further study the clonal development of PSA^{+} vs. $PSA^{-/lo}$ LNCaP cells. In agreement with our 'static' clonal analysis (above), live imaging of single GFP^{+} cells showed that the PSA^{+} LNCaP cells only underwent symmetric division generating clones that contained all PSA^{+} cells (Figure 2F; Supplemental movie 1). By contrast, single GFP^{-} cells generated type I (Figure 2G; Supplemental movie 2), II (Figure 2H; Supplemental movies 3), and III (Figure 2I; Supplemental movie 4) clones. Approximately 15% of the GFP^{-} LNCaP cells underwent ACD during the first cell division with one daughter cell becoming GFP^{+} (Figure 2J). Analysis of the end-point clones derived from single GFP^{-} cells showed that 21% and 11% clones were of type II and III, respectively (Figure 2K).

To further explore asymmetric PCa cell division, we examined Numb partition during or right after mitosis. Numb is a Notch antagonist preferentially segregated into the differentiated daughter cells during asymmetric divisions of neuronal, hematopoietic, and

muscle SCs (Knoblich, 2008; Wu et al., 2007). We observed that in 242 GFP^- LNCaP cells that had just undergone mitosis, 15% of the cells preferentially segregated Numb to the daughter cell that also expressed more PSA (Figure 2L, Figure 3A). In such cells, Numb showed typical cortical concentration (Figure 3A), consistent with its well-established roles in cell polarity and ACD. Using 'mitotic shake-off' strategy, we observed similar asymmetric co-segregation of PSA and Numb in one daughter cell in some GFP^- LNCaP cells (Figure 3B; a–d) whereas in LNCaP cells that underwent symmetric division, Numb was also equally distributed in both cells (Figure 3B, e–h). Finally, we coinfected LNCaP cells with PSAP-GFP and a Numb-DsRed fusion retroviral reporter. The $DsRed^+/GFP^-$ LNCaP underwent ACD at 6 h when Numb was partitioned in only one daughter cell and from 24 h, the $Numb^+$ daughter cell also started to express GFP (i.e., PSA; Figure 3C). These observations indicate that a subset of $PSA^{-/lo}$ LNCaP cells can undergo authentic ACD associated with Numb co-segregation into the differentiated PSA^+ daughter cells.

$PSA^{-/lo}$ PCa Cells Purified from Xenografts Possess Long-Term Clonogenicity, Are Quiescent, and Can Undergo ACD

We used PSAP-GFP or the modified lentivectors to establish LAPC9 (and LAPC4) 'reporter' tumors (Figure S5A). The LAPC4 and LAPC9 xenograft models contain both differentiated and undifferentiated PCa cells and as such, are very useful in elucidating the cellular heterogeneity of PCa (Patrawala et al., 2005, 2006, 2007). Immunostaining using LAPC4 and LAPC9 cells purified from the reporter tumors revealed that most GFP^+ cells stained strongly for PSA whereas $GFP^{-/lo}$ tumor cells were generally negative or weak for PSA (Figure S5B–C). Western blotting (Figure 3D) and qPCR (not shown) also revealed lower protein and mRNA levels of PSA and AR in $GFP^{-/lo}$ LAPC9 cells.

In serum-containing medium, $PSA^{-/lo}$ LAPC9 cells initiated spheres that gradually enlarged and expanded and could be passaged for at least 4 generations whereas PSA^+ cell-initiated spheres aborted by 2^0 generation despite that they formed slightly more 1° spheres (Figure 3E; Figure S5D), suggesting that $PSA^{-/lo}$ LAPC9 cells possess high sphere-propagating capacity. When PSA^+ and $PSA^{-/lo}$ LAPC9 cells were cultured in medium containing CDSS, $PSA^{-/lo}$ cells formed much more (Figure 3F) and larger (Figure S5E) spheres than PSA^+ cells. Interestingly, purified $PSA^{-/lo}$ LAPC4 cells founded more and larger spheres in both serum- (Figure S5F, a–c) and bicalutamide-containing (Figure S5F, d–f) media. Similar to $PSA^{-/lo}$ LNCaP cells, the $PSA^{-/lo}$ LAPC9 cells in the tumors were quiescent as assessed by in vivo BrdU LRC (Figure 3G) and PKH26 dye-retaining (Pece et al., 2010) (Figure S6A) assays. Finally, we infected LAPC9 cells with PSAP-GFP/Pcmv-DsRed (Figure S3A), plated the purified $PSA^{-/lo}$ (i.e., $DsRed^+/GFP^-$) cells on fibroblast feeder, and tracked their developmental fates. Although most $PSA^{-/lo}$ LAPC9 cells underwent symmetric cell division (Figure 3H, top), ~5% cells underwent ACD generating PSA^+ LAPC9 cells (i.e., $DsRed^+/GFP^+$, yellow; Figure 3H, bottom).

$PSA^{-/lo}$ LAPC9 Cells Express Genes Associated with SC Functions and Castration Resistance

Microarray profiling revealed that ~200 genes were over-expressed whereas ~300 genes were under-expressed (F.C ≥1.4, $P<0.05$) in $PSA^{-/lo}$ LAPC9 cells, which fall into distinct functional categories (Figure 3I, Table S3, Table S4). Most prominently, ~27% of genes (>50) overexpressed in $PSA^{-/lo}$ LAPC9 cells were associated with SCs and development, which included SPP1 (osteopontin or OPN), FGFs, ALDH1A1, integrin α2, c-KIT, Bcl-2, IGF-1, CD44, and Nanog (Figure 3I, top; Table S3, Table S4). Overexpression of some of these molecules was confirmed by Western blotting (Figure 4A) and/or qPCR (Figure S6B). Many of the upregulated genes including Bcl-2, IGF-1, IGFBP3, REG4, and Nanog have been implicated in resistance to androgen deprivation (Jeter et al., 2011). Intriguingly, the

PSA$^{-/lo}$ LAPC9 cells overexpressed about 20 neural/glial-related genes (Table S4), suggesting that PSA$^{-/lo}$ cells might be related to or have the ability to generate neuroendocrine-like cells. Finally, many genes preferentially expressed in PSA$^{-/lo}$ LAPC9 cells were shared with those expressed in ESCs or with the genes having either bivalent or H3K27me3 chromatin marks (Figure S6C). The major class of genes upregulated in PSA^{+} LAPC9 cells (26%) was involved in intermediated metabolism and, interestingly, NumbL, the mammalian homolog of Numb, was overexpressed in PSA^{+} cells (Figure 3I, bottom; Table S3).

PSA$^{-/lo}$ PCa Cells Possess Long-Term Tumor-Propagating Capacity in Hormonally Intact Male Mice

Next, we performed limiting-dilution (LDAs) and serial tumor transplantation assays by monitoring tumor latency, incidence, growth rate, and/or endpoint weight. We first implanted 10,000 each of PSA$^{-/lo}$ (i.e., GFP$^{-/lo}$) and PSA^{+} (GFP^{+}) LAPC9 cells subcutaneously in hormonally intact male NOD/SCID mice. Surprisingly, PSA^{+} LAPC9 cells readily regenerated primary (1°) tumors that were about twice as large as those derived from PSA$^{-/lo}$ cells (Figure 4A; Figure S7A). When we infected LAPC9 cells with PSAP-GFP/Pcmv-DsRed and purified out PSA^{+} (GFP^{+}DsRed^{+}) and PSA$^{-/lo}$ (GFP^{-}DsRed^{+}) cells for LDAs, the former demonstrated higher tumor-regenerating capacity (Table 1) and developed larger tumors (not shown). Similarly, when PSA^{+} and PSA$^{-/lo}$ LAPC9 cells were implanted orthotopically in the dorsal prostate (DP), PSA^{+} cells initiated more (Table 1) and larger (not shown) tumors. The PSA^{+} LNCaP cells implanted in testosterone-supplemented male NOD/SCID mice also initiated larger tumors (Table 1). These findings suggest that 'differentiated' PSA^{+} PCa cells are, unexpectedly, tumorigenic in androgen-proficient hosts.

Nevertheless, when PSA^{+} and PSA$^{-/lo}$ LAPC9 cell-derived tumors were serially passaged in intact male mice, PSA$^{-/lo}$ cells maintained relatively constant tumorigenicity whereas PSA^{+} cells displayed decreasing tumorigenicity (Figure 4A–B; Figure S7A). By 2° generation, tumor weights between the two groups became almost equal and starting from the 3° generation, PSA^{+} cells generated tumors 2–3 times smaller than PSA$^{-/lo}$ cell-derived tumors (Figure 4B; Figure S7A). Tumor growth rates also showed contrasting patterns – although the 1° PSA^{+} LAPC9 tumors grew faster than PSA$^{-/lo}$ tumors, starting from the 3° generation, the PSA$^{-/lo}$ tumors grew much faster (not shown). Importantly, although initially there was no significant difference in tumor incidence between the PSA^{+} and PSA$^{-/lo}$ groups, by the 5° generation tumor incidence was lower for PSA^{+} cells and, by the 6° generation, tumor incidence was significantly lower ($P = 0.006$) for PSA^{+} cells (Figure 4B; Figure S7A). Comparing tumor incidence across PSA^{+} generations revealed that the 6° tumor incidence was much lower than that in the earlier (i.e., 1° – 4°) generations ($P = 0.007$; proportion trend test). These observations indicate that PSA$^{-/lo}$ LAPC9 cells are endowed with long-term tumor-propagating capacity in androgen-proficient male hosts.

Similarly, the 1° PSA^{+} LAPC4 tumors were slightly larger than those derived from PSA$^{-/lo}$ cells but later-generation PSA^{+} LAPC4 cells regenerated significantly smaller tumors than the corresponding PSA$^{-/lo}$ or early-generation PSA^{+} cells (Figure S7B). Slightly different from LAPC9, PSA$^{-/lo}$ LAPC4 cells consistently demonstrated higher tumor incidence than PSA^{+} cells across generations (Figure S7B; Table 1).

Consistent with the PSA$^{-/lo}$ LNCaP and LAPC9 cells being able to undergo ACD generating both PSA$^{-/lo}$ and PSA^{+} cells whereas PSA^{+} cells undergoing only symmetric divisions, most tumor cells in PSA^{+} LNCaP cell-derived tumors in male mice were GFP^{+}/PSA^{+} whereas tumors derived from PSA$^{-/lo}$ LNCaP cells contained both GFP^{+}/PSA^{+} and GFP^{-}/PSA^{-} cells (Figure S7C). Likewise, most tumor cells in PSA^{+} LAPC9 cell-derived tumors serially passaged in male mice were GFP^{+}/PSA^{+} whereas tumors derived from

$PSA^{-/lo}$ cells contained both GFP^+/PSA^+ and GFP^-/PSA^- cells (not shown). FACS analysis demonstrated that tumors derived from GFP^+ LAPC9 cells contained mostly GFP^+ cells whereas tumors derived from $PSA^{-/lo}$ LAPC9 cells contained ~20% $GFP^{-/lo}$ cells with the majority of cells being GFP^+ (Figure S7D), indicating that the $GFP^{-/lo}$ PCa cells can undergo self-renewal and recreate the cellular heterogeneity in vivo.

$PSA^{-/lo}$ Cells Harbor CRPC-Regenerating Subpopulation that Can Be Further Enriched by the $ALDH^+CD44^+\alpha2\beta1^+$ Profile

We then implanted purified PSA^+ and $PSA^{-/lo}$ LAPC9 cells in castrated male NOD/SCID mice also treated with bicalutamide (50 mg/kg body weight; 3 times/week). In such 'fully castrated' mice, $PSA^{-/lo}$ LAPC9 cells developed much larger tumors that grew significantly faster than corresponding PSA^+ cells (Figure 4C–D). In female NOD/SCID mice, often used as surrogate androgen-deficient hosts (Klein et al., 1997), $PSA^{-/lo}$ LAPC9 cells similarly initiated larger tumors than PSA^+ cells (Figure 4E). Purified $PSA^{-/lo}$ LNCaP cells also regenerated larger and/or more tumors in fully castrated male or female NOD/SCID mice (Table 1). These results suggest that the $PSA^{-/lo}$ PCa cells are more tumorigenic than PSA^+ cells in androgen-deficient hosts.

Intriguingly, the $PSA^{-/lo}$ LAPC9 cells did not display significantly higher tumor-initiating frequency whether we utilized PSAP-GFP or PSAP-GFP/Pcmv-DsRed lentivectors to purify PSA^+ and $PSA^{-/lo}$ cells (Table 1). We reasoned that the $PSA^{-/lo}$ cell population was still heterogeneous with tumorigenic cells able to initiate CRPC likely representing a minority. cDNA microarray analysis revealed the overexpression of ALDH1A1, integrin α2, and CD44 in $PSA^{-/lo}$ LAPC9 cells (Table S3). ALDH1A1 is the major mediator of Aldefluor phenotype and Aldefluor-hi (i.e., $ALDH^+$) population is enriched in cancer SCs (CSCs) (van den Hoogen et al., 2010) whereas $CD44^+$ PCa cells contain tumor-initiating cells (Patrawala et al., 2006) that can be further enriched by $CD44^+\alpha2\beta^+$ phenotype (Patrawala et al., 2007). Consequently, we purified $ALDH^+CD44^+\alpha2\beta1^+$ and $ALDH^-CD44^-\alpha2\beta1^-$ LAPC9 cells (Figure S7E) from the xenograft tumors maintained in castrated male NOD/SCID mice in which ~90% tumor cells were $PSA^{-/lo}$ and performed serial LDAs in fully castrated mice. Remarkably, $ALDH^+CD44^+\alpha2\beta1^+$ cells, in a cell dose-dependent manner, initiated tumor regeneration with as few as 10 cells (Figure 4F; Table 1). In contrast, $ALDH^-CD44^-\alpha2\beta1^-$ cells only regenerated 1 tumor (out of 22 injections) at the highest cell number (Figure 4F), which likely resulted from cell impurity. Similar differences in tumorigenicity were observed between the two populations in the 2° transplantations (Table 1). The abundance of $ALDH^+CD44^+\alpha2\beta1^+$ cells was higher in castrate tumors than tumors in intact male mice and was maintained during serial transplantations (Figure 4G; data not shown), indicating the self-renewal of these cells in vivo. Combined, these results suggest that the $ALDH^+CD44^+\alpha2\beta1^+$ phenotype in $PSA^{-/lo}$ population further enriches CRPC cells.

To determine what molecules might be involved in determining the tumorigenicity of $PSA^{-/lo}$ PCa cells, we again resorted to our microarray data, which identified increased expression of Nanog, CD44, and OPN, among many others. Overexpression of Nanog, CD44, and OPN was confirmed by qPCR in independently purified $PSA^{-/lo}$ LAPC9 and other PCa cells (Figure S6B; data not shown). We therefore infected $PSA^{-/lo}$ LAPC9 cells with lentivectors encoding shRNA for Nanog (Jeter et al., 2009), OPN, or CD44 (Liu et al., 2011). Knockdown of OPN, CD44, or Nanog (Figure 4H–I) inhibited tumor regeneration of $PSA^{-/lo}$ LAPC9 cells in fully castrated hosts, consistent with our recent findings that CD44 knockdown inhibits PCa metastasis (Liu et al., 2011) and that Nanog overexpression promotes CSC properties and PCa cell resistance to androgen deprivation (Jeter et al., 2011).

$PSA^{-/lo}$ PCa Cells Resist Androgen Deprivation in vivo

We carried out an ADT experiment (Yoshida et al., 2005) to determine whether $PSA^{-/lo}$ PCa cell-derived tumors resist androgen ablation in vivo. We purified PSA^{+} and $PSA^{-/lo}$ LAPC9 cells and injected them in intact male mice. When tumors became palpable, mice were castrated and also treated with bicalutamide. $PSA^{-/lo}$ cell-derived tumors grew much better (Figure 5A) and larger (Figure 5B) in androgen-depleted hosts than PSA^{+} cell-derived tumors. We further attempted to mimic the clinical scenario by correlating % GFP^{+} (PSA^{+}) cells during castration with biochemical (PSA) failure and tumor recurrence (re-growth). When the group of animals bearing LAPC9 tumors was castrated and concomitantly treated with bicalutamide at week 5, tumor growth plateaued, serum PSA levels dipped, and the % GFP^{+} cells declined by week 6 (Figure 5C). However, by week 8, despite continued decrease in GFP^{+} cells (Figure 5C, right), tumor growth resumed (Figure 5C, left, inset) and serum PSA rebounded (Figure 5C, middle, inset), signaling biochemical recurrence (BCR) and tumor recurrence. These observations were remarkably similar to what was observed in PCa patients undergoing ADT (Ryan et al., 2006) and provide evidence that androgen ablation enriches $PSA^{-/lo}$ PCa cells.

The $PSA^{-/lo}$ Cells from Primary Prostate Tumors (HPCa) and Early Xenografts Were also More Clonogenic and Tumorigenic

Are the preceding findings in PCa models (LNCaP, LAPC9, and LAPC4) applicable to patient tumors? Strikingly, low levels of tumor *PSA* mRNA correlated with reduced BCR-free and overall patient survival (Figure 7A). We purified HPCa cells from (untreated) prostatectomy specimens, infected them with PSAP-GFP, separated PSA^{+} and $PSA^{-/lo}$ cells, and performed clonal and sphere assays in serum/androgen-free medium (Jeter et al., 2009; Liu et al., 2011). The results from 3 HPCa samples showed that $PSA^{-/lo}$ cells did not express AR protein (not shown) and possessed significantly higher clonal and sphere-forming capacities than corresponding PSA^{+} cells (Figure 7B–D; Figure S8A). Importantly, we observed clonal development patterns in HPCa cells similar to those observed in LNCaP cells. For instance, most PSA^{+} HPCa12 cell-derived clones were GFP^{+} whereas the $PSA^{-/lo}$ cell-derived holoclones contained $GFP^{-/lo}$ as well as GFP^{+} cells (Figure 7E). Similar type II clones were observed in $PSA^{-/lo}$ cells plated on collagen (Figure 7F) and some $PSA^{-/lo}$ HPCa cells also underwent ACD (Figure 7G). Microarray analysis in 4 pairs of purified $PSA^{-/lo}$ and PSA^{+} HPCa cells revealed preferential expression of many SC/developmental genes in $PSA^{-/lo}$ HPCa cells (Table S5).

Using one of the early-generation (4°) HPCa xenografts, i.e., HPCa58 (Liu et al., 2011), we established reporter tumors similarly to LAPC9 and LAPC4. The reporter tumor was green (Figure 7H) and expressed *PSA* mRNA (Figure 7I). PSA immunostaining revealed a good correlation between GFP and PSA positivity (Figure 7J). When PSA^{+} and $PSA^{-/lo}$ HPCa58 cells were used in sphere assays, the $PSA^{-/lo}$ cells demonstrated higher sphere-forming capacity in both androgen-supplemented (Figure S8B) and androgen-ablated (Figure S8C) conditions. Serial transplantations in male NOD/SCID mice revealed that PSA^{+} HPCa58 cells initiated larger tumors than the corresponding $PSA^{-/lo}$ cells in the first generation; however, upon passaging, $PSA^{-/lo}$ HPCa58 cells developed larger tumors than the corresponding PSA^{+} cells (Figure 7K). Finally, when equal numbers (10,000) of PSA^{+} and $PSA^{-/lo}$ HPCa58 cells were implanted in castrated male NOD/SCID mice treated with bicalutamide, $PSA^{-/lo}$ cells generated larger and more tumors (Figure S8D). Experiments with another HPCa reporter tumor, i.e., HPCa80, revealed that the $PSA^{-/lo}$ HPCa80 cells generated larger tumors than PSA^{+} HPCa80 cells (Figure S8E).

DISCUSSION

PSA$^{-/lo}$ PCa Cells, Tumor PSA mRNA, and Serum PSA: Relevance to PCa

PSA is normally expressed and secreted by prostate luminal cells and represents one of the best-characterized organ-specific differentiation markers. Early studies have shown that PSA protein expression in PCa positively correlates with its degree of differentiation and that both untreated PCa and CRPC contain PSA^{+} and PSA$^{-/lo}$ cancer cells. Our own analysis of ~45 patient tumors confirms the two populations of PCa cells and, importantly, demonstrates that the abundance of PSA$^{-/lo}$ PCa cells is enriched in high-grade and treatment-failed tumors. PSA protein is also reduced or lacking in metastases (Varambally et al., 2005). Strikingly, lower tumor *PSA* mRNA levels positively correlate with worse clinical outcomes including high tumor grade, LN positivity, metastasis, recurrence, and reduced patient survival. The association of PSA$^{-/lo}$ PCa cells and tumor PSA mRNA/protein with poor clinical features is opposite to the positive correlation between serum PSA and the same clinical parameters. Elevated serum PSA levels in advanced PCa may be due to increased access of PCa cells to bloodstream and/or related to increased tumor mass in which PSA$^{-/lo}$ PCa cells can differentiate into PSA^{+} cells.

PSA$^{-/lo}$ PCa Cells and AR

PSA has been thought to be strictly regulated by AR. In clinical samples, however, AR and PSA protein expression is often discordant and heterogeneous with some PCa cells showing little expression of either molecule (Hobisch et al., 1995; Mostaghel et al., 2007; Ruizeveld de Winter et al., 1994; Shah et al., 2004). Discordant AR and PSA expression is also reflected at the mRNA levels in individual primary, hormone-refractory and recurrent tumors as well as in metastases (Figure S2B; unpublished observations). The discordant expression patterns of PSA and AR suggest that PSA expression can be regulated in an AR-independent manner (Hsieh et al., 1993) and that prostate tumors contain AR^{+}/PSA^{+}, AR^{+}/PSA^{-}, AR^{-}/PSA^{+}, and AR^{-}/PSA^{-} PCa cells.

The PSA^{+} PCa cells isolated based on our reporter systems mostly show strong nuclear AR whereas PSA$^{-/lo}$ population contains both AR^{-} and AR^{+} cells. Consequently, PSA^{+} cells resemble AR^{+}/PSA^{+} cells whereas PSA$^{-/lo}$ cells contain both AR^{+}/PSA^{-} and AR^{-}/PSA^{-} PCa cells. AR expression is sometimes upregulated in advanced and recurrent tumors, which we surmise could be related to the expansion of AR^{+}/PSA^{-} PCa cells. Future work that permits fractionation of AR^{+}/PSA^{-} and AR^{-}/PSA^{-} PCa cells should allow us to directly address this postulate. It should be noted that AR possesses PCa-suppressive functions (Niu et al., 2008), AR signaling is attenuated in some advanced PCa (Tomlins et al., 2007), AR is significantly reduced and only detectable in ~40% PCa cells in hormone-refractory metastases (Davis et al., 2006), and AR requirement in PCa may be context dependent (Memarzadeh et al, 2011).

Distinct Biological Properties and Gene Expression Profiles of PSA$^{-/lo}$ PCa Cells

PSA$^{-/lo}$ PCa cells possess high clonogenic capacity, survive better in androgen-deficient conditions, and are refractory to not only androgen deprivation but also drugs. PSA$^{-/lo}$ PCa cells are quiescent, which could partly explain their resistance to various stresses. Importantly, a fraction of PSA$^{-/lo}$ PCa (~15–20% PSA$^{-/lo}$ LNCaP and 5% PSA$^{-/lo}$ LAPC9) cells can undergo authentic ACD, a cardinal feature of SCs. In contrast, PSA^{+} cells undergo mainly symmetric divisions. The distinct division patterns between PSA^{+} and PSA$^{-/lo}$ cells overall are mirrored in the respective tumors they regenerate – although the PSA^{+} cell-derived tumors contain mostly PSA^{+} cells, the PSA$^{-/lo}$ cell-originated tumors contain both PSA$^{-/lo}$ and PSA^{+} cells.

It is presently unclear how $PSA^{-/lo}$ and PSA^{+} cells, both of which are maintained under identical conditions, embark on different developmental fates. Nevertheless, the distinct division modes of $PSA^{-/lo}$ and PSA^{+} cells reinforce their intrinsic biological differences. Significantly, the PSA^{+}, differentiated daughter cell derived from asymmetric division of a PSA^{-} PCa cell also preferentially 'inherits' Numb, one of the best studied cell fate determinants known to be asymmetrically segregated into differentiated daughter cells (Knoblich, 2008). It is interesting that asymmetric segregation of Numb precedes that of PSA (Figure 3J), raising the possibility that Notch signaling may regulate PCa cell ACD.

$PSA^{-/lo}$ LNCaP and LAPC9 cells preferentially express dozens of genes associated with development and SC functions. These SC-associated molecules are functionally important as demonstrated for ASCL-1, IGF-1, and NKX3.1 in LNCaP cells and Nanog, CD44, and OPN in LAPC9 cells. The $PSA^{-/lo}$ LNCaP and LAPC9 cells commonly overexpress hundreds of genes (e.g., BCL2, IGF1, SOX15, BMPR1B, TGFBR1, etc), which fall into distinct GO categories including SC, development, stress response, and wound healing (unpublished observations).

The $PSA^{-/lo}$ LNCaP and LAPC9 cells do express 'unique' gene categories. Thus, $PSA^{-/lo}$ LNCaP cells prominently under-express genes associated with cell-cycle progression and mitosis. In contrast, the $PSA^{-/lo}$ LAPC9 cells overexpress hundreds of signaling molecules whereas under-express genes associated with intermediate metabolism. The observations that $PSA^{-/lo}$ LNCaP cells under-express cell-cycle and mitosis associated genes and that $PSA^{-/lo}$ LAPC9 cells under-express metabolism-associated genes are consistent with the $PSA^{-/lo}$ PCa cells being more quiescent. Intriguingly, $PSA^{-/lo}$ and PSA^{+} LAPC9 cells frequently exhibit reciprocal gene expression patterns (Table S4), suggesting that the two populations of PCa cells may cross talk and reciprocally regulate each other in a 'paracrine' fashion, as hinted by emerging data in other tumor systems (Tang, 2012).

Distinct Tumor-Propagating Properties of $PSA^{-/lo}$ cells: Evidence for a Tumorigenic Pool that Harbors Distinct CSC Subsets

Tumor transplantation experiments in NOD/SCID mice (~2,000 used) reveal that although the tumor-propagating capacities of $PSA^{-/lo}$ PCa cells are maintained across the generations in hormonally intact male mice, the tumor-regenerating ability of the corresponding PSA^{+} PCa cells gradually declines, suggesting that $PSA^{-/lo}$ cells possess long-term tumor-propagating capacity. The $PSA^{-/lo}$ cell-regenerated tumors recreate the original tumor heterogeneity containing both $PSA^{-/lo}$ and PSA^{+} cells. That PSA^{+} cells serially transplanted in androgen-proficient hosts manifest diminishing tumorigenic potential strongly suggests that these cells intrinsically possess more limited self-renewal ability compared to $PSA^{-/lo}$ PCa cells. The unexpected observations that PSA^{+} cells, at the first generation, often demonstrate higher tumorigenic potential than the isogenic $PSA^{-/lo}$ cells caution us to be careful when using tumor regeneration as a yardstick of measuring CSC properties. Preferably, serial transplantation assays should be performed – otherwise misleading or even opposing/contradictory conclusions may be reached.

When transplanted in androgen-deficient hosts, $PSA^{-/lo}$ PCa cells initiate much larger and faster growing tumors than isogenic PSA^{+} cells. Taken together, the biological, molecular and tumorigenic properties of $PSA^{-/lo}$ cells presented herein, coupled with earlier reports on several prostate CSC populations (e.g., Collins et al., 2005; Huss et al., 2005; Maitland et al., 2011; Patrawala et al., 2006; Rajasekhar et al., 2011), suggest that the $PSA^{-/lo}$ cell population may represent a tumorigenic pool that harbors several subsets of stem-like cancer cells. First, $CD133^{+}\alpha2\beta1^{hi}CD44^{+}$ primary PCa cells (Collins et al., 2005), $ABCG2^{+}$ PCa cells *in situ* (Huss et al., 2006), and $Lin^{-}CD44^{+}$ PCa cells in xenografts (Patrawala et al., 2006) all seem to express low levels of AR and lack PSA, suggesting that these PCa cell

subsets may overlap with each other and are all harbored in $PSA^{-/lo}$ population. Second, unbiased whole-genome transcriptome analysis reveals preferential expression of CD44, integrin α2, and ALDH1A1 in $PSA^{-/lo}$ LAPC9 cells. Third, prospectively purified $ALDH^{+}CD44^{+}\alpha2\beta1^{+}$ subpopulation in $PSA^{-/lo}$ cells greatly enriches for more tumorigenic, castration-resistant PCa cells. Finally, $CD44^{+}$ PCa cells freshly purified from a dozen untreated primary tumors express much lower levels of PSA mRNAs than the corresponding $CD44^{-}$ PCa cells (Liu et al., unpublished observations). Future work will further elucidate the interrelationship between various subsets of tumorigenic cells and characterize $PSA^{-/lo}$ PCa cells with respect to their relationship with luminal and basal cells.

$PSA^{-/lo}$ CSCs May Represent an Important Source of CRPC Cells

One of the most significant contributions of the present work is to provide direct experimental evidence that $PSA^{-/lo}$ PCa cells may represent an important source of CRPC cells. *First*, $PSA^{-/lo}$ cells, in vitro, survive androgen deprivation, resist drug/stress treatments, and robustly found holoclones and self-renewing spheres. *Second*, when both PSA^{+} and $PSA^{-/lo}$ cells are implanted in male mice that are subsequently subjected to ADT, the $PSA^{-/lo}$ cell-derived tumors are refractory to castration and continue to develop. *Third*, androgen deprivation greatly enriches the $PSA^{-/lo}$ cells, which could initiate robust tumor development in castrated hosts. These findings closely resemble the AI progression observed in patients and mirror the observed reduction in PSA-producing cells in patient tumors upon androgen depletion (Ryan et al., 2006). We have provided the first *prospective* evidence that $PSA^{-/lo}$ PCa cells, which pre-exist in the tumors, are molecularly and functionally distinct from the differentiated counterparts.

We have shown that under normal (i.e., androgen-proficient) conditions, undifferentiated $PSA^{-/lo}$ cells harbor self-renewing CSCs and likely represent one important source of CRPC cells. Future work will address whether under other conditions such as persistent castrations, PSA^{+} PCa cells may manifest increased plasticity by undergoing de-differentiation, as shown by emerging data in other tumors (Tang, 2012). Altogether, our results suggest that novel therapeutics targeting $PSA^{-/lo}$ cells should be developed and used in conjunction with ADT in order to eradicate all PCa cells and prevent recurrence.

EXPERIMENTAL PROCEDURES

Detailed methods are available online in Supplemental Experimental Procedures (SEP).

Serial tumor transplantation in NOD/SCID mice

GFP^{+} and GFP^{-} PCa cells were sorted out by FACS from 1° tumors originally derived from GFP^{+} and GFP^{-} cells, respectively, and implanted s.c to generate 2° tumors in intact male mice. Sequential tumor transplantation was performed using similar strategies by following that GFP^{+} cells were always purified from tumors originated from purified GFP^{+} cells whereas GFP^{-} cells were from tumors derived initially from GFP^{-} cells. For tumor experiments in castrated mice, male NOD/SCID mice (6–8 weeks) were surgically castrated 1–2 weeks prior to injection. GFP^{+}/GFP^{-} PCa cells were purified out from reporter tumors and injected s.c into the castrated mice, which also received i.p injections of bicalutamide.

Experimental ADT and ‘recurrence’ experiments

For ADT, GFP^{+} and GFP^{-} LAPC9 cells were purified out from AD reporter tumors and injected s.c in intact male NOD/SCID mice. When tumors reached ~60 mm^3, mice were surgically castrated and treated with bicalutamide. Tumor growth was followed by caliper measurement and volumes of individual tumor were normalized to those on day 0 (day of castration). For ‘recurrence’ experiments, unsorted LAPC9 cells from AD reporter tumors

were injected s.c in intact male NOD/SCID mice. Starting from the 4th week, tumor volumes (mm^3) were measured using a digital caliper, blood samples (100–200 μl/mouse) were collected from each animal via saphenous vein for serum PSA measurement (ng/ml) and 2–3 tumors were harvested to determine by FACS the % of GFP^+ cells in individual tumors on weekly basis. For tumor volumes and serum PSA, the values were presented as fold increases over those from the fourth week. At the fifth week, animals were randomly divided into the control group, in which the animals were mock-castrated, and the castrate group, in which the animals were surgically castrated and also treated with bicalutamide.

Time-lapse videomicroscopy

Time-lapse fluorescence videomicroscopy was performed using Nikon Biostation Timelapse system (Liu et al., 2011) as described in SEP.

cDNA microarray

Basic procedures have been described (Bhatia et al., 2008). Total RNA was extracted from pooled purified GFP^+ or GFP^- LNCaP and LAPC9 cells and microarray experiments were performed in triplicates using the 44 K 60-mer "Human Whole Genome Oligo Microarray Kit from Agilent (Agilent Technologies, Santa Clara, CA) with 500 ng of total RNA. For details, please refer to SEP.

Supplementary Material

Refer to Web version on PubMed Central for supplementary material.

Acknowledgments

We thank K. Claypool and P. Whitney for FACS, Histology Core for IHC, R. Fagin for HPCa samples, J. Shen and J. Repass for qPCR, L. Shen and S. Tsavachidis for initial microarray analysis, and other members of the Tang lab for helpful discussions. This work was supported in part by grants from NIH (R01-ES015888 and 1R21CA 150009), Department of Defense (W81XWH-11-1-0331), CPRIT (RP120380), Elsa Pardee Foundation, and MDACC UCF, Center for Cancer Epigenetics, and Laura & John Arnold Foundation RNA Center pilot grant (all to D.G.T) and by two Center Grants (CCSG-5 P30 CA166672 and ES007784). We apologize to the colleagues whose work was not cited due to space constraint.

References

Abrahamsson PA, Lilja H, Falkmer S, Wadström LB. Immunohistochemical distribution of the three predominant secretory proteins in the parenchyma of hyperplastic and neoplastic prostate glands. Prostate. 1988; 12:39–46. [PubMed: 2450341]

Bhatia B, Jiang M, Suraneni M, Patrawala L, Badeaux M, Schneider-Broussard R, Multani AS, Jeter CR, Calhoun-Davis T, Hu L, et al. Critical and distinct roles of p16 and telomerase in regulating the proliferative life span of normal human prostate epithelial progenitor cells. J Biol Chem. 2008; 283:27957–27972. [PubMed: 18662989]

Chan JM, Stampfer MJ, Giovannucci E, Gann PH, Ma J, Wilkinson P, Hennekens CH, Pollak M. Plasma insulin-like growth factor-I and prostate cancer risk: a prospective study. Science. 1998; 279:563–566. [PubMed: 9438850]

Collins AT, Berry PA, Hyde C, Stower MJ, Maitland NJ. Prospective identification of tumorigenic prostate cancer stem cells. Cancer Res. 2005; 65:10946–10951. [PubMed: 16322242]

Davis JN, Wojno KJ, Daignault S, Hofer MD, Kuefer R, Rubin MA, Day ML. Elevated E2F1 inhibits transcription of the androgen receptor in metastatic hormone-resistant prostate cancer. Cancer Res. 2006; 66:11897–11906. [PubMed: 17178887]

Feiner HD, Gonzales R. Carcinoma of the prostate with atypical immunohistological features: clinical and histologie correlates. Am J Surg Pathol. 1986; 10:765–770. [PubMed: 2430476]

Gallee MP, Visser-de Jong E, van der Korput JA, van der Kwast TH, ten Kate FJ, Schroeder FH, Trapman J. Variation of prostate-specific antigen expression in different tumour growth patterns present in prostatectomy specimens. Urol Res. 1990; 18:181–187. [PubMed: 1697709]

Hsieh JT, Wu HC, Cleave ME, von Eschenbach A, Chung LWK. Autocrine regulation of prostate-specific antigen gene expression in a human prostatic cancer (LNCaP) subline. Cancer Res. 1993; 53:2853–2857.

Hobisch A, Culig Z, Radmayr C, Bartsch G, Klocker H, Hittmair A. Distant metastases from prostatic carcinoma express androgen receptor protein. Cancer Res. 1995; 55:3068–3072. [PubMed: 7541709]

Huss WJ, Gray DR, Greenberg NM, Mohler JL, Smith GJ. Breast cancer resistance protein-mediated efflux of androgen in putative benign and malignant prostate stem cells. Cancer Res. 2005; 65:6640–6650. [PubMed: 16061644]

Jeter CR, Badeaux M, Choy G, Chandra D, Patrawala L, Liu C, Calhoun-Davis T, Zaehres H, Daley GQ, Tang DG. Functional evidence that the self-renewal gene NANOG regulates human tumor development. Stem Cells. 2009; 27:993–1005. [PubMed: 19415763]

Jeter CR, Liu B, Liu X, Chen X, Liu C, Calhoun-Davis T, Repass J, Zaehres H, Shen JJ, Tang DG. NANOG promotes cancer stem cell characteristics and prostate cancer resistance to androgen deprivation. Oncogene. 2011; 30:3833–3845. [PubMed: 21499299]

Jiang T, Collins BJ, Jin N, Watkins DN, Brock MV, Matsui W, Nelkin BD, Ball DW. Achaete-scute complex homologue 1 regulates tumor-initiating capacity in human small cell lung cancer. Cancer Res. 2009; 69:845–854. [PubMed: 19176379]

Klein KA, Reiter RE, Redula J, Moradi H, Zhu XL, Brothman AR, Lamb DJ, Marcelli M, Belldegrun A, Witte ON, et al. Progression of metastatic human prostate cancer to androgen independence in immunodeficient SCID mice. Nat Med. 1997; 3:402–408. [PubMed: 9095173]

Knoblich JA. Mechanisms of asymmetric stem cell division. Cell. 2008; 132:583–597. [PubMed: 18295577]

Laffin B, Tang DG. An old player on a new playground: Bmi-1 as a regulator of prostate stem cells. Cell Stem Cell. 2010; 7:639–640. [PubMed: 21112554]

Li H, Chen X, Calhoun-Davis T, Claypool K, Tang DG. PC3 human prostate carcinoma cell holoclones contain self-renewing tumor-initiating cells. Cancer Res. 2008; 68:1820–1825. [PubMed: 18339862]

Liu C, Kelnar K, Liu B, Chen X, Calhoun-Davis T, Li H, Patrawala L, Yan H, Jeter C, Honorio S, et al. The microRNA miR-34a inhibits prostate cancer progenitor cells and metastasis by directly repressing CD44. Nature Med. 2011; 17:211–215. [PubMed: 21240262]

Maitland NJ, Frame FM, Polson ES, Lewis JL, Collins AT. Prostate cancer stem cells: Do they have a basal or luminal phenotype. Horm Canc. 2011; 2:47–61.

Memarzadeh S, Cai H, Janzen DM, Xin L, Lukacs R, Riedinger M, Zong Y, Degendt K, Verhoeven G, Huang J, et al. Role of autonomous androgen receptor signaling in prostate cancer initiation is dichotomous and depends on the oncogenic signal. Proc Natl Acad Sci USA. 2011; 108:7962–7967. [PubMed: 21518863]

Mostaghel EA, Page ST, Lin DW, Fazil L, Colement IM, True LD, Knudsen B, Hess DL, Nelson CC, Matsumoto AM, et al. Intraprostatic androgens and androgen-regulated gene expression persist after testosterone suppression: therapeutic implications for castration-resistant prostate cancer. Cancer Res. 2007; 67:5033–5041. [PubMed: 17510436]

Niu Y, Altuwaijri S, Lai KP, Wu CT, Ricke WA, Messing EM, Yao J, Yeh S, Chang C. Androgen receptor is a tumor suppressor and proliferator in prostate cancer. Proc Natl Acad Sci USA. 2008; 105:12182–12187. [PubMed: 18723679]

Patrawala L, Calhoun T, Schneider-Broussard R, Li H, Bhatia B, Tang S, Reilly JG, Chandra D, Zhou J, Claypool K, et al. Highly purified $CD44^{+}$ prostate cancer cells from xenograft human tumors are enriched in tumorigenic and metastatic progenitor cells. Oncogene. 2006; 25:1696–1708. [PubMed: 16449977]

Patrawala L, Calhoun T, Schneider-Broussard R, Zhou J, Claypool K, Tang DG. Side population is enriched in tumorigenic, stem-like cancer cells, whereas $ABCG2^{+}$ and $ABCG2^{-}$ cancer cells are similarly tumorigenic. Cancer Res. 2005; 65:6207–6219. [PubMed: 16024622]

Patrawala L, Calhoun-Davis T, Schneider-Broussard R, Tang DG. Hierarchical organization of prostate cancer cells in xenograft tumors: the $CD44^{+}\alpha 2\beta 1^{+}$ cell population is enriched in tumor-initiating cells. Cancer Res. 2007; 67:6796–6805. [PubMed: 17638891]

Pece S, Tosoni D, Confalonieri S, Mazzarol G, Vecchi M, Ronzoni S, Bernard L, Viale G, Pelicci PG, Di Fiore PP. Biological and molecular heterogeneity of breast cancers correlates with their cancer stem cell content. Cell. 2010; 140:62–73. [PubMed: 20074520]

Rajasekhar VK, Studer L, Gerald W, Socci ND, Scher HI. Tumour-initiating stem-like cells in human prostate cancer exhibit increased NF-κB signalling. Nat Commun. 2011; 2:162. [PubMed: 21245843]

Roudier MP, True LD, Higano CS, Vesselle H, Ellis W, Lange P, Vessella RL. Phenotypic heterogeneity of end-stage prostate carcinoma metastatic to bone. Hum Pathol. 2003; 34:646–653. [PubMed: 12874759]

Ruizeveld de Winter JA, Janssen PJ, Sleddens HM, Verleun-Mooijman MC, Trapman J, Brinkmann AO, Santerse AB, Schröder FH, van der Kwast TH. Androgen receptor status in localized and locally progressive hormone refractory human prostate cancer. Am J Pathol. 1994; 144:735–746. [PubMed: 7512791]

Ryan CJ, Smith A, Lal P, Satagopan J, Reuter V, Scardino P, Gerald W, Scher HI. Persistent prostate-specific antigen expression after neoadjuvant androgen depletion: an early predictor of relapse or incomplete androgen suppression. Urol. 2006; 68:834–839. [PubMed: 17070363]

Shah RB, Mehra R, Chinnaiyan AM, Shen R, Ghosh D, Zhou M, Macvicar GR, Varambally S, Harwood J, Bismar TA, et al. Androgen-independent prostate cancer is a heterogeneous group of diseases: lessons from a rapid autopsy program. Cancer Res. 2004; 64:9209–9216. [PubMed: 15604294]

Shen MM, Abate-Shen M. Molecular genetics of prostate cancer: new prospects for old challenges. Genes Dev. 2010; 24:1967–2000. [PubMed: 20844012]

Tang DG. Understanding the cancer stem cell heterogeneity and plasticity. Cell Res. 2012 In press.

Tomlins SA, Mehra R, Rhodes DR, Cao X, Wang L, Dhanasekaran SM, Kalyana-Sundaram S, Wei JT, Rubin MA, Pienta KJ, et al. Integrative molecular concept modeling of prostate cancer progression. Nat Genet. 2007; 39:41–51. [PubMed: 17173048]

van den Hoogen C, van der Horst G, Cheung H, Buijs JT, Lippitt JM, Guzmán-Ramírez N, Hamdy FC, Eaton CL, Thalmann GN, Cecchini MG, et al. High aldehyde dehydrogenase activity identifies tumor-initiating and metastasis-initiating cells in human prostate cancer. Cancer Res. 2010; 70:5163–5173. [PubMed: 20516116]

Varambally S, Yu J, Laxman B, Rhodes DR, Mehra R, Tomlins SA, Shah RB, Chandran U, Monzon FA, Becich MJ, et al. Integrative genomic and proteomic analysis of prostate cancer reveals signatures of metastatic progression. Cancer Cell. 2005; 8:393–406. [PubMed: 16286247]

Wang Q, Li W, Zhang Y, Yuan X, Xu K, Yu J, Chen Z, Beroukhim R, Wang H, Lupien M, et al. Androgen receptor regulates a distinct transcription program in androgen-independent prostate cancer. Cell. 2009; 138:245–256. [PubMed: 19632176]

Wang X, Kruithof-de Julio M, Economides KD, Walker D, Yu H, Halili MV, Hu YP, Price SM, Abate-Shen C, Shen MM. A luminal epithelial stem cell that is a cell of origin for prostate cancer. Nature. 2009; 461:495–500. [PubMed: 19741607]

Wu M, Kwon HY, Rattis F, Blum J, Zhao C, Ashkenazi R, Jackson TL, Gaiano N, Oliver T, Reya T. Imaging hematopoietic precursor division in real time. Cell Stem Cell. 2007; 1:541–554. [PubMed: 18345353]

Yoshida T, Kinoshita H, Segawa T, Nakamura E, Inoue T, Shimizu Y, Kamoto T, Ogawa O. Antiandrogen bicalutamide promotes tumor growth in a novel androgen-dependent prostate cancer xenograft model derived from a bicalutamide-treated patient. Cancer Res. 2005; 65:9611–9616. [PubMed: 16266977]

Yu D, Chen D, Chiu C, Razmazma B, Chow YH, Pang S. Prostate-specific targeting using PSA promoter-based lentiviral vectors. Cancer Gene Ther. 2001; 8:628–635. [PubMed: 11593331]

Highlights

- $PSA^{-/lo}$ PCa cells are quiescent and refractory to androgen deprivation, chemotherapeutic drugs, and prooxidants;
- $PSA^{-/lo}$ PCa cells express stem cell genes and can undergo asymmetric cell division;
- $PSA^{-/lo}$ PCa cells possess long-term tumor-propagating capacity in intact male mice;
- $PSA^{-/lo}$ PCa cells are highly tumorigenic and resist androgen ablation in castrated hosts.

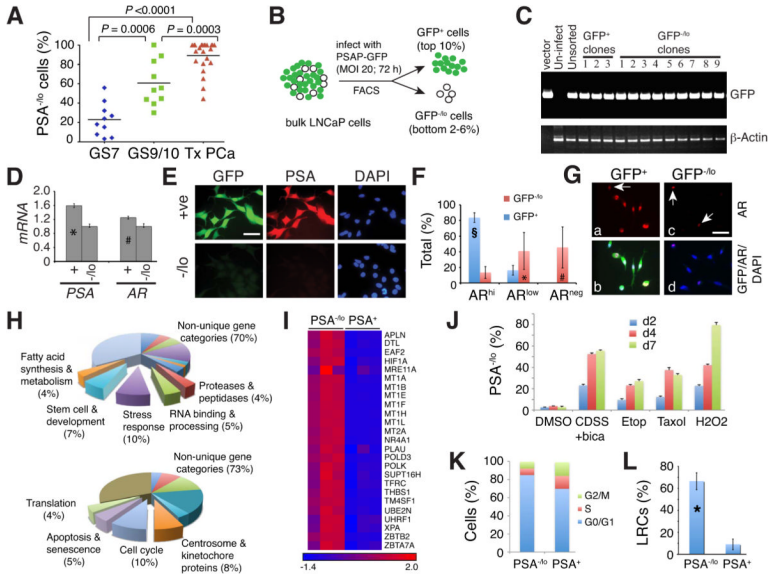

Figure 1. Distinct Molecular and Biological Properties of PSA$^{-/lo}$ and PSA^{+} LNCaP Cells

(A) Abundance of PSA$^{-/lo}$ tumor cells in untreated low-grade (GS7) and high-grade (GS9/10) tumors or in treatment-failed (Tx) PCa. See Table S1 and Figure S1 for relevant information.

(B) Schematic of GFP^{+} and GFP$^{-/lo}$ cell sorting.

(C) Genomic PCR of GFP sequence in clonally derived LNCaP cells. β-Actin, control for DNA; PSAP-GFP vector, positive control for GFP. Shown are results from 3 GFP^{+} and 9 GFP$^{-/lo}$ (1–3, type I; 4–6, type II; 7–9, type III; see Figure S4F for clone types) clones.

(D) qPCR analysis of *PSA* and *AR* mRNA in GFP^{+} and GFP$^{-/lo}$ LNCaP cells (n=3). $^{*}P = 0.005$; $^{\#}P = 0.047$.

(E) Representative microphotographs (scale bar, 20 μm) of PSA staining in GFP^{+} and GFP$^{-/lo}$ LNCaP cells (n=4).

(F–G) GFP$^{-/lo}$ LNCaP cells express lower levels of nuclear AR. F. Cells that expressed high (AR^{hi}), low (AR^{low}) and no (AR^{neg}) nuclear AR were counted and the results expressed as % of total (mean ± S.D; $^{\S}P = 6.97E09$; $^{*}P = 0.05$; $^{\#}P = 0.008$). G. Representative images (bar, 20 μm). In panels a–b, all cells are AR^{hi} with only one AR^{low} (arrow) cell. In panels c–d, all cells are AR^{neg} with two cells being AR^{low} (arrows).

(H) Distinct gene expression profiles of PSA$^{-/lo}$ and PSA^{+} LNCaP cells. Shown are pie charts of gene categories (% indicated) overexpressed (top) and under-expressed (below) in PSA$^{-/lo}$ cells.

(I) Heatmap presentation of representative anti-stress genes overexpressed in PSA$^{-/lo}$ LNCaP cells. The scale bar depicts relative expression levels (log scale) derived from raw values of each gene divided by its respective S.D across all 6 samples and centered at 0.

(J) PSA$^{-/lo}$ LNCaP cells are resistant to androgen deprivation (i.e., CDSS plus bicalutamide) as well as chemotherapeutics and hydrogen peroxide. Shown are % PSA$^{-/lo}$ cells in PSAP-GFP infected LNCaP cells treated with the conditions indicated for 2, 4, and 7 days (d). Differences between all individual treatments and DMSO are statistically significant ($P < 0.01$).

(K) PSA$^{-/lo}$ LNCaP cells are slow-cycling. Cell cycle analysis in purified PSA$^{-/lo}$ vs. PSA^{+} LNCaP cells. Shown are the mean % cells in different phases of the cell cycle ($n = 2$).

(L) PSA$^{-/lo}$ LNCaP cells are quiescent. Shown is the % label (i.e., BrdU) retaining cells (LRCs) in purified PSA$^{-/lo}$ vs. PSA^{+} LNCaP cells (mean ± S.D; $n = 3$). $^{*}P < 0.0001$.

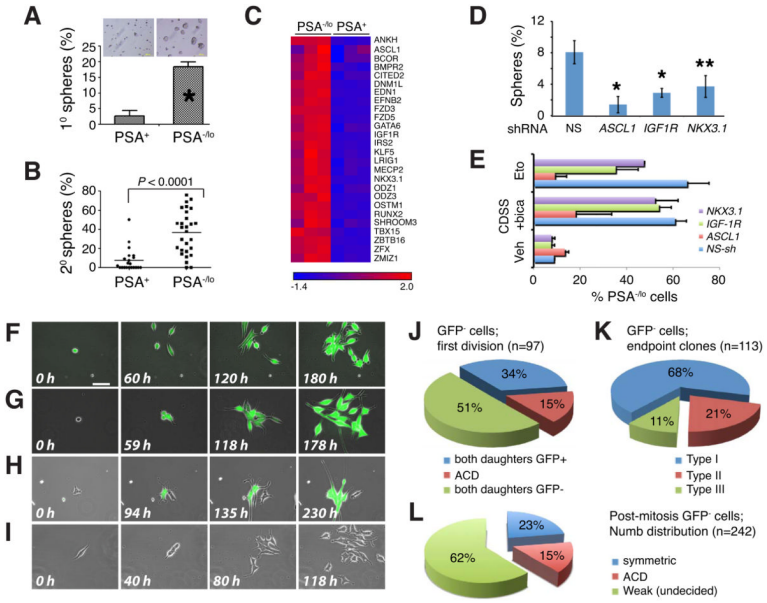

Figure 2. Distinct biological properties and division mode of PSA$^{-/lo}$ LNCaP Cells

(A) PSA$^{-/lo}$ LNCaP cells possess high sphere-forming capacity. Shown is the sphere forming efficiency (%; *$P < 0.0001$) 10 d after plating. Insets, spheres generated from PSA^{+} (left) and PSA$^{-/lo}$ cells.

(B) PSA$^{-/lo}$ LNCaP cells possess higher 2° sphere-forming capacity than PSA^{+} cells. Individual 1° spheres in (A) were picked, dissociated, and used in 2° sphere assays.

(C) Heatmap presentation of some SC-associated genes overexpressed in PSA$^{-/lo}$ LNCaP cells.

(D) Knocking down of *ASCL1, IGF-1R*, or *NKX3.1* in PSA$^{-/lo}$ LNCaP cells reduced sphere formation.

(E) Knocking down of *ASCL1, IGF-1R*, or *NKX3.1* inhibited expansion of PSA$^{-/lo}$ (i.e., GFP^{-}) cells. LNCaP cells that had been stably knocked down for the 3 genes were infected with PSAP-GFP and then treated with DMSO (vehicle), CDSS plus bicalutamide (20 μM), or etoposide (Eto., 50 μM) for 7 d.

(F–I) Single PSA^{+} (F) and PSA$^{-/lo}$ (G–I) LNCaP cells were tracked under a time-lapse video microscope. Images in F show symmetric cell division from a GFP^{+} LNCaP cell (representative of 52 movies; see Supplemental Movie 1 for an example) and images in G–I represent type I, II, and III clones, respectively, derived from single GFP^{-} cells (from 292 movies; see Supplemental Movies 2–4 for examples). Scale bar, 20 μm.

(J) Quantification of cell division mode in GFP^{-} cells during the first cell division (n = 97 movies).

(K) Quantification of the type of clones derived from GFP^{-} cells at the end of recording (n = 113 movies).

(L) Asymmetric Numb segregation during divisions of GFP^{-} LNCaP cells in the single thymidine block and post-mitosis Numb staining experiment.

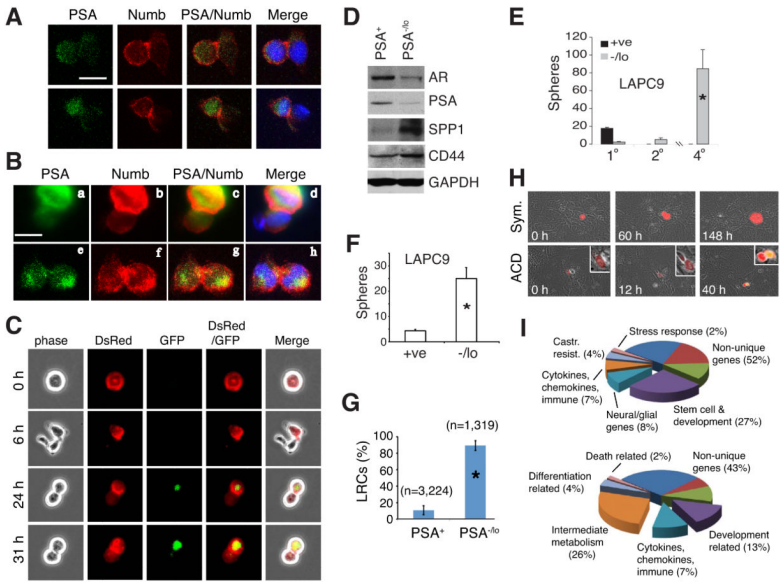

Figure 3. Distinct biological properties of PSA$^{-/lo}$ LNCaP and LAPC9 Cells

(A) Two representative GFP^{-} LNCaP cells co-segregating PSA and Numb into one daughter cell during the first cell division (scale bar, 20 μm).

(B) Different distribution patterns of PSA and Numb during asymmetric (a–d) and symmetric (e–h) division of LNCaP cells assessed in the mitotic shake-off experiments. Images shown are representative of about five dozens of cells for each mode of cell division (scale bar, 20 μm).

(C) Asymmetric co-segregation of Numb and PSA during ACD of PSA$^{-/lo}$ LNCaP cells assessed by time-lapse videomicroscopy. Shown are images of a PSA^{-} (i.e., DsRed^{+}/GFP^{-}) LNCaP cell undergoing ACD by asymmetrically segregating Numb into one daughter cell, which subsequently acquired GFP (PSA) positivity (representative of a total of 188 similar movies analyzed).

(D) Western blotting analysis of the molecules indicated in purified PSA^{+} and PSA$^{-/lo}$ LAPC9 cells.

(E–F) Purified PSA^{+} and PSA$^{-/lo}$ LAPC9 cells were cultured (10,000 cells/well) in anchorage independent conditions in either IMDM-15% FBS (E) or IMDM-15% CDSS (F) for 3 weeks and spheres were enumerated. Shown in B are serial sphere passaging (see also Figure S5D). *$P < 0.01$.

(G) PSA$^{-/lo}$ LAPC9 cells were quiescent as analyzed by in vivo LRC assays. *$P < 0.0001$.

(H) PSA$^{-/lo}$ (i.e., DsRed^{+}/GFP^{-}) LAPC9 cells undergo symmetric (top) or asymmetric (bottom) cell divisions assessed by time lapse. Images are representative of 65 movies analyzed.

(I) Distinct gene expression profiles of PSA$^{-/lo}$ and PSA^{+} LAPC9 cells. Shown are pie charts of gene categories (% indicated) over-expressed (top) and under-expressed (below) in PSA$^{-/lo}$ cells.

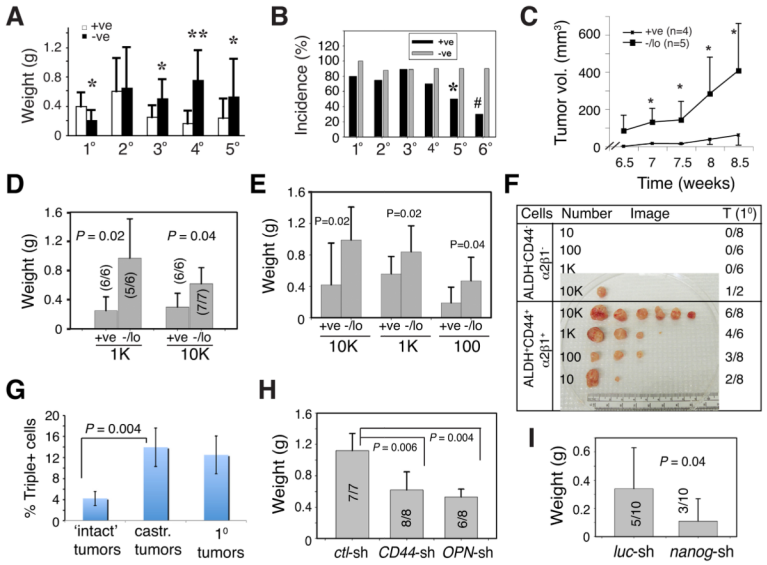

Figure 4. PSA$^{-/lo}$ PCa Cells Possess High and Long-Term Tumor Propagating Capacity

(A–B) Tumor weights (A; mean ± S.D, *P < 0.05, **P < 0.01) and incidence (B; *P = 0.045, #P = 0.006) of PSA^{+} (+ve) and PSA$^{-/lo}$ (−/lo) LAPC9 cells serially transplanted in male NOD/SCID mice (also see Figure S7A).

(C–D) GFP^{+} (+ve) and GFP^{-} (−/lo) LAPC9 cells were acutely purified out and implanted s.c in castrated male NOD/SCID mice treated with bicalutamide. (C) Tumor volumes measured in animals with 1,000 cell injections starting from 6.5 weeks post implantation (mean ± S.D; *P < 0.05; tumors harvested at 66 d for 1,000 cells and 60 d for 10,000 cells). Shown in D are incidence and weight.

(E) Purified GFP^{+} (+ve) and GFP^{-} (−ve) LAPC9 cells were implanted s.c in female NOD/SCID mice. Tumors were harvested at 78 d (for 100 cells), 66 (for 1,000 cells) or 53 (for 10,000 cells) d post implantation.

(F) Triple marker-positive and –negative LAPC9 cells were purified from AI tumors and re-implanted, at the cell doses indicated, in fully castrated NOD/SCID mice.

(G) The % of triple marker-positive LAPC9 cells in three types of tumors, i.e., 'intact' tumors maintained in hormonally intact male mice, 'castrated' tumors maintained in castrated animals, and the 1° tumors derived from the triple marker-positive cells.

(H) Knockdown of OPN or CD44 inhibits tumor regeneration in PSA$^{-/lo}$ LAPC9 cells. PSA$^{-/lo}$ LAPC9 cells infected with control shRNA (ctl-sh), or CD44 or OPN shRNAs were implanted s.c in male NOD/SCID mice. Bars represent tumor weights (mean ± S.D).

(I) Nanog knockdown inhibits tumor regeneration. Shown are tumor weights and incidence. luc-sh, luciferase-shRNA; nanog-sh, Nanog-shRNA.

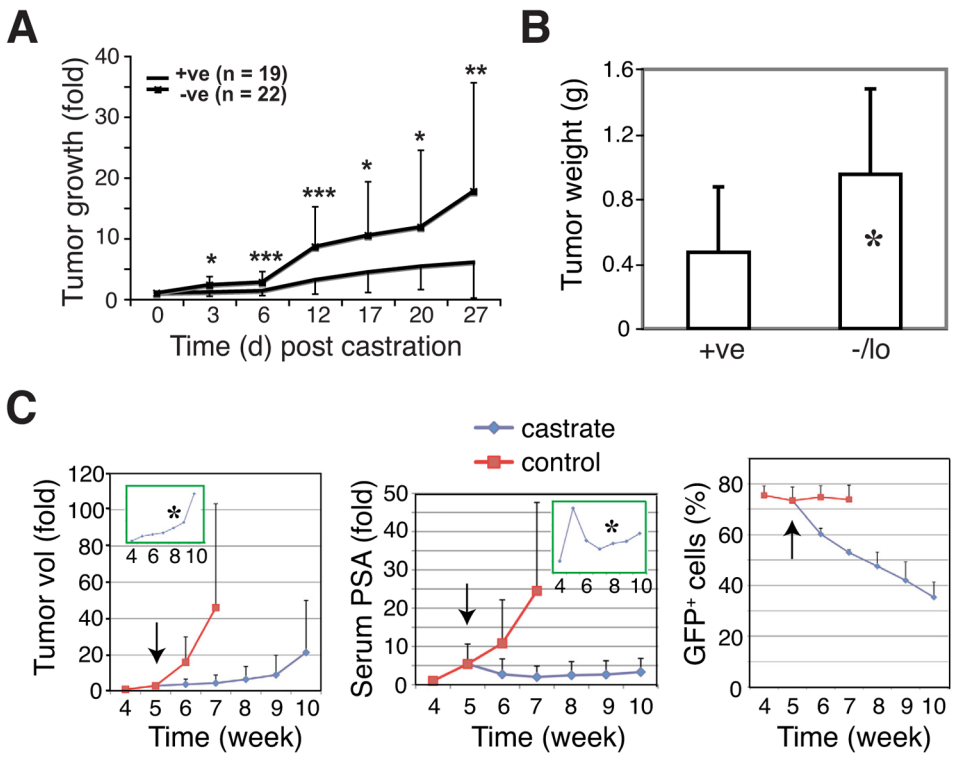

Figure 5. PSA$^{-/lo}$ PCa Cells are More Resistant to Experimental ADT

(A–B) Purified PSA^{+}/PSA$^{-/lo}$ LAPC9 cells (10,000 each) were injected s.c in intact male mice and when tumors became palpable, mice were castrated and treated with bicalutamide (time 0). Tumors were measured at the indicated time points and results are presented as fold increase in tumor growth over time 0 (F; *P<0.05; **P<0.01; ***P<0.001). Shown in B are tumor weights (mean ± S.D; *P<0.05) from one group of animals at the end of experiments (see Table 1 for incidence).

(C) 'Recurrence' experiments. Shown are measurements of tumor volume (left), serum PSA (middle) and the % of GFP^{+} LAPC9 cells in the tumors (right) starting from the fourth week after implantation. Arrows indicate the time of castration (i.e., the fifth week). Insets: tumor vol. (left) and PSA (middle) plotted for the castrate group only (asterisks indicate when tumors 'recurred' at 8 weeks).

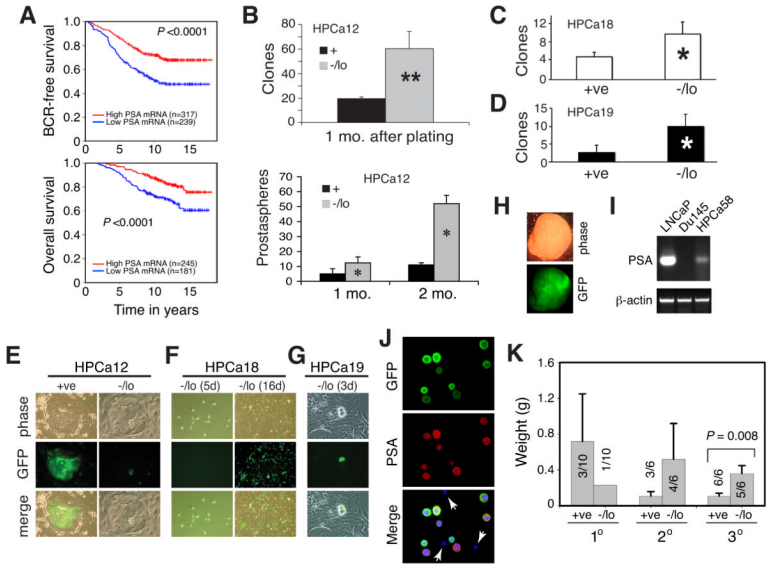

Figure 6. Distinct biological and tumor-propagating properties of PSA^{+} and PSA$^{-/lo}$ HPCa cells

(A) Meta-analysis showing lower tumor PSA mRNAs correlating with reduced BCR-free or overall patient survival. Data was based on the Nakagawa study.

(B) PSA^{+} and PSA$^{-/lo}$ HPCa12 cells were plated (2,000 cells/well) in serum/androgen-free PrEBM medium on Swiss 3T3 feeders for holoclone analysis (the upper panel; **P<0.01) or in low-attachment plate for sphere-formation assays (the lower panel; *P<0.05).

(C–D) PSA^{+}/PSA$^{-/lo}$ HPCa18 (C) and HPCa 19 (D) cells were plated (100 cells/well) and cultured on Swiss 3T3 feeder plate for 18 days and individual holoclones were enumerated. *P<0.05.

(E–G) PSA^{+} and PSA$^{-/lo}$ HPCa cells were purified from 3 patient tumors, infected, FACS-purified, and plated (at 1 cell/well in 96 microwell plate) on either fibroblasts (E and G) or collagen (F). Images in E were taken 12 d post plating.

(H–K) Experiments with HPCa58 early xenograft tumors. HPCa58 cells were purified out from the 4° HPCa58 xenografts, infected with PSAP-GFP, and implanted s.c in male NOD/SCID-γ mice to establish reporter tumors. H. A representative reporter tumor. I. RT-PCR of PSA mRNA. J. PSA immunostaining in GFP^{+} HPCa58 cells on cytospun slides (small white arrows, GFP^{-}cells that were also PSA^{-}). K. Tumor weights (mean ± S.D) and incidence of serially transplanted PSA^{+} (+ve) and PSA$^{-/lo}$ (−/lo) HPCa58 cells (10,000 cells/injection).

Table 1

Tumor-initiating frequency (TIF) of PSA^+ and $PSA^{-/lo}$ PCa cells in NOD/SCID mice

Cells	Cell dose						TIF (95% interval)*	P value*
	10^5	10^4	10^3	10^2	10	1		
[1]**LNCaP**								
PSA^+ (male)		2/4 (1.0 g)						
$PSA^{-/lo}$ (male)		3/5 (0.3 g)						
PSA^+ (castr.)		0/6						
$PSA^{-/lo}$ (castr.)		2/6 (1.3 g)						
PSA^+ (female)		1/6 (0.5 g)	1/6 (0.05 g)				1/30,110 (1/7,199 – 125,944)	
$PSA^{-/lo}$ (female)		4/5 (1.4 g)	5/7 (0.7 g)				1/2,674 (1/986 – 7,250)	0.0005
[2]**LAPC9**								
[a]PSA^+ (male)		2/2	5/6	4/10	4/10	1/8	1/204 (1/88 – 473)	
[a]$PSA^{-/lo}$ (male)		1/2	4/6	4/10	2/10	0/8	1/552 (1/243 – 1,254)	0.0335
[b]PSA^+ (male)/DP	1/1	3/4	3/7				1/4,156 (1/1,518 – 11,382)	
[b]$PSA^{-/lo}$ (male)/DP	1/1	1/4	1/7				1/20,187 (1/5,125 – 79,523)	0.0399
[a]PSA^+ (castr.)			2/4	3/10	1/10	0/8	1/615 (1/238 – 1,589)	
[a]$PSA^{-/lo}$ (castr)			2/4	2/10	2/9	1/8	1/196 (1/77 – 499)	0.075
[b]PSA^+ (castr.)		6/6	6/6				1/1 (1/1 – 1,071)	
[b]$PSA^{-/lo}$ (castr)		7/7	5/6				1/559 (1/206 – 1,515)	0.224
[b]PSA^+ (female)		6/6	4/6	5/8			1/425 (1/180 – 1,006)	
[b]$PSA^{-/lo}$ (female)		6/6	5/6	6/8			1/235 (1/92 – 605)	0.254
[c]$ALDH^{hi}CD44^+\alpha2\beta1^+$ (castr.) 1^0		6/8	4/6	3/8	2/8	0/8	1/448 (1/193 – 1,043)	
[c]$ALDH^{lo}CD44^-\alpha2\beta1^-$ (castr.) 1^0		1/2	0/6	0/6	0/8	0/8	1/21,298 (1/3,126 – 145,130)	648 e-150
[c]$ALDH^{hi}CD44^+\alpha2\beta1^+$ (castr.) 2^0			7/8	5/8	0/8	0/8	1/283 (1/125 – 645)	
[c]$ALDH^{lo}CD44^-\alpha2\beta1^-$ (castr.) 2^0		2/3	0/8	0/8			1/13,802 (1/3,366 – 53,421)	2.23 e-09
[3]**LAPC4**								
PSA^+ (male) 3^0		6/10	4/8				1/6,895(1/3,374 – 14,088)	
$PSA^{-/lo}$ (male) 3^0		10/10	8/8				1/1(1/1 – 860)	9.65 e-08

[1] PSA^{+} (i.e., GFP^{+}) and $PSA^{-/lo}$ ($GFP^{-/lo}$) LNCaP cells were purified and implanted subcutaneously in 50% Matrigel in 3 types of NOD/SCID mice, i.e., intact male mice supplemented with testosterone pellets, surgically castrated (castr.) male mice also treated with bicalutamide, or female mice. All tumors were harvested 3 – 4.5 months after implantation.

[2] For experiments in a, LAPC9 cells acutely purified from xenograft tumors were infected with PSAP-GFP/Pcmv-DsRed (MOI 20; 72 h). Purified PSA^{+} (i.e., $GFP^{+}DsReD^{+}$) and $PSA^{-/lo}$ ($GFP^{-}DsRed^{+}$) cells at the indicated numbers were injected subcutaneously into the inatct or castrated male mice. For experiments in b, PSA^{+} (i.e., GFP^{+}) and $PSA^{-/lo}$ (i.e., $GFP^{-/lo}$) LAPC9 cells were purified out from reporter tumors. Cells at the indicated numbers were implanted subcutaneously or orthotopically (in the DP) in 50% Matrigel in the 3 types of hosts. All tumors were harvested in ~2 months. For experiments in c, the triple marker-positive and -negative LAPC9 cells were purified from the xenograft tumors long-term maintained in castrated NOD/SCID mice and injected at the indicated cell doses. Tumors were harvested ~2 months post-implantation. Then triple marker-positive and -negative cells were purified from the two tumors derived from 10 marker-positive cell injections and used in secondary transplantations, which were harvested 73 days later.

[3] Shown were the tumor LDAs performed with the third-generation LAPC4 reporter tumors (see Figure S7B).

[*] TIF and statistical differences (P values) were determined using the Limdil function of the Statmod package (http://bioinf.wehi.edu.au/software/elda/index.html).

Cell Stem Cell. Author manuscript; available in PMC 2013 May 04.